Climate Change, Firms, and Aggregate Productivity*

Andrea Caggese† Andrea Chiavari‡ Sampreet Singh Goraya§
Carolina Villegas-Sanchez¶

Abstract: This paper develops a general equilibrium framework to study how temperature affects firm-level demand, productivity, and input allocation, and uses it to derive an aggregate damage function for climate change. Using matched data for Italian firms and climate variation, we find that extreme temperatures reduce both productivity and the marginal product of capital. Our model estimates aggregate productivity losses from local temperature fluctuations ranging from 1.6% to 17.8%, depending on adaptation and scenario. For a given scenario, these losses are about four times larger than in representative-firm models, which overlook frictions and heterogeneity. Embedding our framework into Integrated Assessment Models would revise upward the economic costs of climate change.

Keywords: Climate Change, Aggregate Productivity, Firms, Allocative Efficiency.

*This version: April 26, 2026. The first version circulated in October 2023. We thank Matteo Alpino, Lint Barrage, Andrew Bernard, Douglas Gollin, Banu Demir, Maarten De Ridder, Dave Donaldson, Farid Farrokhi, Stephie Fried, Kerem Cosar, Jeremy Majerovitz, Asier Mariscal, Eduardo Morales, Ishan Nath, Michael Peters, Sophie Piton, Stephen Redding, Richard Rogerson, Federico Rossi, Karthik Sastry, Anant Sudarshan, Lucian Taylor, Rick Van Der Ploeg, John Van Reenen, Christopher Woodruff, and the conference participants of the Finpro-CEPR Rome, BSE Summer Forum, ENRI meeting in Luxembourg, EEA, London Junior Macro, LSE Environment Week, Lancaster Climate Change and Global Economy, Tilburg Growth International Finance and Trade, University of Mannheim conference and seminar participants at CREST-ENSAI, Princeton, Duke, ESADE, Illinois Urbana-Champaign, Oxford, CREI, Houston, Virginia, University of Barcelona, ETH CEPE, IMF, San Francisco Fed, New York Fed, CERGE-EI, University of Oslo, NYU Abu Dhabi for useful comments and suggestions. We thank Robert Wojciechowski for his excellent research assistance. We thank Antoine Gervais for sharing his tradability data with us. We acknowledge financial support from the EIBURS grant on "Intangibles, Technology Diffusion and Public Policies: Implications for Firm Investment, Market Structure and Aggregate Productivity".

†UPF, Barcelona GSE, and CREI, andrea.caggese@upf.edu
‡University of Oxford, andrea.chiavari@economics.ox.ac.uk
§Stockholm School of Economics, sampreet.goraya@hhs.se
¶ESADE, URL, ECB and CEPR, carolina.villegas@esade.edu

1 Introduction

The rising levels of CO_2 in the atmosphere are significantly increasing global temperatures and altering weather patterns, leading to climate change (IPCC, 2021). Since Nordhaus (1977), with its latest version in Barrage and Nordhaus (2023), the literature has relied on Integrated Assessment Models (IAMs) to quantify the aggregate costs of climate change, the social cost of carbon, and explore the potential for policy interventions. This approach extends the standard neoclassical growth model by incorporating climate-induced economic losses through an *aggregate damage function*, which links aggregate productivity to temperature changes within the standard aggregate production function. Despite the aggregate damage function being a key component of IAMs, no consensus has yet emerged regarding its measurement—a critical gap given that damage function estimates directly determine optimal climate policy.

The standard approach to measuring damage functions follows a two-step process. First, parameters are estimated using historical temperature fluctuations and economic outcomes. Second, these estimates predict future economic damages under different climate scenarios. Most studies perform the first step using aggregate economic data, but this approach faces inherent limitations. Aggregate regressions struggle to separate climate effects from policy responses and other confounding factors. Moreover, they cannot distinguish between channels that directly impact firm productivity from those affecting allocative efficiency. A "bottom-up" approach—estimating firm-level damages and aggregating them—avoids policy-driven confounding and isolates distinct channels, improving projection accuracy as these channels may respond differently to future climate scenarios.

In this paper, we develop a microfounded aggregate damage function grounded in firm-level analysis, offering a framework for its measurement and making three contributions. First, we introduce a micro-to-macro framework that links firm-level damages from temperature increases to aggregate productivity, emphasizing two channels: a direct effect that reduces productivity and/or demand and an indirect effect arising from input adjustment frictions. Second, using standard firm-level data, we provide causal estimates of both direct and indirect effects. To the best of our knowledge, this is the first study to offer causal evidence of significant indirect effects driven by frictions in firm-level capital adjustment. Finally, we show that the channels identified in our framework result in substantial aggregate productivity damages. Both direct and indirect effects play important roles, with considerable heterogeneity in productivity damages even within narrowly defined geographic regions.

Our framework models monopolistically competitive heterogeneous firms producing with

capital, labor, and materials, with their scale of operations *directly* influenced by local temperature through its effects on productivity and demand. This relationship captures several well-documented channels: temperature may reduce labor efficiency through its effects on workers' performance, attendance, or health; lower capital productivity as machinery and equipment operate less efficiently under extreme conditions; and shift consumer spending patterns and local demand, particularly for non-tradable goods consumed locally.[1]

However, these direct effects do not fully account for the total productivity losses incurred by firms. When frictions—such as adjustment costs or spatial and financial constraints—limit firms' ability to adjust inputs in response to temperature changes, firms may be compelled to retain inputs they would otherwise discard. For example, if extreme heat reduces a firm's optimal scale of operation but it cannot adjust its capital stock while maintaining optimal labor and materials, it operates with excess capital. This lowers the revenue-based marginal product of capital due to the law of diminishing returns, amplifying the initial productivity loss. To fix ideas, consider an extreme temperature event that hits half the regions in a country, preventing affected firms from operating 20% of the time. Under costless input adjustment and constant returns to scale, aggregate productivity would remain unchanged—firms would simply scale down proportionally. But if affected firms cannot reduce inputs while unaffected firms scale up to meet demand, aggregate productivity falls by roughly 10%, reflecting the weighted average of productivity across firms.

To capture this *indirect* effect, we introduce reduced-form, input-specific wedges, following Restuccia and Rogerson (2008) and Hsieh and Klenow (2009). These wedges, which we allow to vary with temperature, capture the gap between an input's revenue-based marginal product and its user cost, influencing how firms adjust different inputs in response to temperature changes.

Our model shows that, at the firm level, productivity losses are driven by the temperature-semielasticity of two factors: firm sales and the revenue-based marginal product of inputs. Through the lens of the model, these semielasticities allow us to separately identify and quantify both direct and indirect effects—where direct effects capture the contribution of firm-level productivity to aggregate productivity, and indirect effects arise from frictions that distort input allocation. At the macro level, the model delivers a novel closed-form characterization of the aggregate productivity damage function, linking it to firm-level temper-

[1]The demand-side impacts of temperature are underscored in Busse et al. (2015) for the case of durable goods, while its effects on productivity have been explored extensively (e.g., Seppanen et al., 2006; Zhang et al., 2018; Somanathan et al., 2021), as summarized in Heal and Park (2016) and Lai et al. (2023).

ature-semielasticities without relying on aggregate equilibrium prices, thereby ensuring robustness to general equilibrium considerations.

We implement our framework using Italian data, an ideal setting given the country's frequent episodes of very high temperatures and substantial regional variation in both climate and economic development. European temperatures have risen at more than twice the global average over the past 30 years, and Italy is among the most affected.[2] We merge firm-level data from Orbis (1999–2013), covering roughly 75% of Italy's aggregate gross output (Kalemli-Özcan et al., 2024), with daily temperature and rainfall data from Copernicus Climate Change Services at an $\sim 11 \times 11$, km grid resolution. Firms are matched to climate data based on their headquarters' postcode location.[3]

Empirically, we follow standard practice in the literature by exploiting short-run temperature variation to isolate the effect of climate on economic activity.[4] Specifically, we adopt the firm-level methodology of Somanathan et al. (2021), aggregating daily temperatures at each grid point to the annual level by counting the number of days falling within different temperature intervals, following the approach of Deschênes and Greenstone (2011).[5] Our analysis reveals an inverted U-shaped effect of temperature on sales, with extremely high or low temperatures negatively affecting firms. We find that extreme temperatures reduce labor and material inputs but not capital usage among affected firms, suggesting stronger frictions in capital adjustment than for other inputs. Consequently, we estimate an inverted U-shaped relationship between temperature and the revenue-based marginal product of capital, with no significant effect on the marginal products of other inputs. This captures the indirect effect of temperature on firms. Finally, while distinguishing between productivity and demand effects is not essential for our quantitative aggregation, we examine their relative importance by comparing tradable and non-tradable sectors. Based on prior literature, we assume similar productivity effects across sectors but greater demand sensitivity for non-tradables.[6] We find no significant differences in temperature effects between the two, suggesting that temperature primarily affects firms through productivity rather than demand.

Quantitatively, we construct the aggregate damage function from our causal estimates un-

[2]Source: Report on the State of the Climate in Europe, 2021, by the World Meteorological Organization.

[3]Most of our sample consists of single-establishment SMEs, and results are robust to excluding larger or multi-establishment firms.

[4]Examples of macro-level studies using short-run temperature variation to assess the effects of climate change include Dell et al. (2012), Dell et al. (2014), Bilal and Känzig (2024), and Nath et al. (2024). Micro-level approaches using similar variation include Acharya et al. (2023) and Ponticelli et al. (2023), among others.

[5]Alternative aggregation methods, such as the degree-day approach or nonlinear transformations of average annual temperature as in Burke et al. (2015), yield similar results.

[6]For instance, Almunia et al. (2021) document lower demand sensitivity for tradable goods.

der different warming scenarios, incorporating both mean temperature increases and greater variability. This distinction is novel in counterfactual analysis and matters for three reasons: extreme events are projected to rise exponentially with mean warming[7]; our inverted U-shaped firm-level estimates imply variability alone can reduce aggregate productivity; and the short-term indirect allocative effects we identify apply mainly to variability, since in the long run inputs should fully reallocate to the most productive locations. Therefore, in our baseline scenario we only apply allocative effects to the projected increase in the dispersion of temperatures around the mean. In other words, even though firms can reallocate inputs efficiently in response to a gradual increase in temperatures over many decades, they cannot easily do so in response to sudden extreme temperature events, which are expected to become more frequent in the future. In the counterfactuals, we also take into account that firms can adapt to both changes in mean and variability of temperatures. We incorporate adaptation by comparing historically exposed regions—likely already adapted—to newly exposed regions, predicting which will adapt in future and applying correspondingly smaller damages.

Our baseline exercise uses the RCP4.5 scenario, which implies for Italy an average increase in temperatures of around 2℃ in 2071–2099 compared to 1981–2010. In this scenario we find that aggregate productivity declines by 4.23 percent, and a substantial part of this total effect (21 percent) is caused by the indirect allocative channel despite, as explained above, it only applies to the increase in temperature variability. These negative effects of local temperature fluctuations are large relative to previous studies on temperate countries such as Italy. We find that adaptation reduces the expected losses only modestly, from 4.23 percent to 3.35 percent. We also find that such losses are much smaller (a decline by 1.64%) if only mean temperature increases are considered, while temperature variability is held constant. We show that damages are highly nonlinear: under RCP8.5 (≈4℃ warming), losses reach 17.81% without adaptation and 14.97% with adaptation—over four times greater than under RCP4.5 despite only doubling mean warming—reflecting both the non-linear firm-level effects and the broader geographic spread of extremes in severe scenarios.

We demonstrate the value of our micro-to-macro approach by contrasting its predictions with those from standard firm-level studies and integrated assessment models (IAMs). Firm-level studies using representative-firm frameworks (e.g., Zhang et al., 2018; Somanathan et al., 2021) typically estimate firm-level losses based on simple average temperature scenarios and predict aggregate productivity declines four times smaller than our estimates when

[7]See projections by IPCC, 2021. We quantify this relation for Italy, based on the study by Fischer and Schär (2010), in a 0.08 points increase in standard deviation for every 1℃ rise in average temperature.

applied to our data. The novel indirect channel accounts for 68% of this gap; the rest reflects general-equilibrium mechanisms: first, the roundabout nature of material production creates output–input feedback loops that amplify losses (Jones, 2011); and second, the covariance between firm size and temperature sensitivity concentrates damages in more productive regions—a higher covariance indicating that temperature-related productivity damages are concentrated in regions with larger firms.

We conclude the analysis by constructing aggregate damage functions at the NUTS3 level to explore the regional impact of climate change on productivity across Italian provinces. This analysis reveals heterogeneous effects, ranging from mildly positive to severely negative outcomes. Notably, as poorer southern regions are expected to face greater shifts toward extreme temperature ranges, climate change is likely to exacerbate existing regional inequalities in Italy. Our findings underscore this dynamic by showing a negative relationship between expected productivity losses and current GDP per capita.

Finally, we discuss some limitations of our framework and interpret the results. Our static framework does not account for the extensive margin, such as firm entry and exit, which could influence the outcomes. For example, unproductive firms may exit affected regions, improving the selection of firms, or firms might relocate to cooler areas, enhancing allocative efficiency. While our sample provides limited evidence for the latter, our analysis lays the groundwork for future models to address these dynamics.

Literature Review. This paper contributes to the literature on firm heterogeneity that uses the reduced-form wedge approach to evaluate the aggregate productivity impacts of shocks, frictions, and policies, including studies by Restuccia and Rogerson (2008), Hsieh and Klenow (2009), Gopinath et al. (2017), Osotimehin (2019), and Baqaee and Farhi (2020). Building on this foundation, we analyze aggregate productivity losses under climate scenarios. Our work is related to Bau and Matray (2023), who develop a framework to assess the effects of observed policies on aggregate productivity but without enabling counterfactual analysis, and Sraer and Thesmar (2023), who incorporate counterfactual analysis but focus solely on changes in frictions. We extend this literature by introducing a novel decomposition of aggregate productivity changes that facilitates counterfactual analysis in general equilibrium, capturing changes in productivity and frictions caused by shocks, using causally estimated firm-level semi-elasticities as inputs.

Our work is closely related to the macro-climate literature employing Integrated Assessment Models (IAMs), pioneered by Nordhaus (1977) and further expanded in dynamic versions by Golosov et al. (2014), Krusell and Smith (2022), and Barrage and Nordhaus (2023). These

studies calibrate aggregate damage functions to ensure that output losses align with historical temperature-induced changes in aggregate estimates (see Nordhaus and Moffat (2017) for a review).

Recent contributions by Cruz and Rossi-Hansberg (2023) and Bilal and Rossi-Hansberg (2023) expand IAMs to incorporate the spatial implications of climate change, using structural models with migration and capital accumulation to match observed regional losses to historical temperature changes. These models are critical for understanding dynamic responses, aggregate consequences, and the social cost of carbon. However, estimating the aggregate damage function—a core IAM component—at country or regional levels remain challenging due to standard identification issues in aggregate regressions. Our framework addresses these challenges by examining firm-level mechanisms and distinguishing direct productivity effects from indirect effects caused by input adjustment frictions. This approach complements the growing body of work that leverages granular data and quantitative macroeconomic models to study climate impacts (e.g., Desmet and Rossi-Hansberg, 2015; Barrage, 2020; Conte et al., 2022; Fried, 2022; Nath, 2024; Balboni et al., 2024; Castro-Vincenzi, 2022; Castro-Vincenzi et al., 2024) by microfounding the aggregate damage function at the firm level and providing an empirical framework for its measurement.

Finally, we contribute to the empirical literature estimating climate-induced losses using historical temperature changes. Aggregate empirical designs include Dell et al. (2012, 2014), Burke et al. (2015), Hsiang et al. (2017), Burke and Tanutama (2019), Kalkuhl and Wenz (2020), Kahn et al. (2021), Newell et al. (2021), Bastien-Olvera et al. (2022), Casey et al. (2023), Nath et al. (2024), Leduc and Wilson (2023), and Bilal and Känzig (2024). Although these approaches have the advantage of encompassing many channels and equilibrium effects, they face identification challenges common to most cross-country empirical settings, such as omitted variables and confounding factors. Our paper instead estimates the effects of local temperature fluctuations on local firm-level economic outcomes. We view this approach as complementary to these papers, and in particular to recent research estimating the effects of global temperature changes on global GDP (e.g., Bilal and Känzig (2024)). The global approach captures a broader range of climate damages–such as droughts, extreme winds, and precipitation–but faces challenges in identifying causal effects due to confounding global factors. In contrast, panel data approaches that exploit local temperature shocks and impose model-based structure improve causal identification and help uncover the specific channels through which temperature affects economic activity. Firm-level approaches aimed at addressing these challenges include Zhang et al. (2018), Addoum et al. (2020), Somanathan et al.

(2021), and Ponticelli et al. (2023),[8] but they face limitations in informing aggregate counterfactuals. Specifically, general equilibrium effects remain unmeasured because they are absorbed into the intercept—a limitation known as the "missing intercept problem" (Moll, 2021). We complement both approaches by presenting a novel framework that combines careful causal firm-level identification—where we provide, to our knowledge, the first causal evidence of firm-level indirect effects driven by input-adjustment frictions and their implications for productivity—with a methodology that allows for closed-form aggregation consistent with broad general equilibrium effects.

Outline. The rest of the article is organized as follows. Section 2 describes a theoretical model. Section 3 describes data and measurement. Section 4 lays out the empirical strategy. Section 5 presents the main results. Section 6 provides the aggregate effects. Section 7 concludes.

2 Structural Framework

In this section, we present a framework to microfound the impact of temperature on aggregate productivity—the aggregate damage function central to IAMs—through the different effects of temperature on firms.

2.1 Firm-Level Variables

We build our framework on a closed-economy version of Melitz (2003).[9] We consider an economy at time t populated by a large number N of monopolistically competitive firms i, producing differentiated varieties, and operating in a grid-cell g.[10] In this economy, aggregate output Y is a CES aggregate of N firms:

$$Y_t = \left(\sum_{i=1}^{N_t} \left(e^{d_{it}(T_{g(i)t})} Y_{it} \right)^{\frac{\sigma-1}{\sigma}} \right)^{\frac{\sigma}{\sigma-1}}, \tag{1}$$

[8] Other studies exploring the micro-level impact of climate change on other outcomes include Deschênes and Greenstone (2011), Kala et al. (2012), Graff Zivin and Neidell (2014), Cohn and Deryugina (2018), Diffenbaugh and Burke (2019), Colmer (2021), Albert et al. (2021), Pankratz and Schiller (2024), Custodio et al. (2024), Cascarano et al. (2022), Balboni (2025), Acharya et al. (2023), Liu and Xu (2024), and Bettarelli et al. (2025).

[9] The model is static, and firm decisions at time t do not depend on past choices, nor they affect future outcomes. For convenience, we introduce the time subscript from the outset, as it will be useful in the empirical application where we will be using panel data.

[10] The grid-cell is the finest geographical unit for which we have data on temperatures. It coincides with an area of 0.1deg^2, which corresponds approximately to 121km^2. This is approximately the size of Turin (130km^2) and $1/10th$ the size of Rome ($1,285\text{km}^2$). Section 3 describes the data in more detail.

where Y_{it} is the output of firm i, $e^{d_{it}(T_{g(i)t})}$ is a *temperature-dependent demand shifter* with $T_{g(i)t}$ being the temperature in a grid-cell g, and σ denotes the elasticity of substitution between varieties. The notation $g(i)$ means that the grid-cell g varies for different firms i. The presence of a temperature-dependent demand shifter, $e^{d_{it}(T_{g(i)t})}$, suggests that temperature changes in a given grid-cell can influence the demand faced by firms within that cell. Note that, since temperature fluctuations are spatially correlated across grid-cells, in our empirical analysis we show that our results are robust to using spatially adjusted standard errors based on the method proposed by Conley (2010). Furthermore, the functional form assumed for $d_{it}(T_{g(i)t})$, along with other temperature-dependent variables in the model, allows for the possibility that factors beyond grid-cell-level temperature may also affect demand. Section 4 details the specific functional forms used in the empirical analysis.

We denote by P_{it} the price of firm i and by P_t the price of aggregate output Y_t.[11] The demand faced by each firm i is given by

$$Y_{it} = \left(e^{d_{it}(T_{g(i)t})}\right)^{\sigma-1} \left(\frac{P_{it}}{P_t}\right)^{-\sigma} Y_t. \tag{2}$$

The production function of each firm is Cobb-Douglas in productivity, capital, labor, and materials:

$$Y_{it} = e^{z_{it}(T_{g(i)t})} \prod_{X \in \mathcal{X}} X_{it}^{\alpha^X}, \quad \text{with} \quad \sum_{X \in \mathcal{X}} \alpha^X = 1, \tag{3}$$

where $e^{z_{it}(T_{g(i)t})}$ is the *temperature-dependent productivity* for firm i in grid-cell g and $\mathcal{X} \equiv \{K, L, M\}$ with K being capital, L being labor, and M being materials. The term, $e^{z_{it}(T_{g(i)t})}$, implies that temperature changes in a given grid-cell may impact the productivity of firms operating within that cell. Under the Cobb-Douglas production function assumption, this term captures different forms of productivity, including both labor-augmenting and capital-augmenting productivity.

The problem of a firm is given by

$$\begin{aligned} \Pi_i &= \max_{\{P_{it}, Y_{it}\}} P_{it} Y_{it} - \mathcal{C}(Y_{it}), \\ \text{s.t.} \quad Y_{it} &= \left(e^{d_{it}(T_{g(i)t})}\right)^{\sigma-1} \left(\frac{P_{it}}{P_t}\right)^{-\sigma} Y_t; \end{aligned} \tag{4}$$

[11] P_t is a CES aggregate of firm level prices P_{it}, as defined by equation 50 in Appendix A

where

$$\mathcal{C}(Y_{it}) = \min_{X} \left\{ \sum_{X \in \mathcal{X}} e^{\tau_{it}^{X}(T_{g(i)t})} P_t^X X_{it} \quad \middle| \quad Y_{it} - e^{z_{it}(T_{g(i)t})} \prod_{X \in \mathcal{X}} X_{it}^{\alpha^X} \right\}, \tag{5}$$

where $e^{\tau_{it}^{X}(T_{g(i)t})}$ are *temperature-dependent input-specific wedges* for firm i in grid-cell g and P_t^X is the price of input X.

The model highlights two types of temperature-related effects: direct and indirect. The *direct* effect of temperature is represented by the temperature-dependent demand and productivity terms. The former captures potential changes in demand patterns across firms, as reported in Busse et al. (2015) for the case of durable goods purchases. The latter encompasses a range of effects. For example, recent research reviewed by Heal and Park (2016) and Lai et al. (2023) demonstrates that extreme temperatures impair labor productivity by affecting health, labor supply, and concentration.[12] Extreme heat may also reduce capital productivity, as suggested by case studies indicating that machines such as cell phones, data centers, cars, and lithium-ion batteries become less efficient at high temperatures (e.g., Garimella et al., 2023).

The *indirect* effect of temperature in the model is summarized by reduced-form wedges, as in Restuccia and Rogerson (2008) and Hsieh and Klenow (2009), representing frictions that affect the marginal products or costs of specific inputs, such as adjustment costs, spatial, and financial frictions. These frictions may be directly influenced by temperature, affecting the reduced-form wedge. Even if not directly impacted, their presence can constrain the adjustment of inputs in response to temperature-induced changes in demand or productivity, which would still manifest as changes in the wedges. For instance, in response to the direct effect of extreme temperatures reducing demand or productivity, frictions that limit capital adjustment may cause some firms to hold excess capital but not labor or materials, resulting in a higher capital wedge without corresponding increases in labor or material wedges. Our objective is to estimate how these wedges respond to temperature changes and quantify their impact on aggregate productivity.

Profit maximization yields the standard condition that the firm's output price is a fixed markup over its marginal cost:

$$P_{it} = \mathcal{M} \cdot \mathcal{C}'(Y_{it}), \tag{6}$$

[12] Additional evidence is provided by Gould et al. (2024) and Filomena and Picchio (2024) for Italy, while Somanathan et al. (2021) shows reduced productivity and increased absenteeism in Indian manufacturing plants during hot days.

where $\mathcal{M} \equiv \sigma/(\sigma-1)$. The solution of the minimization problem is given by

$$\mathcal{C}(Y_{it}) = \prod_{X \in \mathcal{X}} \left(\frac{e^{\tau_{it}^X(T_{g(i)t})} P_t^X}{\alpha^X} \right)^{\alpha^X} \frac{Y_{it}}{e^{z_{it}(T_{g(i)t})}}. \tag{7}$$

Combining equations (2), (6), and (7), firm i sales can hence be expressed just as a function of the primitives of the model as

$$P_{it}Y_{it} = \left(e^{\tilde{z}_{it}(T_{g(i)t})}\right)^{\sigma-1} \left(\mathcal{M} \prod_{X \in \mathcal{X}} \left(\frac{e^{\tau_{it}^X(T_{g(i)t})} P_t^x}{\alpha^X} \right)^{\alpha^X} \right)^{-(\sigma-1)} P_t^\sigma Y_t, \tag{8}$$

with

$$e^{\tilde{z}_{it}(T_{g(i)t})} \equiv e^{d_{it}(T_{g(i)t})} e^{z_{it}(T_{g(i)t})}, \tag{9}$$

where $e^{\tilde{z}_{it}(T_{g(i)t})}$ is defined through the rest of the paper as the firm level *temperature-dependent demand-adjusted productivity*, and combines the firm productivity and the demand shifter responses to temperature. Taking logarithms in equation (8) we recover the following log-linear relation:

$$\begin{aligned} p_{it}y_{it} = (\sigma-1) &\left(\tilde{z}_{it}(T_{g(i)t}) - \sum_{X \in \mathcal{X}} \alpha^X \tau_{it}^X(T_{g(i)t}) \right) \\ &- (\sigma-1) \left(\mu + \sum_{X \in \mathcal{X}} \alpha^X \left(p_t^X - \log \alpha^X \right) \right) + \sigma p_t + y_t, \end{aligned} \tag{10}$$

with lowercase letters indicating logarithms. $p_{it}y_{it}$ is the logarithm of sales for firm i in period t. In Section 4, we explain how we estimate an empirical counterpart of equation (10). Unlike the existing literature that has conducted similar regressions, our theoretical framework has the advantage of identifying the various channels through which temperature shocks impact firm-level revenues. More specifically, sales may respond to temperature because this can affect (i) the firm demand-adjusted productivity through $\tilde{z}_{it}(T_{g(i)t})$ or (ii) the input-specific wedges through $\tau_{it}^X(T_{g(i)t})$. Formally, the temperature-semielasticity of sales is given by

$$\frac{\partial p_{it}y_{it}}{\partial T_{g(i)t}} = (\sigma-1) \left(\frac{\partial \tilde{z}_{it}(T_{g(i)t})}{\partial T_{g(i)t}} - \sum_{X \in \mathcal{X}} \alpha^X \frac{\partial \tau_{it}^X(T_{g(i)t})}{\partial T_{g(i)t}} \right) \tag{11}$$

Equation (11) shows that, conditional on a measure of the elasticity of substitution between varieties, σ, and the production function elasticities, α^X, if one can measure the temperature-

semielasticity of the input-specific wedges, $\frac{\partial \tau_{it}^X(T_{g(i)t})}{\partial T_{g(i)t}}$, then the temperature-semielasticity of the demand-adjusted productivity, $\frac{\partial \tilde{z}_{it}(T_{g(i)t})}{\partial T_{g(i)t}}$, can be recovered. If this is not the case, however, one would incorrectly attribute the effect of temperature on input-specific wedges to demand-adjusted productivity.

Thus, to estimate the effect of temperature on input-specific wedges we note that the optimality conditions of our model imply that individual input demand is given by:

$$e^{\tau_{it}^X(T_{g(i)t})} P_t^X X_{it} = \alpha^X \mathcal{C}(Y_{it}), \quad \forall X \in \mathcal{X}, \tag{12}$$

which can be rearranged, using equation (6), as

$$MRPX_{it} \equiv \alpha^X \frac{P_{it} Y_{it}}{X_{it}} = \mathcal{M} e^{\tau_{it}^X(T_{g(i)t})} P_t^X. \tag{13}$$

Taking logarithms in equation (13) we recover the following log-linear relation:

$$\log MRPX_{it} = \tau_{it}^X(T_{g(i)t}) + \mu + p_t^X. \tag{14}$$

Equations (13) and (14) have two important insights. First, conditional on the production function elasticity α^X, the revenue-based marginal product of input X ($MRPX$) of firm i can be measured just by observing firm-level sales $P_{it}Y_{it}$ and firm-level input quantities $X_{it} \in \{K_{it}, L_{it}, M_{it}\}$. Second, in equilibrium the effect of temperature on $\log MRPX_{it}$ only depends on its input-specific wedge $\tau_{it}^X(T_{g(i)t})$, and not on the other input-specific frictions.[13] Hence, having the necessary data to empirically measure firm-level sales and $MRPX$, we can use equations (10) and (14) to estimate the temperature-semielasticity of sales and of input-specific wedges, and then use equation (11) to recover the temperature-semielasticity of the demand-adjusted productivity. We provide a detailed procedure for this in Section 4.

[13] It also depends on the logarithm of the markup, μ, and of the input price, p_t^X. Regarding the latter, to the extent that its variations are similar across all firms in a given industry, they are absorbed by sector-year effects in our empirical specification. Regarding the former, assuming a CES aggregator in our model rules out any direct effect of temperature on markups. However, while this channel might be accommodated by the temperate-dependent input-specific wedges, in the empirical analysis in Section 5 we find no *prima facie* effect of temperature on the revenue-based marginal product of materials and labor (which are common measures of firm-level markups used by the literature; see Loecker and Warzynski, 2012), validating the CES assumption. Furthermore, the empirical specification of equation (14) will further generalize this formula to account for other potential factors.

2.2 Aggregate Variables

To quantify the effects of temperature on aggregate productivity—and thereby trace the aggregate damage function central to IAMs—we use changes in the Solow residual as a proxy for changes in aggregate productivity. Appendix A reports the details of all the calculations.

Before introducing the Solow residual in our framework, we demonstrate that aggregate gross output TFP can be expressed as

$$TFP_t = \frac{Y_t}{\prod_{X \in \mathcal{X}} X_t^{\alpha^X}}, \tag{15}$$

$$= \left(\sum_{i=1}^{N_t} \left(e^{\tilde{z}_{it}(T_{g(i)t})} \right)^{\sigma-1} \prod_{X \in \mathcal{X}} \left(e^{\tau_{it}^X (T_{g(i)t})} \right)^{-(\sigma-1)\alpha^X} \right)^{\frac{\sigma}{\sigma-1}}$$

$$\times \prod_{X \in \mathcal{X}} \left(\sum_{i=1}^{N_t} \frac{\left(e^{\tilde{z}_{it}(T_{g(i)t})} \right)^{\sigma-1}}{e^{\tau_{it}^X (T_{g(i)t})}} \prod_{X \in \mathcal{X}} \left(e^{\tau_{it}^X (T_{g(i)t})} \right)^{-(\sigma-1)\alpha^X} \right)^{-\alpha^X}; \tag{16}$$

with $X_t = \sum_{i=1}^{N_t} X_{it}$ standing for real aggregate capital, labor, and materials.

Similarly to Hsieh and Klenow (2009) and Gopinath et al. (2017), we can use equation (16) to also recover the upper bound of aggregate gross output TFP in this economy. This is obtained by equalizing all input-specific wedges $e^{\tau_{it}^X (T_{g(i)t})}$ across firms. The resulting expression is given by

$$TFP_t^* = \left(\sum_{i=1}^{N_t} \left(e^{\tilde{z}_{it}(T_{g(i)t})} \right)^{\sigma-1} \right)^{\frac{1}{\sigma-1}}. \tag{17}$$

Equation (17) represents the upper bound of aggregate TFP in a counterfactual, frictionless scenario, reminiscent of the aggregate productivity in Melitz (2003). Throughout the paper, we refer to this counterfactual, frictionless measure of aggregate TFP as "efficient"—a term commonly used in the literature, albeit with some flexibility in its interpretation.[14]

Equations (16) and (17) show that conditional on the elasticity of substitution between varieties σ and the production function elasticities α^X, aggregate gross output TFP and its efficient counterpart are just a function of two measurable objects: $e^{\tilde{z}_{it}(T_{g(i)t})}$ and $e^{\tau_{it}^X (T_{g(i)t})}$. Given our framework, the firm-level demand-adjusted productivity $e^{\tilde{z}_{it}(T_{g(i)t})}$ can be expressed

[14] While we label this counterfactual TFP as efficient, we refrain from using it for normative assessments. This is because it may not always lie within the set of achievable allocations. For instance, if some frictions in the data arise from technological constraints like adjustment costs, this counterfactual TFP would be unattainable.

as

$$e^{\tilde{z}_{it}(T_{g(i)t})} = \left(\frac{(P_t Y_t)^{-\frac{1}{\sigma-1}}}{P_t} \right) \left(\frac{(P_{it} Y_{it})^{\frac{\sigma}{\sigma-1}}}{\prod_{X \in \mathcal{X}} X_{it}^{\alpha^X}} \right). \tag{18}$$

Thus, conditional on a measure of the elasticity of substitution between varieties σ and the production function elasticities α^X, equation (18) can be measured just with data on nominal aggregate output $P_t Y_t$, the aggregate price deflator P_t, firm-level sales $P_{it} Y_{it}$, and firm-level inputs X_{it}. Moreover, firm-level input-specific wedges $e^{\tau_{it}^X(T_{g(i)t})}$ can be measured using equation (13). Hence, using standard firm-level data and leveraging the structure of our framework, we can measure empirically each element in equations (16) and (17). By taking logs and fully differentiating equations (16) and (17), we derive expressions that relate changes in both aggregate gross output TFP and efficient aggregate gross output TFP to variations in grid-cell-level temperatures, resulting in:

$$\begin{aligned}
\Delta \log TFP_t &\equiv \Delta \log TFP_t \left(e^{\tilde{z}_{it}(T_{g(i)t})}, e^{\tau_{it}^X(T_{g(i)t})}, \Delta T_{g(i)t} \right) \\
&\approx \sum_{i=1}^{N_t} \lambda_{it} \sum_{X \in \mathcal{X}} \frac{\alpha^X}{e^{\tau_{it}^X(T_{g(i)t})}} \Omega_t^X \\
&\times \left[\left(\sigma \frac{e^{\tau_{it}^X(T_{g(i)t})}}{\Omega_t^X} - (\sigma - 1) \right) \left(\frac{\partial \tilde{z}_{it}(T_{g(i)t})}{\partial T_{g(i)t}} - \sum_{X \in \mathcal{X}} \alpha^X \frac{\partial \tau_{it}^X(T_{g(i)t})}{\partial T_{g(i)t}} \right) + \frac{\partial \tau_{it}^X(T_{g(i)t})}{\partial T_{g(i)t}} \right] \\
&\times \Delta T_{g(i)t},
\end{aligned} \tag{19}$$

and

$$\Delta \log TFP_t^* \equiv \Delta \log TFP_t^* \left(e^{\tilde{z}_{it}(T_{g(i)t})}, \Delta T_{g(i)t} \right) \approx \sum_{i=1}^{N_t} \lambda_{it}^* \frac{\partial \tilde{z}_{it}(T_{g(i)t})}{\partial T_{g(i)t}} \Delta T_{g(i)t}, \tag{20}$$

where $\lambda_{it} \equiv \lambda_{it} \left(e^{\tilde{z}_{it}(T_{g(i)t})}, e^{\tau_{it}^X(T_{g(i)t})} \right)$ and $\lambda_{it}^* \equiv \lambda_{it}^* \left(e^{\tilde{z}_{it}(T_{g(i)t})} \right)$ are firm-level weights, and $\Omega_t^X \equiv \Omega_t^X \left(e^{\tilde{z}_{it}(T_{g(i)t})}, e^{\tau_{it}^X(T_{g(i)t})} \right)$ is an aggregate object, all detailed in Appendix A.1.

Equations (19) and (20) represent a novel contribution of this paper, playing a central role in our analysis. These equations enable the calculation of *counterfactual* changes in aggregate TFP and TFP^* resulting from temperature variations at the grid-cell level, affecting both demand-adjusted productivity and input-related frictions. Notably, while these equations hold in general equilibrium, they require only data on the distribution of demand-adjusted productivity, $e^{\tilde{z}_{it}(T_{g(i)t})}$, input-specific wedges, $e^{\tau_{it}^X(T_{g(i)t})}$, and their corresponding semielas-

ticities, $\partial \tilde{z}_{it}(T_{g(i)t})/\partial T_{g(i)t}$ and $\partial \tau_{it}^{X}(T_{g(i)t})/\partial T_{g(i)t}$, without needing information on the effect of grid-cell-level temperatures on aggregate prices. Therefore, this approach avoids reliance on estimating the effects of grid-cell-level temperatures on aggregate prices, circumventing the well-known "missing intercept" problem in cross-sectional data. Finally, while the data requirements may appear substantial, the distributions of demand-adjusted productivity and input-specific wedges can be derived using equations (13) and (18), and the semielasticities, central to our empirical analysis, are detailed in Section 4.

We now have all the necessary elements to decompose the change in aggregate gross output TFP into two components: an efficient component and a component associated with input-related frictions. The final expression for the changes in aggregate gross output TFP is as follows:

$$\Delta \log TFP_t = \underbrace{\Delta \log TFP_t^*}_{\Delta \text{ Technology}} - \underbrace{(\Delta \log TFP_t^* - \Delta \log TFP_t)}_{\Delta \text{ Allocative Efficiency}}. \tag{21}$$

The Δ Technology term captures changes in TFP^*, as described in equation (20). Intuitively, it reflects the changes in aggregate TFP driven by the effect of temperature on demand-adjusted productivity, $e^{\tilde{z}it(Tg(i)t)}$, in an economy without allocative frictions—where aggregate output cannot be increased by reallocating inputs across firms. This term isolates the direct impact of temperature on firm-level demand and productivity.

The Δ Allocative Efficiency term captures deviations from the efficient allocation, reflecting the impact of temperature shocks on aggregate TFP through changes in allocative efficiency. This term is influenced by changes in both demand-adjusted productivity, $e^{\tilde{z}_{it}(T_{g(i)t})}$, and input-specific wedges, $e^{\tau_{it}^{X}(T_{g(i)t})}$. While changes in the latter directly indicate shifts in firm-level resource allocation relative to a counterfactual frictionless benchmark, and thus affect aggregate allocative efficiency, changes in the former impact aggregate allocative efficiency only if the economy's initial allocation is distorted by frictions. For instance, if firms with inefficiently high levels of inputs experience a temperature shock that reduces their demand-adjusted productivity, it not only diminishes the Δ Technology term but also decreases the Δ Allocative Efficiency term by pushing their allocation of inputs even further from the frictionless optimum. However, this effect is not always negative. Temperature-induced changes in demand-adjusted productivity can either enhance or diminish aggregate allocative efficiency, depending on the initial distribution of input-specific wedges and inputs. Thus, this term is the outcome of the indirect effect due to the presence of frictions and echoes the covariance argument between wedges and productivity highlighted in the misallocation

literature (e.g., Gopinath et al., 2017) and ultimately remains a quantitative question.

Until now, our analysis has not required explicit assumptions about the supply of aggregate inputs. However, because our focus is on the impact of climate change on the Solow residual—defined in terms of value-added—we modify (21) accordingly, as detailed in Appendix A.2. In brief, this adjustment assumes that aggregate labor and capital are in fixed supply, while the use of the final good as materials introduces a simple roundabout production structure, as described in Jones (2011) and Baqaee and Farhi (2020). This results in the following measure for changes in the Solow residual:

$$\Delta \log Solow_t \approx \frac{Y_t}{GDP_t} \left(\Delta \log TFP_t^* - \left(\Delta \log TFP_t^* - \Delta \log TFP_t \right) \right), \tag{22}$$

where Y_t is gross output and GDP_t is value-added, i.e., gross output net of materials.

Equation (22) shows that the impact of climate change on the Solow residual exceeds its effect on gross output TFP due to a multiplier effect equal to the ratio of gross output to GDP. This arises from the roundabout nature of material production, where materials are produced using output. Initial productivity losses reduce output, which subsequently lowers material production, further constraining output. This feedback loop amplifies the initial productivity losses, creating a multiplier mechanism.

Therefore, to compute the counterfactual impact of climate change on aggregate productivity and decompose it into a technology component and a component related to allocative efficiency, we simultaneously utilize equations (19), (20), and (22).

3 Data

This section presents the two main data sources used for the empirical analysis.

3.1 Firm-Level Data

The Italian firm-level data is obtained from Orbis, provided by Bureau van Dijk between the years 1999-2013. Orbis offers harmonized cross-country financial information for both private and public firms collected from various national data sources, primarily business registers. The dataset covers, on average, 75 percent of the official Italian gross output reported in Eurostat. One major advantage of Orbis over other datasets is that it includes many small private firms. In fact, Kalemli-Özcan et al. (2024) show that Orbis closely mimics the official size distribution reported in Eurostat Structural and Business Statistics (SBS). The cleaning process follows

Kalemli-Özcan et al. (2024) and Gopinath et al. (2017) and is explained in Appendix B.

The final dataset includes information on approximately 4.3 million observations corresponding to 1 million firms. We measure sales (PY) by operating revenue, materials (M) by expenditure on materials, labor (L) by the cost of employment, and capital (K) by the book value of tangible fixed assets. All monetary values are deflated using Eurostat two-digit industry price deflators, and capital is deflated using the country-specific price of investment from the World Development Indicators. The dataset also includes the primary sector of economic activity at the four-digit industry level and, importantly, firm-level zip codes, enabling geolocation. This geolocation is used to link the data to the climate variables.

We compute the marginal revenue product of input $X \in L, M, K$ using equation (13), with α^X, the elasticity of output with respect to X, measured via the cost shares approach (Foster et al., 2008) and taking the median firm-level cost share within each four-digit industry (De Loecker et al., 2020) to address measurement error and adjustment frictions.[15] The production function elasticities are given by $\alpha^M = \text{med}\left\{\frac{P_t^M M_{it}}{r_t K_{it}+W_t L_{it}+P_t^M M_{it}}\right\}$, $\alpha^L = \text{med}\left\{\frac{W_t L_{it}}{r_t K_{it}+W_t L_{it}+P_t^M M_{it}}\right\}$, $\alpha^K = 1-\alpha^L-\alpha^M$, where $r_t K_{it}$ is the rental cost of tangible capital, $W_t L_{it}$ is the wage bill, and $P_t^M M_{it}$ is the expenditure on materials.[16] We recover median production function elasticities $\{\alpha^X\}_{X\in\{M,L,K\}}$ equal to $\{0.53,\ 0.36,\ 0.11\}$, well within the range found by the literature.[17] For instance, Gandhi et al. (2020) reports values for materials, labor, and capital ranging from 0.50-0.67, 0.22-0.52, and 0.04-0.16, respectively.

3.2 Climate Data

The meteorological data are sourced from Copernicus, the European Union's flagship Earth Observation Programme, using E-OBS, a daily gridded land-only observational dataset for Europe.[18] For further details, see Cornes et al. (2018) and Appendix B.2.1. This dataset is constructed using observations from National Meteorological and Hydrological Services (NMHSs) and other data-holding institutions across Europe. It incorporates contributions from 84 organizations and includes data collected from over 23,000 meteorological stations. Additional

[15] We use the production function elasticities both to calculate the aggregate counterfactual based on equation (19) and to compute the revenue-based marginal products in equation (13). For the latter, since our regression framework includes firm and sector-time fixed effects, these elasticities are absorbed into the error term and are therefore not required to identify the temperature-semielasticity of each revenue-based marginal product.

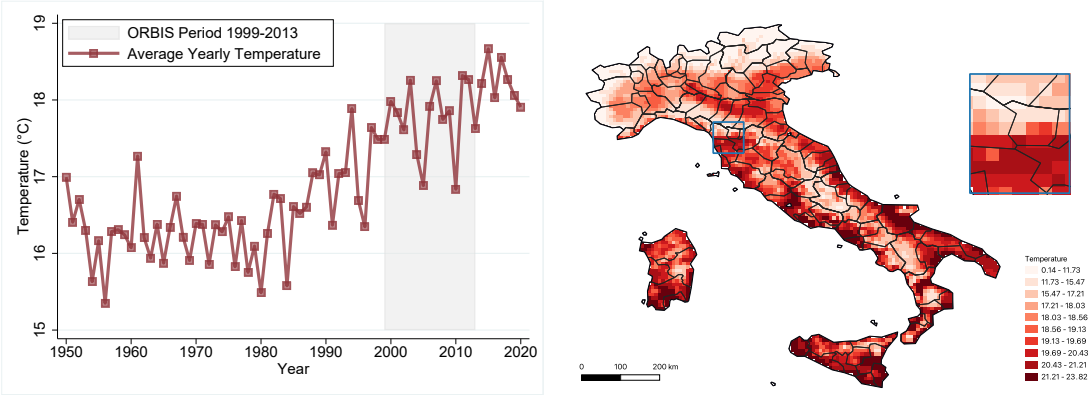
[16] We measure the user cost of capital as $r_t = i_t - \mathbb{E}_t\pi_{t+1} + \delta + RP$. We use the real interest, $i_t - \mathbb{E}_t\pi_{t+1}$, from Gopinath et al. (2017), a depreciation rate, δ, of 10% as usually done in the literature, and a risk premium, RP, of 5% as calculated in Caballero et al. (2017).

[17] The inclusion of aggregate median elasticities in the text serves the sole purpose of facilitating a meaningful comparison with the existing literature. However, in the calculations, only the sector-level elasticities are used.

[18] See https://doi.org/10.24381/cds.151d3ec6.

information on the dataset's high station coverage is provided in Appendix B.2.2.

Figure 1: Average Yearly Temperature



(a) 1950-2020 Trend **(b) 1999 Cross Section**

Note. Figure 1a shows the evolution of the average yearly temperature in Italy between 1950-2020. The grey areas show the time frame (1999-2013) for which Orbis data is available. Figure 1b shows the average yearly temperature across all the grid-cells in Italy in 1999. It also plots regional boundaries at the NUTS 3 level.

We use daily temperature and rainfall data with a horizontal grid resolution of 0.1° (approximately 11 km × 11 km, or 121 km^2), covering the period 1950–2020. Temperatures are recorded in degrees Celsius (°C), and rainfall is measured in millimeters (mm). Following Somanathan et al. (2021), daily temperature is represented by the maximum temperature, which typically occurs during working hours and serves as a proxy for heat exposure during peak economic activity. Rainfall is recorded as total daily precipitation, including rain, snow, and hail, expressed as the equivalent height of liquid water per square meter. While our primary variable of interest is temperature, rainfall is included as a control variable in the empirical analysis, as detailed in Section 4.

Figure 1a shows the evolution of the average yearly maximum temperature over the entire sample period. The average yearly maximum temperature is volatile and rising over time. Table 1 presents summary statistics for our climate data during the period 1999–2013, which corresponds to the subperiod for which firm-level data is available and forms the basis of our analysis. Summary statistics for the entire sample period are provided in Table B.2 in Appendix B.2.3. Additionally, Figure 1b illustrates the average yearly temperature in 1999 for each grid cell, overlaid with the boundaries of NUTS 3 regions in Italy. The average yearly temperature ranges from 0.14°C to 23.82°C, highlighting substantial variation across grid cells and regions. This pronounced temperature heterogeneity makes Italy an exceptional setting for studying the economic impacts of climate change. The coexistence of wide temperature gradients and diverse locations of economic activity—from production sites in colder areas like

the Alps to warmer coastal regions—provides a unique opportunity to analyze firm responses to varying climatic conditions.

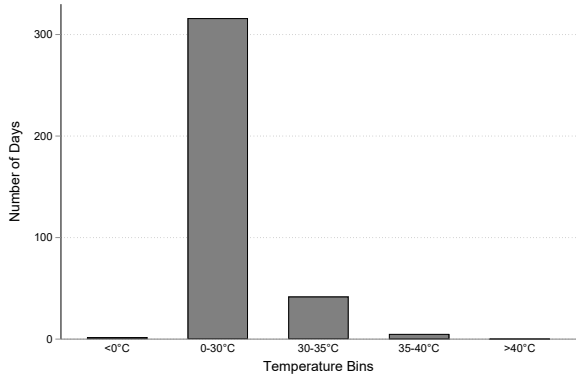
Table 1: Summary Statistics of Climate Data (1999-2013)

	Overall		Within Grid-Cell	
	Temperatures (°C)	Rainfalls (mm)	Temperatures (°C)	Rainfalls (mm)
Mean	17.74	2.28	17.74	2.28
Median	17.65	0.00	17.51	1.01
Min	-24.94	0.00	0.35	0.00
Max	43.71	258.40	33.62	26.99

Note. Table 1 shows summary statistics of temperature in degrees Celsius (°C) and rainfalls in millimeters (mm) for the period 1999-2013. The first two columns report statistics for the overall sample. The last two columns report statistics on the variation within the average grid-cell, that is, they show the average temperature distribution among the different grid-cells.

Our main empirical specification follows Somanathan et al. (2021), aggregating daily temperatures to the annual level by counting the number of days falling within specific temperature bins, as introduced by Deschênes and Greenstone (2011). We use the following bins: $\{(-\infty, 0°\text{C}], (0°\text{C}, 30°\text{C}], (30°\text{C}, 35°\text{C}], (35°\text{C}, 40°\text{C}], (40°\text{C}, +\infty)\}$. To summarize the yearly temperature distribution, we construct a vector $\boldsymbol{T} = \{T^1, T^2, T^3, T^4, T^5\}$, which counts the number of days in each bin for every grid cell and year. These non-overlapping bins fully capture the observed temperature distribution, with more bins at the high end to assess the economic impact of future climate change. In Section 5, we present a robustness exercise using a smaller benchmark bin, specifically $(15°\text{C}, 30°\text{C}]$. Additionally, we consider two alternative specifications for daily maximum temperatures: one based on a degree-day approach and another using a quadratic formulation of daily maximum temperatures.

Figure 2: Average Distribution of Days Within Temperature Bins



Note. Figure 2 shows the number of days per year within each temperature bin of the vector $\boldsymbol{T}$. We construct this figure averaging across all grid-cells and years.

Figure 2 shows the distribution of days within each temperature bin of the vector $\boldsymbol{T}$ av-

eraged across grid-cells and years. Most of the days clearly belong to the $[0°\text{C}, 30°\text{C})$ range, which we will use as the reference bin in the regression framework. Importantly, all temperature bins have a non-zero average number of days. Table B.3 in Appendix B.3 reports summary statics for the distribution of days within each temperature bin across grid-cells.

3.3 Main Combined Data

To construct our final dataset, we merge firm-level data from Orbis with temperature data from Copernicus by assigning each firm to a specific grid cell in the Copernicus dataset. The Copernicus data includes latitude and longitude for its grid cells. We determine each firm's geographical coordinates in Orbis using their reported postcode to the business registry. Postcodes act as unique identifiers for specific locations, enabling precise localization. To convert postcodes into geographical coordinates, we use the Python package "pgeocode."[19] Using the firms' coordinates and the latitude and longitude of the Copernicus grid cells, we assign each firm to its nearest grid cell by calculating the minimum distance between the two.

One limitation of our data is that we only have information on the firm's headquarters address, with no details about production plant locations. For firms whose headquarters are in a different grid cell than their production plants, temperature data may be incorrectly assigned—a scenario more likely for large, multi-plant firms. However, in our sample of Orbis-Italian firms, only 1% are publicly listed, 3–4% are foreign-owned, and 2% have consolidated financial statements, suggesting that such firms represent a small minority. Robustness checks confirm that these cases do not drive our results. Furthermore, if production locations are misassigned to grid cells, the firm's response to the incorrectly assigned temperature would likely be weaker or negligible, biasing our results downward. This implies a conservative bias in our estimates, offering a more benign interpretation of this potential source of mismeasurement.

4 Empirical Strategy

This section outlines our empirical approach to identifying the effects of temperature on firm-level demand-adjusted productivity and input-specific wedges.

In Section 2, we left the temperature-dependent factors as unspecified functions. Here, we specify the functional forms used in the empirical analysis for demand-adjusted productivity and input-specific wedges. Specifically, we assume that firm-level outcomes and input-

[19] The pgeocode package (https://pypi.org/project/pgeocode/) utilizes data from GeoNames (https://www.geonames.org), an open-source project providing detailed postal code and location information.

specific wedges consist of a temperature-dependent component, $F(T_{g(i)t})$, and a temperature-independent component, $\boldsymbol{W}_{it}$, such that:

$$e^{\tilde{z}_{it}(T_{g(i)t})} \equiv e^{F^{\tilde{z}}(T_{g(i)t})+G^{\tilde{z}}(\mathbf{W}_{it})}, \tag{23}$$

$$e^{\tau^X_{it}(T_{g(i)t})} \equiv e^{F^{\tau^X}(T_{g(i)t})+G^{\tau^X}(\mathbf{W}_{it})}, \quad \text{with} \quad \forall X \in \mathcal{X}; \tag{24}$$

where $F(\cdot)$ is a non-linear function of temperature in the grid-cell to which firm i belongs and $G(\mathbf{W}_{it})$ is a function of alternative explanatory variables. Thus, to measure the effect of changes in temperature on firm-level outcomes, we estimate the following equation:

$$Outcome_{it} = \sum_{\ell} \beta_\ell T^{\ell}_{g(i)t} + \delta Rain_{g(i)t} + \boldsymbol{\lambda'}\mathbf{X}_{r(i)t} + \gamma_{s(i)t} + \alpha_i + \varepsilon_{it}, \tag{25}$$

where i denotes a firm, t stands for year and $g(i)$ denotes the grid-cell to which firm i belongs. $Outcome_{it}$ denotes log firm-level outcomes or log revenue-based marginal product of a given input X, $\log MRPX_{it}$. We approximate the non-linear temperature function $F(\cdot)$ by the variable $T^{\ell}_{g(i)t}$, denoting number of days in temperature bin ℓ, that each grid cell $g(i)$ experienced during a given year (see Section 3.2 for a description). We set the interval $[0°\text{C}, 30°\text{C})$ as the reference temperature bin since it covers the average temperature faced by most grid-cells in our data. For robustness, as detailed in Section 5, we use two alternative specifications for $F(\cdot)$: a degree-day measure and a quadratic specification of daily maximum temperatures.

$G(\mathbf{W}_{it})$ includes potential confounding factors at the firm, grid-cell, region, and sector level. Outcome variables may also respond to other climate factors related to temperature. To address this, we include $Raing(i)t$, which represents the average yearly rainfall in each grid cell. For robustness, Section 5 introduces a nonlinear specification of rainfall, similar to $F(\cdot)$, to account for rainfall nonlinearity and the potential effects of floods, the primary extreme weather event in Italy caused by heavy precipitation. We include firm fixed effects (α_i) to control for unobserved time-invariant characteristics at the firm level. To account for regional shocks, we add regional trends, $\mathbf{X}r(i)t$, which include time trends at the NUTS 2 regional level ($r(i)$ indicates the region of firm i) and dummies for the Great Recession (2008–2009) and the Sovereign Debt Crisis (2012–2013), reflecting the uneven regional impact of these crises in Italy. Similarly, to control for sectoral and aggregate productivity trends, we include sector-time fixed effects ($\gamma s(i)t$), where $s(i)$ denotes the NACE 4 sector of firm i. These fixed effects capture sector-specific and broader economic fluctuations. Standard errors are clustered at the grid-cell level to account for potential serial correlation that could downwardly bias the

estimates. To further address spatial autocorrelation in weather patterns, as highlighted by Auffhammer et al. (2013), we include a robustness check in Section 5 using spatially adjusted standard errors based on the method proposed by Conley (2010).

The regression specification given by equation (25) is the empirical counterpart of equations (10) and (14). The coefficient of interest is β_ℓ, which captures the effect of an extra day into the temperature bin ℓ relative to the reference temperature bin. Thus, $\beta_\ell < 0$ implies that the given firm-level outcome declines β_ℓ percent for each extra day into the temperature bin ℓ relative to the reference temperature bin. Our coefficient of interest, β_ℓ, is identified by comparing firms with similar time-invariant characteristics that experience the same grid-cell rainfall levels, regional development trends, exposure to the Great Recession (GR) and Sovereign Debt Crisis (SDC), and sectoral dynamics but are exposed to different grid-cell temperature changes over time. The key identification assumption is that, after controlling for regional and sectoral fixed effects, temperature fluctuations are exogenous to any other time-varying factors influencing demand, productivity, or inputs.

There are at least three potential challenges to the validity of our results, but as we explain below, these challenges do not fully align with our findings and would likely bias our estimates downward. First, there is the possibility of a contemporaneous shock that affects both temperatures and productivity simultaneously. For example, regions experiencing a surge in economic activity might face increased congestion or pollution, leading to both a rise in temperatures and a decline in productivity. However, this explanation does not fully align with our findings, as we observe output decreases directly linked to elevated temperatures. A second identification challenge arises from shocks that influence both productivity and its responsiveness to temperature. For instance, higher firm unionization might lead to tougher bargaining discussions, including grievances about working under extreme temperatures. In this scenario, there is a potential for overestimating the impact of temperatures, as it may also encompass the effects of unionization itself. However, by controlling for sector-year fixed effects and considering that these phenomena are widespread across all firms in a sector, concerns should be mitigated. Third, if firms could accurately anticipate temperature increases at the grid-cell level and choose their locations accordingly, this could introduce selection bias. To address this, we include regional trends in our analysis, allowing us to estimate deviations from these trends and capture the effects of unanticipated temperature shocks. This approach suggests that our estimates are best interpreted as short- to medium-run elasticities.

5 Results

In this section, we present the firm-level effects of temperature on several objects of interest and we discuss potential channels and heterogenous effects.

5.1 Sales, Inputs, and Marginal Revenue Products

We estimate the effect of temperature on firm-level outcomes using the regression specification outlined in equation (25). We estimate the effect of temperature on sales and its impact on firms' inputs—materials, labor, and capital—to better understand the response of marginal revenue products of inputs. Columns 1-4 of Table 2 report the results.

Table 2: Average Effect of Temperature on Sales and Inputs

	Output / Expenditure Variables				**Marginal Revenue Products**		
Dependent Variable	**Sales**	**Materials**	**Labor**	**Capital**	**MRPM**	**MRPL**	**MRPK**
	(1)	(2)	(3)	(4)	(5)	(6)	(7)
Temperature bins							
$(-\infty, 0℃]$	-0.094^{***}	-0.068^{**}	-0.070^{***}	-0.036^{*}	-0.018	0.008	-0.030
	(0.019)	(0.029)	(0.019)	(0.021)	(0.019)	(0.013)	(0.022)
$(30℃, 35℃]$	-0.017^{*}	-0.022	0.002	0.003	0.006	-0.012^{**}	-0.014
	(0.009)	(0.014)	(0.007)	(0.010)	(0.008)	(0.006)	(0.010)
$(35℃, 40℃]$	-0.046^{***}	-0.060^{**}	-0.003	0.004	0.011	-0.021	-0.045^{**}
	(0.017)	(0.025)	(0.016)	(0.019)	(0.014)	(0.013)	(0.021)
$(40℃, +\infty)$	-0.807^{***}	-0.557^{**}	-0.369^{**}	0.033	-0.209	-0.019	-0.578^{**}
	(0.194)	(0.242)	(0.187)	(0.217)	(0.156)	(0.145)	(0.231)
Fixed effects							
Firm	✓	✓	✓	✓	✓	✓	✓
Sector × Year	✓	✓	✓	✓	✓	✓	✓
GR and SDC × Region	✓	✓	✓	✓	✓	✓	✓
Controls							
Rainfall	✓	✓	✓	✓	✓	✓	✓
Region trends	✓	✓	✓	✓	✓	✓	✓
Observations	4,687,524	4,687,524	3,767,578	4,328,710	4,687,524	3,767,578	4,328,710

Note. All dependent variables are in logs. Temperature bins are constructed as explained in Section 3.2. Rows 1-4 present the effect on the log of the dependent variable of adding an extra day in the given temperature range respectively. Standard errors are clustered at the grid-cell level and reported in parentheses. *, **, and *** denote 10, 5, and 1% statistical significance respectively.

The estimates reveal that temperature has an inverted U-shaped effect on sales, materials, and labor, indicating that extreme temperatures, whether high or low, tend to suppress these firm-level outcomes. For instance, one additional day above 40 degrees Celsius is estimated to reduce sales by 0.807%, while one extra day below 5 degrees Celsius decreases sales by 0.094%.[20] These losses are measured relative to the reference temperature bin $[0°\text{C}, 30°\text{C})$.

[20] Assuming production is evenly distributed across all effective working days in a year (approximately 220 in Italy, accounting for 250 working days minus 30 holidays), an extra day above 40 degrees Celsius equates to

The response of capital, however, is notably weaker, particularly at higher temperatures. This is significant for our analysis, as it suggests that while materials and, to a lesser extent, labor exhibit substantial and meaningful responses to extreme temperatures, capital adjustments are minimal, consistent with the widely recognized view that capital is subject to greater adjustment frictions compared to materials and labor.

We next estimate the effect of temperature on the firm-level revenue-based marginal product of each input using the regression specification in equation (25). The results, shown in columns 5-7 of Table 2, reveal an inverted U-shaped relationship between temperature and revenue-based marginal products, which is statistically significant and substantial only for $MRPK$. This indicates that extreme temperatures—whether high or low—reduce the revenue-based marginal product of capital. Specifically, an additional day above 40℃ decreases $MRPK$ by 0.578%, while an extra day below 5℃ reduces it by 0.030%. These findings are consistent with the patterns reported in Table 2. The results further show that $MRPM$ and $MRPL$ remain unaffected by temperature fluctuations, as materials and labor adjust in response to temperature changes to align with sales. In contrast, $MRPK$ is significantly impacted because capital adjustments are constrained, leaving firms with excess capital that cannot be reallocated effectively. This finding highlights the unique role of capital adjustment frictions and represents a novel contribution of our paper.[21]

The finding that materials are flexible to adjust aligns with a large body of literature in firm dynamics, which identifies materials as the most flexible input. Moreover, the minimal impact of temperature on the $MRPL$ suggests that, despite Italy's traditionally rigid labor market institutions, firms demonstrate considerable flexibility in adjusting their labor input. This adaptability operates through both intensive margins (adjusting hours worked) and extensive margins (utilizing fixed-term contracts), the latter facilitated by labor market reforms since the mid-1990s (Caggese and Cuñat, 2008). This labor input flexibility allows firms to maintain optimal labor allocation even when facing temperature shocks. The finding that capital is difficult to adjust aligns with the extensive literature on capital adjustment costs (e.g., Cooper and Haltiwanger, 2006). Our analysis shows a significant decline in $MRPK$ during high-temperature episodes. While factors such as increased cooling needs or temporary shutdowns might be expected to raise $MRPK$, we observe the opposite. This reflects

nearly a two-day loss in sales ($100 \times 2/220 \approx 0.807$), and an extra day below 5 degrees Celsius corresponds to about a one-third-day loss in sales ($100 \times 0.3/220 \approx 0.094$).

[21] The model assumes no unemployed inputs. Thus, when firms reduce labor and material inputs due to temperature shocks, these inputs are assumed to be reallocated to more productive uses within the year. While some inputs may remain temporarily unemployed in reality, affecting aggregate output, this has less relevance for aggregate productivity, which is the primary focus of our analysis.

the quasi-fixed nature of capital investments and the associated adjustment costs: firms are unable to efficiently scale down capital inputs during temporary production declines, leading to a reduced output-to-capital cost ratio.

Our main results are robust to various concerns and alternative specifications. Table C.4 in Appendix C.1 demonstrates that splitting the $(0°\text{C}, 30°\text{C}]$ range into smaller bins—$(0°\text{C}, 15°\text{C}]$ and $(15°\text{C}, 30°\text{C}]$—produces estimates consistent with the benchmark specification. Tables C.5 and C.6 in Appendix C.1 confirm the robustness of our findings under alternative regression specifications. First, we control for firm age, a well-documented determinant of firm heterogeneity (Fort et al., 2013), and find no changes to our results. Second, we test alternative temperature specifications, including a piecewise linear model based on degree days (Somanathan et al., 2021) and a quadratic model of daily maximum temperatures (Dell et al., 2012; Burke et al., 2015). Third, we include a specification with nonlinear rainfall controls to account for the effects of precipitation and floods. Finally, we address spatial autocorrelation by adjusting standard errors using the method of Conley (2010), allowing for dependence within radii of 80 km and 150 km.[22] Across all robustness checks, our findings remain consistent with the benchmark results reported in this section.

Finally, we show that our results are robust across various sample cuts. First, Tables C.7 and C.8 in Appendix C.2 present additional specifications to evaluate the sensitivity of our estimates to firms potentially assigned incorrect temperatures, as discussed in Section 3.3. These specifications exclude specific types of firms, such as foreign firms, listed firms, firms reporting consolidated accounts, and large firms, with the exclusion criteria detailed in Appendix C.2. Crucially, our analysis shows that the inclusion or exclusion of these firms does not affect our estimates, indicating that the concerns raised in Section 3.3 about potentially misclassified firms do not materially impact our findings. Second, we address the issue of differing sample sizes due to limited data availability for employment measures. As shown in Tables C.7 and C.8 in Appendix C.2, ensuring consistency in the number of observations across variables does not alter the patterns presented in this section.

5.2 Demand-Adjusted Productivity

Having estimated the effects of temperature on both sales and the revenue-based marginal product of inputs, we leverage the structural framework and equation (11) to recover the impact of temperature on firm-level demand-adjusted productivity. In Section 5.3.1, we fur-

[22] These radii are a conservative choice, as Italy spans approximately 549 km x 549 km, totaling 301,340 km^2.

ther detail how we disentangle demand effects from productivity effects. Importantly, the effect of temperature on the revenue-based marginal product not only offers novel evidence of a previously underexplored channel through which extreme temperatures affect firms but also enables a more accurate measurement of demand-adjusted productivity. Neglecting this channel would lead to an underestimation of the temperature effect, as noted in equation (11).

To compute these estimates, we require the elasticity of substitution across varieties, denoted as σ, and the production function elasticities, α^X. For the latter, we use the elasticities described in Section 2, and assume an elasticity of substitution $\sigma = 4$ between varieties. This value implies an average cost-weighted markup of 33 percent, consistent with estimates from De Loecker et al. (2020) and our own for Italy, where we find a materials cost-weighted markup of 27 percent. It also aligns with the mean value reported by Broda and Weinstein (2006).[23] This elasticity estimate is further supported by both firm-level and macroeconomic studies. For instance, Bernard et al. (2003) report a value of $\sigma = 3.79$ in a firm-level export model, while Christiano et al. (2015), using a New-Keynesian model with financial frictions, estimate $\sigma = 3.78$. Additionally, we obtain the temperature-semielasticities of sales and revenue-based marginal products from Table 2, and we set the temperature-semielasticity of $MRPM$ and $MRPL$ to zero as they are statistically insignificant and small.[24]

Table 3 summarizes the effect of temperature on demand-adjusted productivity, under the parameters specified above. Notice that the temperature-semielasticities of the demand-adjusted productivity vary across sectors as production function elasticities are sector-specific. Thus, we report both an unweighted average and a sales-weighted average across sectors.[25]

Table 3: Average Effect of Temperature on Demand-Adjusted Productivity

	Temperature Bins			
	$(-\infty, 0°C]$	$(30°C, 35°C]$	$(35°C, 40°C]$	$(40°C, \infty)$
Variable				
β^z_ℓ, unweighted	-0.031	-0.005	-0.021	-0.337
β^z_ℓ, weighted	-0.031	-0.005	-0.019	-0.321

Note. Table 3 reports the temperature-semielasticity for demand-adjusted wedges for each temperate bin. Temperature bins are constructed as explained in Section 3.2. Row 1 reports the unweighted average across sectors. Row 2 reports the sales-weighted average across sectors.

We observe that the temperature-semielasticity of demand-adjusted productivity exhibits the previously identified inverted U-shaped pattern. This result is not entirely unexpected, as

[23] Based on three-digit goods (SITC-3) data over the period 1990–2001.

[24] We do the same for the calculation implemented in Section 6.

[25] Table C.9 in the appendix C.4 shows how the effect of temperature on demand-adjusted productivity varies across sectors. High capital intensive sectors experience larger losses.

equation (11) shows that this semielasticity is a linear combination of the earlier ones, subject to rescaling. Quantitatively, our analysis indicates that an additional day with temperatures exceeding 40 degrees Celsius decreases demand-adjusted productivity by 0.337 percent, while an additional day with temperatures below 0 degrees Celsius reduces it by 0.031 percent. These findings highlight the significant impact of extreme temperatures—both high and low—on demand-adjusted productivity as reflected in the data.

5.3 The Demand Channel and Adaptation Effects

This section investigates potential differences between tradable and non-tradable sectors, shedding light on the roles of demand versus efficiency. Additionally, it explores the possibility of firm adaptation to climate change.

5.3.1 Demand versus Productivity

Although the model does not require separating demand from productivity to conduct the aggregate counterfactual analysis in equation (21), we aim to understand which of these two margins is more affected by temperature. To this end, we extend our empirical strategy to disentangle the effects of temperature on firms' demand and productivity. While firms operating in a specific area are likely to experience similar productivity impacts from extreme temperatures, we observe that firms producing tradable goods are less exposed to local temperature-related demand shocks, as a significant portion of their demand originates from outside the local market, potentially from abroad.[26] Therefore, if temperature changes occur in the grid cell where their production is located, these firms' productivity will be affected. However, their demand will remain either unaffected or less affected, as they do not rely heavily on sales within that grid cell.

Thus, we set to identify the effect of temperature on demand and productivity separately using the following regression specification:

$$\begin{aligned} Outcome_{it} = &\sum_{\ell} \beta_{1,\ell} T^{\ell}_{g(i)t} + \delta_1 Rain_{g(i)t} + \boldsymbol{\lambda_1'} \mathbf{X}_{r(i)t} \\ &+ \left(\sum_{\ell} \beta_{2,\ell} T^{\ell}_{g(i)t} + \delta_2 Rain_{g(i)t} + \boldsymbol{\lambda_2'} \mathbf{X}_{r(i)t} \right) \times I^{NT}_{s(i)} + \gamma_{s(i)t} + \alpha_i + \varepsilon_{it}, \end{aligned} \tag{26}$$

[26] For instance, the lower demand sensitivity of sales for firms producing tradable goods has been empirically documented by Almunia et al. (2021) during the Great Recession. Furthermore, examining this dimension in our data is a natural choice, given that a significant proportion of Italian firms engage in the production of tradable goods and exporting, as highlighted by Caggese and Cuñat (2013).

where $I^{NT}_{s(i)}$ is an indicator function that takes the value of one if firm i belongs to sectors s selling non-tradable goods, as described below, and the other variables are described in the main specification in Section 4. In this specification, the estimated coefficients $\beta_{1,\ell}$ capture the temperature-semielasticity of sales, which is common to firms both in the tradable and non-tradable sectors and that therefore captures common productivity effects. Instead, the coefficients $\beta_{2,\ell}$ reflect the differential impact of temperature on firms in the non-tradable sector, which we interpret as the semielasticity of the demand effect.

We employ three distinct measures to classify firms into tradable and non-tradable sectors. First, based on the World Input-Output Database (WIOD), we identify tradable sectors as those where the proportion of exports in total value-added for each NACE 2-digit sector in Italy exceeds the median. Recognizing that tradability involves more than international trade, we further identify firms whose goods and services are predominantly locally demanded. To achieve this, we employ two additional metrics. First, we use the classification provided by Gervais and Jensen (2019) which utilizes a dataset on the distribution of output and demand across regions of the United States to construct measures of trade costs for nearly a thousand service and manufacturing industries.[27] Secondly, we adapt the tradability measure from Mian and Sufi (2014), which links high regional employment concentration to greater tradability. Using a similar approach, we measure the geographical (NUTS 2) concentration of each NACE 2 sector in Italy, defining a sector as tradable if its wage bill concentration exceeds the median.

Table 4 presents the results. Column 1 reports the estimated average effect of temperature on sales, as shown in Table 2. Columns 2 to 4 provide (i) the coefficient for the common effect of temperature on sales across both tradable and non-tradable sectors and (ii) the coefficients for the additional effect of temperature on sales in non-tradable sectors, capturing the demand effect. In Column 2, tradable sectors are defined as those with a proportion of exports in total value-added above the median, based on WIOD data for each NACE 2-digit sector. Column 3 uses the tradability measure from Gervais and Jensen (2019), while Column 4 applies the tradability measure from Mian and Sufi (2014) using Italian data.

We observe that the interaction coefficient is largely insignificant and modest across intervals, except for the $(35°\text{C}, 40°\text{C}]$ interval, where it is negative in two out of three specifications. Conversely, the common coefficient for extreme temperatures is highly significant, substantial in size, and similar to the average effect. These findings suggest that non-tradable firms are only slightly more affected by temperature, indicating a minor but nonzero role of temperature in demand and a more substantial impact on productivity. This does not contra-

[27] We thank Antoine Gervais for sharing his data with us.

Table 4: Effect of Temperature on Sales of Tradable versus Non-Tradable Sectors

Dependent Variable	**Sales** (1)	**Sales** (2)	**Sales** (3)	**Sales** (4)
Temperature Bins				
$(-\infty, 0°C]$	-0.094***	-0.090***	-0.096***	-0.113***
	(0.019)	(0.024)	(0.024)	(0.026)
$(30°C, 35°C]$	-0.017*	-0.006	-0.006	-0.025**
	(0.009)	(0.009)	(0.011)	(0.010)
$(35°C, 40°C]$	-0.046***	-0.017	-0.013	-0.024
	(0.017)	(0.019)	(0.020)	(0.021)
$(40°C, +\infty)$	-0.807***	-0.758***	-0.835***	-1.046***
	(0.194)	(0.260)	(0.297)	(0.310)
Temperature Bins$\times I^{NT}_{s(i)}$				
$(-\infty, 5°C]$		-0.006	0.005	0.032
		(0.030)	(0.026)	(0.029)
$(30°C, 35°C]$		-0.019	-0.016	0.014
		(0.015)	(0.012)	(0.012)
$(35°C, 40°C]$		-0.049*	-0.046*	-0.036
		(0.027)	(0.023)	(0.023)
$(40°C, +\infty)$		-0.087	0.022	0.385
		(0.352)	(0.357)	(0.383)
Fixed Effects				
Firm	✓	✓	✓	✓
Sector × Year	✓	✓	✓	✓
GR and SDC × Region	✓	✓	✓	✓
Controls				
Rainfalls	✓	✓	✓	✓
Region Trends	✓	✓	✓	✓
Observations	4,687,524	4,684,661	4,593,020	4,687,524

Note. All dependent variables are in logs. Temperature bins are constructed as explained in Section 3.2. The variable $I^{NT}_{s(i)}$ is an indicator set to one if firm i belongs to a non-tradable sector s, as described in Section 3. Column 2 defines tradable sectors using WIOD, where exports exceed the median proportion of total value-added for NACE 2-digit sectors. Column 3 applies the tradability measure from Gervais and Jensen (2019), while Column 4 adapts Mian and Sufi (2014)'s measure to Italy using wage bill data. Rows 1-4 show the effect on log sales of an additional day in each temperature range. Rows 5-8 show the additional effect on log sales for non-tradable goods. Standard errors are clustered at the grid-cell level and reported in parentheses. *, **, and *** denote 10, 5, and 1% statistical significance respectively.

dict the view that customer demand for certain goods, particularly durables, varies with daily weather (e.g., Busse et al., 2015), but suggests that such variations may be offset over the year, reducing the annual effect. Consequently, our results indicate that most of the temperature effect on the demand-adjusted productivity wedge stems from its impact on productivity.[28]

5.3.2 Adaptation

In the next section, we use the estimates presented in Section 5.1 to predict the aggregate productivity effects of temperature increases due to climate change. For this purpose, considering adaptation is important, as neglecting the fact that firms adopt climate-mitigating

[28] This aligns with existing literature highlighting the influence of temperature on labor productivity, as reviewed by Pankratz and Schiller (2024) and Lai et al. (2023), with additional evidence for Italy provided by Gould et al. (2024) and Filomena and Picchio (2024).

measures in response to climate change may lead to overestimating the overall effect.[29]

We build on recent literature on adaptation, including Auffhammer (2018), Heutel et al. (2021), Carleton et al. (2022), and Nath (2024), by exploiting variation in long-term climate exposure. Firms in different regions experience distinct climates, not only in average temperature but also in variability. Greater exposure to extreme temperatures may lead to differing adaptation patterns and temperature semielasticities. We examine the impact of operating in grid cells with varying exposure to extreme temperatures, arguing that regional adaptation is better modeled based on temperature variability rather than averages. This is very relevant in Italy, where coastal areas often have higher average temperatures but fewer extreme heat events compared to inland regions. Our findings align with earlier estimates showing that firms are more affected by extreme temperatures than by small deviations from the average. To test this hypothesis we estimate the following regression:

$$\begin{aligned} Outcome_{it} = &\sum_{\ell} \beta_{1,\ell} T^{\ell}_{g(i)t} + \delta_1 Rain_{g(i)t} + \boldsymbol{\lambda_1'} \mathbf{X}_{r(i)t} \\ &+ \left(\sum_{\ell} \beta_{2,\ell} T^{\ell}_{g(i)t} + \delta_2 Rain_{g(i)t} + \boldsymbol{\lambda_2'} \mathbf{X}_{r(i)t} \right) \times I^{H}_{g(i)} + \gamma_{s(i)t} + \alpha_i + \varepsilon_{it}, \end{aligned} \tag{27}$$

where $I^{H}_{g(i)}$ is an indicator set to one if firm i operates in adapted grid-cells g, defined as those experiencing more extreme temperatures during the year, and the other variables are described in equation (25).[30] The full results are show in Table C.10 in the appendix. We find significant differences in the effects of extremely high temperatures. One additional day over 40 degrees causes a reduction in sales by 1.86 percent in non-adapted regions, and only by 0.78 percent in adapted regions. Firms in adapted regions also experience a lower fall in their marginal return to capital, although this coefficient is imprecisely estimated. Conversely, we find smaller and insignificant effects of adaptation regarding the exposure to high but less extreme temperatures. Overall, we take these results as suggestive evidence of relatively small adaptation effects, broadly in line with those found in the literature (Nath, 2024).

[29] Note that our model and empirical strategy already incorporate two aspects of adaptation. First, the model allows for input reallocation, with empirical evidence showing materials and labor respond to temperature changes, while capital does not. Second, since firm-level data are annual and temperature measures are daily, actions firms take to boost production in response to temperature increases during the year, such as extending working hours during cooler periods, are already captured in our semielasticities.

[30] Specifically, we define extreme days as those with maximum temperatures above 30 degrees or below 0 degrees. For each location and year, we calculate the ratio of days with extreme temperatures to days with moderate temperatures (maximum daily temperatures between 0 and 30 degrees). Adapted locations are those with an average yearly ratio over the sample period exceeding the national mean. We also consider as robustness check locations above the national median.

6 Aggregate Effects

This section documents the aggregate productivity losses resulting from various warming scenarios and highlights their heterogeneous regional impact.

6.1 Aggregate Productivity Loss

While our reduced-form estimates indicate that climate change reduces firm-level productivity and the revenue-based marginal product of capital, they do not reveal whether these effects significantly impact aggregate productivity. To assess this, we estimate the effect of climate change on the Solow residual, a proxy for aggregate productivity, using equations (19), (20), and (22), which we restate compactly as:

$$\Delta \log Solow_t \approx \frac{Y_t}{GDP_t}\Bigg(\underbrace{\Delta \log TFP_t^* \left(e^{\tilde{z}_{it}(T_{g(i)t})}, \Delta T_{g(i)t} \right)}_{\Delta \text{Technology}} - \underbrace{\left(\Delta \log TFP_t^* \left(e^{\tilde{z}_{it}(T_{g(i)t})}, \Delta T_{g(i)t} \right) - \Delta \log TFP_t \left(e^{\tilde{z}_{it}(T_{g(i)t})}, e^{\tau_{it}^X(T_{g(i)t})}, \Delta T_{g(i)t} \right) \right)}_{\Delta \text{Allocative Efficiency}} \Bigg). \tag{28}$$

Equation (28) indicates that to quantify the counterfactual effect of climate change on aggregate productivity, we require: (i) the demand-adjusted productivity $e^{\tilde{z}_{it}(T_{g(i)t})}$ and the temperature-semielasticity; (ii) input-specific wedges $e^{\tau_{it}^X(T_{g(i)t})}$ and the temperature-semielasticity; and (iii) counterfactual changes in grid-cell-level temperatures $\Delta T_{g(i)t}$. For the elasticity of substitution between the varieties σ and the production function elasticities α^X we use the same values as in Section 5.2. We next turn to explain how we use the empirical results from Section 5 to measure each of these elements.

6.1.1 Measurement and Identification

Demand-adjusted productivity. We compute demand-adjusted productivity in the data using equation (18). For the temperature-semielasticity of the demand-adjusted productivity, we follow the calculations in Section 5.2 as reported in Table 3.

Input-specific wedges. We compute input-specific wedges with our firm-level data using equation (13) as explained in Section 3. To calculate the temperature-semielasticity of the input-specific wedges we use the findings from Section 5.1 and proceed as follows: (i) we set the temperature-semielasticity of labor and materials inputs to zero, as no significant effects

of temperature were observed (see columns 4-6 of Table 2), and (ii) we use the estimated temperature-semielasticity of capital input from Table 2.

6.1.2 Counterfactual changes in grid-cell-level temperatures.

As mentioned in the introduction, the estimation of aggregate productivity losses from climate change requires a two step procedure. Until now we have described the first step, the estimation of the temperature-semielasticities of demand-adjusted productivity and of production inputs. The second step requires applying these estimates to counterfactual changes in grid-cell-level temperatures under different climate change scenarios.

These scenarios are complex: i) They involve mean temperature changes; ii) They involve changes in the dispersion of temperatures; iii) These mean and dispersion changes might apply differently to the different damage channels identified in the previous sections. While existing studies typically only consider (i), one novel aspect of this paper is to consider carefully also (ii) and (iii), as explained in details below.

i) Our benchmark case for the change in mean temperatures is the RCP4.5 scenario from the Copernicus EURO-CORDEX climate model, which offers the advantage of capturing heterogeneous temperature increases across different regions (NUTS3) within Italy, aligning closely with realistic climate change models.[31] We also consider the more extreme RCP8.5 scenario from the same model. The RCP4.5 and RCP8.5 scenarios imply average mean temperature increases across Italy, in 2071–2099 compared to 1981–2010, of approximately 2℃ and 4℃, respectively (Evin et al., 2021). As robustness checks we consider threee alternative scenarios in which temperature increases uniformly across regions by $1°C$, $2°C$ and $4°C$. We refer to the counterfactual experiments that incorporate these changes in the distribution of mean temperatures as **Mean Shift (MS)**.

ii) There is wide consensus among leading climate scientists that future increases in mean temperatures will be accompanied by more frequent extreme temperature events. The influential Sixth Assessment Report of the Intergovernmental Panel on Climate Change shows that an extreme temperature event that was occurring once every 50 years pre-1900, is now 4.8 times more likely and it will become 13.9 times more likely if average global temperature increases additionally by $2°C$ (IPCC, 2021). Fischer and Schär (2010) show for Europe a projected substantial increase in temperature variability beyond the simple increase in mean temperatures.

[31] For a summary description of the RCP scenarios, see https://climate.copernicus.eu/sites/default/files/2021-01/infosheet3.pdf. For a more detailed description of the predictions for the EURO-CORDEX climate model, see Evin et al. (2021)

Our finding of a U-shaped relation between temperatures fluctuations and climate damages implies that changes in dispersion matter beyond the effect of the mean changes, and therefore it is important to take them into account. To disentangle these two components, we define a set of **Mean Preserving (MP)** experiments in which we keep the mean of the temperature distribution constant while we change its variability. Consistent with the projections in Fischer and Schär (2010), we assume that temperature dispersion increases by 0.08 for every additional degree increase in mean temperatures. Finally we define a set of **Full** experiments, in which we change both the mean and variability of the temperature distribution.

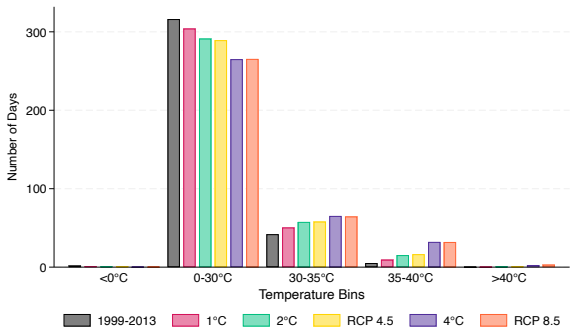
Figure 3 shows the average counterfactual distributions of days within each temperature bin across grid cells. The subfigures report the average annual number of days in each bin for the baseline period (1999–2013) and for warming scenarios that shift mean daily temperatures upward (for example, by 1℃, 2℃, or 4℃), increase variability while keeping the mean unchanged, or combine both effects. Details on the construction of these counterfactual distributions are provided in Appendix D.1.1.

iii) Finally, we consider how these mean and dispersion changes might apply differently to the efficiency and allocative damage channels identified in the previous sections. In particular, equation (28) clarifies that overall losses are composed of the "ΔTechnology" term, which measures the predicted direct effects on productivity, and "ΔAllocative Efficiency" which measures the predicted indirect allocative effects. In the Mean Preserving ("MP") counterfactuals, we isolate the impact of increased temperature variability by holding the mean constant. This implicitly assumes the economy fully adapts to permanent shifts in average temperatures, such that residual economics damages arise solely from larger fluctuations around the mean. This assumption is arguably too extreme when measuring the direct "ΔTechnology" term, and the literature typically assumes no or only partial adaptation when projecting economic damages from future changes in mean temperatures.

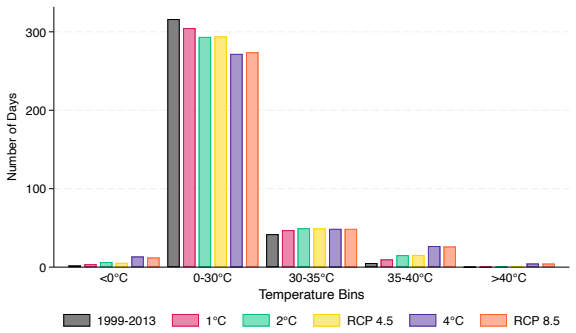
However, this assumption is desirable when projecting the economic damages of the "ΔAllocative Efficiency" channel, as this channel quantifies short-term allocation problems caused by local temperature shocks. If temperature dispersion increases, then these losses are expected to rise, while they should not be affected by long-run gradual increases in mean temperatures, since capital can fully reallocate to the most productive locations over time.

Therefore, in our benchmark projections– referred to as "**Long-run**"– we apply the "Full" distribution of temperature changes when computing "ΔTechnology", and only the increase in dispersion from the "MP" distribution when computing "ΔAllocative Efficiency". In other words, allocative efficiency losses arise solely from greater temperature variability, whereas

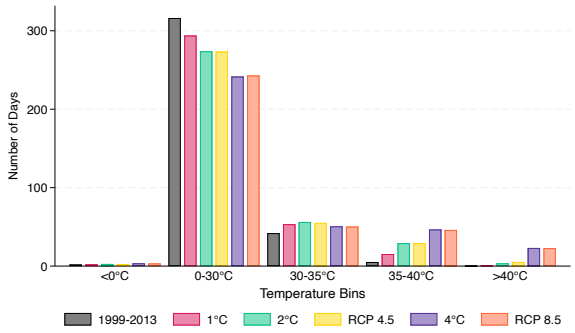
Figure 3: Counterfactual Average Distribution of Days Within Temperature Bins



(a) Mean Shift (MS) distributions



(b) Mean Preserving (MP) distributions



(c) Full distributions

Note. Figure 3 shows the average number of days per year within each temperature bin of the vector $\boldsymbol{T}$. In Figure 3a, we compare distributions with mean-shift in daily temperature: the first column (grey) reports the data for the period 1999-2013. The second column (pink) reports the warming scenario where the daily temperature increases by 1℃. The third column (green) reports the warming scenario where the daily temperature increases by 2℃. The fourth column (orange) reports the warming scenario from the RCP4.5, where temperature increases by approximately 2℃. The fifth column (blue) reports the warming scenario where the daily temperature increases by 4℃. The sixth column (red) reports the warming scenario from the RCP8.5, where temperature increases by approximately 4℃. In Figure 3b, we compare the distributions with mean-preserving spread of the daily temperature while keeping mean the same. In Figure 3c, we compare the distributions, we compare distribution with the combined effect of the increase in the mean and higher standard deviation in the daily temperatures.

technology losses reflect the combined effects of both the mean shift and increased variability on direct productivity.

6.1.3 Results

Table 5 quantifies the aggregate productivity losses resulting from climate change across various climate scenarios, distinguishing between the effects of pure technology ("ΔTechnology") and changes in allocative efficiency ("ΔAllocative Efficiency").

In Panel A, row 3 shows the results for our benchmark "RCP4.5 Long-run" scenario described in the previous section. Aggregate productivity declines by 4.23 percent. In economic terms, this equates to a GDP loss of about 89.17 billion USD in 2021, based on Italy's GDP of

approximately 2.108 trillion USD that year.[32] 81 percent of the overall effect is caused by firm-level productivity reductions, with allocative efficiency declines accounting for 21 percent.

Row 1 and row 2 of Panel A show the separate results for the scenarios that either include only mean temperature changes ("MS") or only dispersion changes ("MP"). Compared to Row 3, Row 1 shows that losses are much smaller when considering only mean temperature changes, which highlights the importance of considering also the temperature variability component of climate change.

Panel C repeats the analysis in Panel A adding adaptation. We use our estimates in Table C.10, which show adapted regions have significantly lower temperature elasticity of sales than non-adapted regions for extreme ($\geq$ 40°) temperatures. When computing aggregate productivity losses with adaptation, we first predict which regions will become adapted in the future based on their new counterfactual temperature distributions. Then, we apply the adaptation-adjusted elasticities for sales while holding other parameters constant. We find that, under the baseline warming scenario of RCP4.5, aggregate productivity losses amount to 3.35 percent in the long run – 21 percent lower than the losses under no adaptation. Therefore, our results suggest adaptation offers only limited protection against future productivity losses.

Panels B and D repeat the analysis with and without adaptation for the RCP8.5 scenario. Results underscore the nonlinear and convex nature of climate change's impact on productivity losses. While average temperature increases are only about twice as large as in the RCP4.5 scenario, aggregate productivity losses are more than four times greater – amounting to 17.81 percent without adaptation and 14.97 percent with adaptation. This pattern is partly explained by the inverted U-shaped relationship between temperature and firm-level economic outcomes documented in Section 5, whereby a linear increase in hot days results in a convex rise in productivity losses. Moreover, as average temperatures rise, climate change significantly increases the number of regions exposed to extreme heat. As shown in Table D.11 in the appendix, the average number of +40℃ days per year rises from 0.04 to 5.21 in the RCP4.5 scenario and surges to 22.67 in the RCP8.5 scenario, see Table D.14.

Finally, to demonstrate that our findings are not driven by the specific scenarios considered, Table D.15 in Appendix D.2 reports aggregate damages under three alternative warming scenarios: 1℃, 2℃ and 4℃. In the 1℃ "long-run" scenario with adaptation, aggregate productivity losses amount to 1.15 percent, rising to 4.36 percent under the 2℃ scenario and to 18.59 percent under the 4℃ scenario.

[32] To calculate the GDP loss, we multiply the 2021 Italian GDP in US dollars (2.108 trillion US dollars) by the percentage loss (4.23 percent): 0.0423×2.108 trillion US dollars = 89.17 billion US dollars.

Taken together, the results in Table 5 provide several important insights. Relative to existing studies, our approach identifies substantially larger negative effects of temperature fluctuations on firm productivity for a country with a temperate climate like Italy, as discussed in greater detail in Section 6.2. An important portion of these larger effects is explained by two additional factors typically omitted from micro-founded economic models of aggregate climate damages. First, climate change projections point not only to shifts in average temperatures but also to increases in the frequency of extreme events and in temperature dispersion. Second, there are indirect costs caused by reductions in allocation efficiency. We highlight that while this latter channel, by construction, applies only to temperature dispersion, it still generates substantial additional losses across all scenarios.[33]

Finally, note that our framework is static. While this choice has advantages, it does not account for the extensive margin, such as firm entry and exit, due to limited data on these dynamics. Neglecting this margin likely biases our results through two channels. First, unproductive firms in affected regions may exit, improving firm selection. Second, firms in these regions might close and relocate their capital to cooler areas, enhancing long-term allocative efficiency (although we find limited evidence for this in our sample). These additional channels might potentially dampen the magnitude of our aggregate productivity effects from climate change, but exacerbate the regional inequality effects we document in Section 6.3.

6.2 Discussion

In this section, we highlight the benefits of a model-based approach for estimating the aggregate effects of temperature on productivity. We compare our findings with existing literature and address the main caveats of our approach, acknowledging its limitations and suggesting areas for future research.

6.2.1 Advantage of Theory-Based Aggregation of Firm-Level Climate Damages

As discussed, a key advantage of our approach is its closed-form expression, which links micro-level temperature effects to aggregate productivity outcomes.

To illustrate the added value of our framework in assessing aggregate productivity losses

[33] To our knowledge, only two other studies perform empirical analyses related to these factors, separately. Regarding the first, Bettarelli et al. (2025) use quarterly data on U.S. public firms from Compustat to analyze the response of firms' investment decisions to temperature uncertainty, measured as the standard deviation of daily temperatures within quarters. Regarding the second, Liu and Xu (2024) estimate the impact of extreme temperatures on the dispersion of marginal revenue products of capital at the industry level across several countries.

Table 5: Effect of Climate Change on Aggregate Productivity

	ΔTotal	ΔTechnology	ΔAllocative Efficiency
Panel A: RCP4.5			
RCP4.5 MS	1.64%	0.85%	0.78%
RCP4.5 MP	2.14%	1.24%	0.90%
RCP4.5 Long-run	4.23%	3.33%	0.90%
Panel B: RCP8.5			
RCP8.5 MS	5.35%	2.75%	2.60%
RCP8.5 MP	7.04%	4.10%	2.93%
RCP8.5 Long-run	17.81%	14.88%	2.93%
Panel C: RCP4.5 + Adaptation			
Adaptation MS	1.38%	0.66%	0.72%
Adaptation MP	1.67%	0.92%	0.76%
Adaptation + Long-run	3.35%	2.59%	0.76%
Panel D: RCP8.5 + Adaptation			
Adaptation MS	4.29%	2.06%	2.23%
Adaptation MP	5.59%	3.18%	2.41%
Adaptation + Long-run	14.97%	12.56%	2.41%

Note. This table reports the percentage losses in aggregate productivity due to climate change. Column 1 reports total productivity losses (ΔTotal), while columns 2 and 3 decompose these into losses from within-firm technology reductions (ΔTechnology) and misallocation (Δ Allocative Efficiency). Panels differ by temperature scenario and model assumptions: **RCP Scenarios:** Use Representative Concentration Pathways where RCP4.5 is approx. 2℃ and RCP8.5 is approx. 4℃ increase in average temperature, respectively. **RCP4.5 MS:** Assumes a mean-shift (MS) in temperature. "MP" consider mean-preserving spread to capture increased variability. "Long-run" assumes allocative efficiency effects due to mean shifts in temperature are zero and Δ technology captures both mean shifts and variability effects. **Adaptation:** includes adaptation effects captured by the regression model in Equation 27. Comparisons across rows isolate the effect of average temperature increases, variability increases, and the combination of the average + variability increases. We assume $\beta = 0.08$, where a 1°C increase in mean temperature increases the standard deviation in temperature distribution by $\beta * 100$ percent.

from climate change, we compare our results with best practices from firm-level studies (e.g., Zhang et al., 2018, Somanathan et al., 2021). These studies typically apply estimated firm-level productivity losses directly to a mean-shift in temperature, calculating the following simple average:

$$\overline{\widehat{\Delta \tilde{z}_{it}}} = \sum_{i=1}^{N_t} \frac{\widehat{\Delta \tilde{z}_{it}}}{N_t}, \quad \text{where} \quad \widehat{\Delta \tilde{z}_{it}} \equiv \frac{\partial \tilde{z}_{it}(T_{g(i)t})}{\partial T_{g(i)t}} \Delta T_{g(i)t}. \tag{29}$$

We consider the RCP4.5 warming scenario ("MS") that is closest to the approach followed in the papers mentioned above. Applying the formulae as in Equation 29 to our empirical estimates results in a productivity decline of 0.39 percent. In contrast, our theory-based aggregation yields a decline of 1.64 percent—more than four times larger. This discrepancy can

be understood through the following decomposition within our framework:

$$\Delta \log Solow_t - \overline{\widehat{\Delta \tilde{z}_{it}}} = \underbrace{\left(\frac{Y_t}{GDP_t} - 1\right)\overline{\widehat{\Delta \tilde{z}_{it}}}}_{\text{Roundabout material production}} + \underbrace{\frac{Y_t}{GDP_t}\mathbb{C}\left(\lambda^*_{it}, \widehat{\Delta \tilde{z}_{it}}\right)}_{\text{Size and losses covariance}} - \underbrace{\frac{Y_t}{GDP_t}\left(\Delta \log TFP^*_t - \Delta \log TFP_t\right)}_{\Delta \text{ Allocative Efficiency}}, \tag{30}$$

where $\overline{\widehat{\Delta \tilde{z}_{it}}}$ and $\widehat{\Delta \tilde{z}_{it}}$ are defined in equation (29), and λ^*_{it} is defined in Section 2.

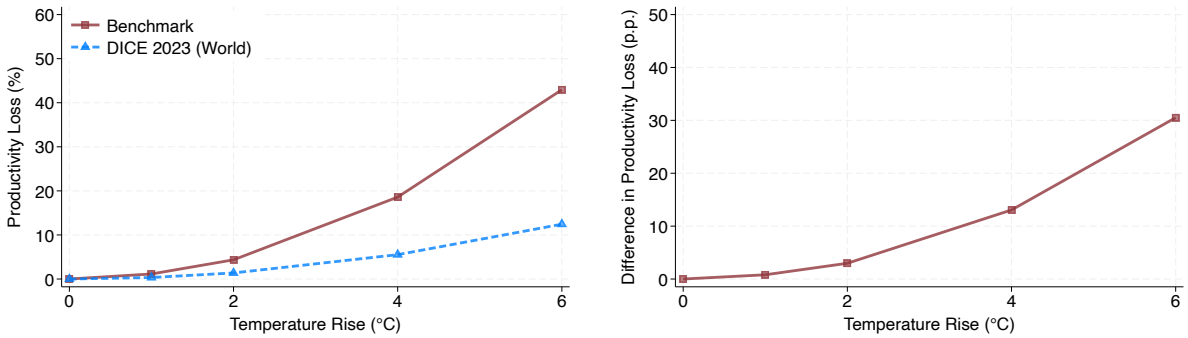
Three factors account for the difference between our theory-based approach and the reduced-form approach. First, the roundabout nature of material production acts as a multiplier, as described in Section 2. Greater material usage in the economy increases the ratio of Y_t/GDP_t, amplifying the difference between the two approaches. Second, the covariance between efficient firm-level weights and estimated productivity losses plays a role. When firm-level losses positively covary with firms' initial efficient sizes, the divergence becomes more pronounced. Finally, changes in allocative efficiency further amplify the difference, as this factor has not been accounted for in previous empirical studies. Overall, we find that the first term explains 29 percent of the difference, the second term 3 percent, and the third term 68 percent. In summary, while causal estimates of firm-level damages are valuable, a theory-based aggregation that incorporates multiple channels, general equilibrium effects, and amplification mechanisms is essential for accurately capturing the significant impact of climate change on aggregate productivity losses.

6.2.2 Comparison with the Literature

Figures 4a and 4b compare our aggregate productivity losses, to the damage functions used in the latest iteration of the DICE model by Barrage and Nordhaus (2023). This model serves as a benchmark, representing the standard calibration approach in the literature (e.g., Golosov et al., 2014, Krusell and Smith, 2022, Hassler et al., 2016, Fernández-Villaverde et al., 2024). Its global damage function is given by $0.003467 \times \Delta T^2$. Details of our productivity loss calculations are provided in Section 6.1.1.

The left figure shows productivity losses across different models, while the right figure highlights the differences between losses in our benchmark results, as well as the losses for the world from the DICE model, relative to our model with adaptation in the long run. All models display a convex, nonlinear relationship that steepens with higher temperature in-

Figure 4: Differences Across Productivity Loss Functions



(a) Productivity Loss Across Models **(b) Additional Losses relative to DICE 2023**

Note. Figure 4a compares productivity losses (in percent) due to temperature increases across three specifications: "Mean Shift" scenario that captures the change in average temperature. "Full" scenario combines mean-shift and variability in temperature together. "Adaptation + Long-run" scenario assumes allocative efficiency effects due to mean shifts in temperature are zero and includes adaptation effects captured by the regression model in Equation 27. In Figure 4b, we compare the "Adaptation + Long-run" losses with those of the losses from the DICE model adjusted for Europe).

creases. Recasting our results into the functional form of an aggregate damage function, our model implies a loss of $0.0145 \times \Delta T^2$. This indicates that productivity losses are larger in our framework, especially under more extreme climate change scenarios.

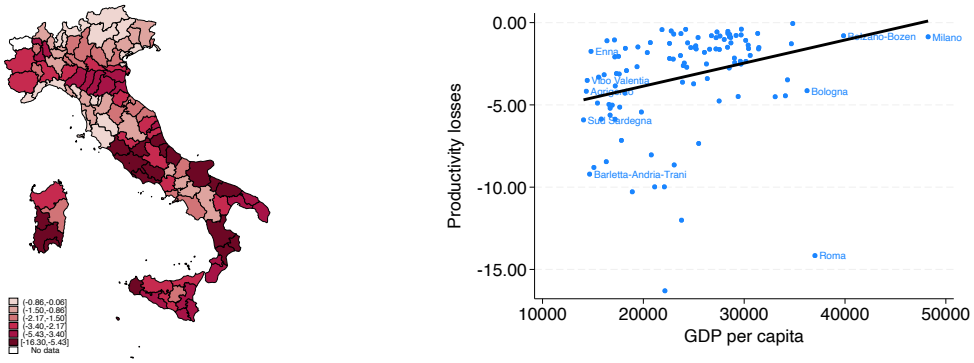
It is important to interpret the evidence presented here accurately. Our estimated losses are not intended as a superior proxy for the loss functions modeled in the above-mentioned studies. Those works aim to assess the overall economic impact of temperature increases across various channels, including changes in mortality, crop yields, coastal erosion, and labor supply. In contrast, our findings highlight significant losses from a single, largely independent channel, emphasizing the value of detailed micro-data in reassessing the total economic costs of climate change. However, we acknowledge that integrating all these effects into a unified framework and evaluating their relative importance lies beyond the scope of this study.

6.3 Regional Heterogeneity

This section examines the impact of climate change on productivity losses at the province level (NUTS 3) in Italy. Using the methodology described in Section 2, we apply equation (22) to each province to estimate the magnitude and spatial distribution of these losses under the baseline warming scenario of RCP4.5. We are taking into account both adaptation and "long-run" effects as explained in the previous section.

The results in Figure 5a reveal significant regional variations in productivity losses across

Figure 5: Regional Productivity Losses for RCP4.5 Warming Scenario



(a) Regional Productivity Losses **(b) Regional Losses and GDP Per Capita**

Note. Figure 5a shows the productivity losses across NUTS 3 regions with RCP4.5 Warming Scenario, calculated using equation (19). Productivity losses are expressed as a percentage, and darker colors represent larger losses. Figure 5b plots regional losses against average GDP per capita in our sample.

Italian provinces under the RCP4.5 warming scenario. While climate change negatively impacts productivity overall, the effects are uneven. Some regions see negligible productivity loss of up to 0.06 percent, whereas others experience substantial losses, with reductions as high as 16.30 percent.

Our analysis highlights regional disparities in climate change-induced productivity losses between southern and northern Italy. Southern regions face significant negative impacts due to an increase in extreme heat days, while northern alpine areas benefit from fewer days below 0 degrees Celsius, leading to moderate productivity losses or even modest gains.

These findings highlight how firm-level losses, characterized by an inverted U-shaped pattern, translate into significant regional differences based on historical temperatures. To further examine the relationship between predicted productivity losses and inequality, Figure 5b plots those losses against GDP per capita. While some wealthy northern regions experience considerable productivity losses, as noted in Section 6.2.1, we observe an overall positive correlation, indicating climate change will likely exacerbate regional inequality in Italy.

7 Conclusion

We present a novel micro-to-macro framework to quantify the aggregate productivity impacts of climate change, rooted in firm-level data and a general equilibrium model. Our findings underscore the importance of incorporating both direct productivity effects and indirect effects stemming from input adjustment frictions. These mechanisms amplify the economic costs of climate change, with aggregate productivity losses estimated to be significantly larger than

those derived from representative firm models or standard IAM methodologies.

Our analysis reveals a highly nonlinear relationship between temperature increases and aggregate productivity losses, driven by firm-level dynamics and geographic variation in temperature extremes. Using Italian firm-level data combined with detailed climate information, we identify an inverted U-shaped effect of temperature on firm sales, with extreme high or low temperatures significantly reducing productivity. Extreme temperatures decrease labor and material inputs but leave capital usage largely unchanged, reflecting greater frictions in capital adjustment compared to other inputs. As a result, we find an inverted U-shaped relationship between extreme temperatures and the revenue-based marginal product of capital, while the marginal products of other inputs remain unaffected.

These findings underscore the importance of indirect effects, driven by input adjustment frictions, in amplifying the overall impact of temperature on firms. Using the estimated semi-elasticities from our empirical analysis, we quantify these impacts in a general equilibrium model. We consider projected temperature changes that reflect both predicted increases in average temperatures, and increases in temperature variability, thus reflecting the fact that climate change will lead to more frequent extreme temperature events.

Under a scenario that implies on average 2℃ warming, we estimate aggregate productivity losses as large as 4.23 percent, while a scenario with average 4℃ warming leads to a sharp increase to 17.81 percent, illustrating the compounding effects of temperature on economic outcomes. A substantial part of this total effect (around 20 percent) is caused by the indirect allocative channel, despite we conservatively assume it only applies to the increase in temperatures variability around the mean. We also find that adaptation reduces the expected losses only modestly, between 15 and 21 percent.

This research contributes to the broader climate economics literature by complementing existing approaches and addressing some of their limitations. First, we show that indirect effects—driven by input frictions and allocative inefficiencies—are quantitatively significant, accounting for a substantial share of total losses. Second, our closed-form aggregate damage function, derived from firm-level semi-elasticities, provides a robust methodology for integrating these findings into IAMs, offering a more comprehensive assessment of climate-related damages. Notably, our framework predicts higher aggregate losses compared to traditional IAMs, emphasizing the need to revise upward the economic costs of climate change and the social cost of carbon.

References

Acharya, V. V., A. Bhardwaj, and T. Tomunen (2023): "Do Firms Mitigate Climate Impact on Employment? Evidence from U.S. Heat Shocks," NBER Working Paper no.31967.

Addoum, J. M., D. T. Ng, and A. Ortiz-Bobea (2020): "Temperature Shocks and Establishment Sales," *The Review of Financial Studies*, 33, 1331–1366.

Albert, C., P. Bustos, and J. Ponticelli (2021): "The Effects of Climate Change on Labor and Capital Reallocation," NBER Working Paper no.28995.

Almunia, M., P. Antràs, D. Lopez-Rodriguez, and E. Morales (2021): "Venting out: Exports During a Domestic Slump," *American Economic Review*, 111, 3611–62.

Auffhammer, M. (2018): "Quantifying Economic Damages from Climate Change," *Journal of Economic Perspectives*, 32, 33–52.

Auffhammer, M., S. M. Hsiang, W. Schlenker, and A. Sobel (2013): "Using weather data and climate model output in economic analyses of climate change," *Review of Environmental Economics and Policy*, 7(2), 181–198.

Balboni, C. (2025): "In Harm's Way? Infrastructure Investments and the Persistence of Coastal Cities," *American Economic Review*, 115, 77–116.

Balboni, C., J. Boehm, and M. Waseem (2024): "Firm adaptation and production networks: Structural evidence from extreme weather events in Pakistan," PEDL Working Paper.

Baqaee, D. R. and E. Farhi (2020): "Productivity and Misallocation in General Equilibrium," *The Quarterly Journal of Economics*, 135, 105–163.

Barrage, L. (2020): "The Fiscal Costs of Climate Change," in *AEA Papers and Proceedings*, vol. 110, 107–112.

Barrage, L. and W. D. Nordhaus (2023): "Policies, Projections, and the Social Cost of Carbon: Results from the DICE-2023 Model," NBER Working Paper no.31112.

Bastien-Olvera, B. A., F. Granella, and F. C. Moore (2022): "Persistent Effect of Temperature on GDP Identified from Lower Frequency Temperature Variability," *Environmental Research Letters*, 17, 084038.

Bau, N. and A. Matray (2023): "Misallocation and Capital Market Integration: Evidence From India," *Econometrica*, 91, 67–106.

Bernard, A. B., J. Eaton, J. B. Jensen, and S. Kortum (2003): "Plants and Productivity in International Trade," *American Economic Review*, 93, 1268–1290.

Bettarelli, L., D. Furceri, M. Ganslmeier, and M. Schiffbauer (2025): "The Economic Costs of Temperature Uncertainty," Tech. rep., International Monetary Fund.

Bilal, A. and D. R. Känzig (2024): "The Macroeconomic Impact of Climate Change: Global vs. Local Temperature," NBER Working Paper no.32450.

Bilal, A. and E. Rossi-Hansberg (2023): "Anticipating Climate Change Across the United States," NBER Working Paper no.31323.

Broda, C. and D. E. Weinstein (2006): "Globalization and the Gains from Variety," *The Quarterly Journal of Economics*, 121, 541–585.

Burke, M., S. M. Hsiang, and E. Miguel (2015): "Global Non-Linear Effect of Temperature on Economic Production," *Nature*, 527, 235–239.

Burke, M. and V. Tanutama (2019): "Climatic Constraints on Aggregate Economic Output," NBER Working Paper no.25779.

Busse, M. R., D. G. Pope, J. C. Pope, and J. Silva-Risso (2015): "The Psychological Effect of Weather on Car Purchases," *The Quarterly Journal of Economics*, 130, 371–414.

Caballero, R. J., E. Farhi, and P.-O. Gourinchas (2017): "Rents, Technical Change, and Risk

Premia Accounting for Secular Trends in Interest Rates, Returns on Capital, Earning Yields, and Factor Shares," *American Economic Review*, 107, 614–620.

Caggese, A. and V. Cuñat (2008): "Financing Constraints and Fixed-Term Employment Contracts," *The Economic Journal*, 118, 2013–2046.

——— (2013): "Financing Constraints, Firm Dynamics, Export Decisions, and Aggregate Productivity," *Review of Economic Dynamics*, 16, 177–193.

Carleton, T., A. Jina, M. Delgado, M. Greenstone, T. Houser, S. Hsiang, A. Hultgren, R. E. Kopp, K. E. McCusker, I. Nath, et al. (2022): "Valuing the Global Mortality Consequences of Climate Change Accounting for Adaptation Costs and Benefits," *The Quarterly Journal of Economics*, 137, 2037–2105.

Cascarano, M., F. Natoli, and A. Petrella (2022): "Entry, Exit and Market Structure in a Changing Climate," Banca d'Italia Working Paper No.1418.

Casey, G., S. Fried, and E. Goode (2023): "Projecting the Impact of Rising Temperatures: The Role of Macroeconomic Dynamics," *IMF Economic Review*, 1–31.

Castro-Vincenzi, J. (2022): "Climate hazards and resilience in the global car industry," *Princeton University manuscript*.

Castro-Vincenzi, J., G. Khanna, N. Morales, and N. Pandalai-Nayar (2024): "Weathering the storm: Supply chains and climate risk," NBER Working Paper no.32218.

Christiano, L. J., M. S. Eichenbaum, and M. Trabandt (2015): "Understanding the Great Recession," *American Economic Journal: Macroeconomics*, 7, 110–167.

Cloyne, J., C. Ferreira, M. Froemel, and P. Surico (2023): "Monetary Policy, Corporate Finance, and Investment," *Journal of the European Economic Association*, 21, 2586–2634.

Cohn, J. and T. Deryugina (2018): "Firm-level Financial Resources and Environmental Spills," NBER Working Paper no.24516.

Colciago, A., V. Lindenthal, and A. Trigari (2019): "Who Creates and Destroys Jobs over the Business Cycle?" De Nederlandsche Bank Working Paper No. 628.

Colmer, J. (2021): "Temperature, Labor Reallocation, and Industrial Production: Evidence from India," *American Economic Journal: Applied Economics*, 13, 101–24.

Conley, T. G. (2010): "Spatial Econometrics," in *Microeconometrics*, ed. by A. C. Cameron and P. K. Trivedi, New York: Springer, 303–328.

Conte, B., K. Desmet, and E. Rossi-Hansberg (2022): "On the Geographic Implications of Carbon Taxes," NBER Working Paper no.30678.

Cooper, R. W. and J. C. Haltiwanger (2006): "On the nature of capital adjustment costs," *The Review of Economic Studies*, 73, 611–633.

Cornes, R. C., G. van der Schrier, E. J. van den Besselaar, and P. D. Jones (2018): "An Ensemble Version of the E-OBS Temperature and Precipitation Data Sets," *Journal of Geophysical Research: Atmospheres*, 123, 9391–9409.

Cruz, J.-L. and E. Rossi-Hansberg (2023): "The Economic Geography of Global Warming," *The Review of Economic Studies*, 91, 899–939.

Custodio, C., M. A. Ferreira, E. Garcia-Appendini, and A. Lam (2024): "Does Climate Change Affect Firm Output? Identifying Supply Effects," Available at SSRN: https://ssrn.com/abstract=3724940.

De Loecker, J., J. Eeckhout, and G. Unger (2020): "The Rise of Market Power and the Macroeconomic Implications," *The Quarterly Journal of Economics*, 135, 561–644.

Dell, M., B. F. Jones, and B. A. Olken (2012): "Temperature Shocks and Economic Growth: Evidence from the Last Half Century," *American Economic Journal: Macroeconomics*, 4, 66–95.

——— (2014): "What Do We Learn from the Weather? The New Climate-Economy Literature," *Journal of Economic Literature*, 52, 740–98.

Deschênes, O. and M. Greenstone (2011): "Climate Change, Mortality, and Adaptation: Evidence from Annual Fluctuations in Weather in the U.S." *American Economic Journal: Applied Economics*, 3, 152–185.

Desmet, K. and E. Rossi-Hansberg (2015): "On the Spatial Economic Impact of Global Warming," *Journal of Urban Economics*, 88, 16–37.

Diffenbaugh, N. S. and M. Burke (2019): "Global Warming has Increased Global Economic Inequality," *Proceedings of the National Academy of Sciences*, 116, 9808–9813.

Evin, G., S. Somot, and B. Hingray (2021): "Balanced estimate and uncertainty assessment of European climate change using the large EURO-CORDEX regional climate model ensemble," *Earth System Dynamics*, 12, 1543–1569.

Fernández-Villaverde, J., K. Gillingham, and S. Scheidegger (2024): "Climate Change through the Lens of Macroeconomic Modeling," NBER Working Paper no.32963.

Filomena, M. and M. Picchio (2024): "Unsafe Temperatures, Unsafe jobs: The Impact of Weather Conditions on Work-Related Injuries," *Journal of Economic Behavior & Organization*, 224, 851–875.

Fischer, E. M. and C. Schär (2010): "Consistent geographical patterns of changes in high-impact European heatwaves," *Nature geoscience*, 3, 398–403.

Fort, T. C., J. Haltiwanger, R. S. Jarmin, and J. Miranda (2013): "How Firms Respond to Business Cycles: The Role of Firm Age and Firm Size," *IMF Economic Review*, 61, 520–559.

Foster, L., J. Haltiwanger, and C. Syverson (2008): "Reallocation, Firm Turnover, and Efficiency: Selection on Productivity or Profitability?" *American Economic Review*, 98, 394–425.

Fried, S. (2022): "Seawalls and Stilts: A Quantitative Macro Study of Climate Adaptation," *The Review of Economic Studies*, 89, 3303–3344.

Gandhi, A., S. Navarro, and D. A. Rivers (2020): "On the Identification of Gross Output Production Functions," *Journal of Political Economy*, 128, 2973–3016.

Garimella, S., M. T. Hughes, and The Conversation US (2023): "Physicists Explain How Heat Kills Machines and Electronics," .

Gervais, A. and J. B. Jensen (2019): "The Tradability of Services: Geographic Concentration and Trade Costs," *Journal of International Economics*, 118, 331–350.

Golosov, M., J. Hassler, P. Krusell, and A. Tsyvinski (2014): "Optimal taxes on fossil fuel in general equilibrium," *Econometrica*, 82, 41–88.

Gopinath, G., Ş. Kalemli-Özcan, L. Karabarbounis, and C. Villegas-Sanchez (2017): "Capital Allocation and Productivity in South Europe," *The Quarterly Journal of Economics*, 132, 1915–1967.

Gould, C. F., S. Heft-Neal, A. K. Heaney, E. Bendavid, C. W. Callahan, M. Kiang, J. S. G. Zivin, and M. Burke (2024): "Temperature Extremes Impact Mortality and Morbidity Differently," NBER Working Paper no.32195.

Graff Zivin, J. and M. Neidell (2014): "Temperature and the Allocation of Time: Implications for Climate Change," *Journal of Labor Economics*, 32, 1–26.

Hassler, J., P. Krusell, and A. A. Smith Jr (2016): "Environmental Macroeconomics," in *Handbook of Macroeconomics*, Elsevier, vol. 2, 1893–2008.

Heal, G. and J. Park (2016): "Reflections—Temperature Stress and the Direct Impact of Climate Change: A Review of an Emerging Literature," *Review of Environmental Economics and Policy*, 10, 347–362.

Heutel, G., N. H. Miller, and D. Molitor (2021): "Adaptation and the Mortality Effects of

Temperature across U.S. Climate Regions," *Review of Economics and Statistics*, 103, 740–753.

Hsiang, S., R. Kopp, A. Jina, J. Rising, M. Delgado, S. Mohan, D. Rasmussen, R. Muir-Wood, P. Wilson, M. Oppenheimer, et al. (2017): "Estimating Economic Damage from Climate Change in the United States," *Science*, 356, 1362–1369.

Hsieh, C.-T. and P. J. Klenow (2009): "Misallocation and Manufacturing TFP in China and India," *The Quarterly Journal of Economics*, 124, 1403–1448.

IPCC (2021): *Summary for Policymakers*, Cambridge, United Kingdom and New York, NY, USA: Cambridge University Press, 3–32.

Jones, C. I. (2011): "Misallocation, Economic Growth, and Input-Output Economics," NBER Working Paper no.16742.

Kahn, M. E., K. Mohaddes, R. N. Ng, M. H. Pesaran, M. Raissi, and J.-C. Yang (2021): "Long-term Macroeconomic Effects of Climate Change: A Cross-country Analysis," *Energy Economics*, 104, 105624.

Kala, N., P. Kurukulasuriya, and R. Mendelsohn (2012): "The Impact of Climate Change on Agro-Ecological Zones: Evidence from Africa," *Environment and Development Economics*, 17, 663–687.

Kalemli-Özcan, S., B. E. Sørensen, C. Villegas-Sanchez, V. Volosovych, and S. Yeşiltaş (2024): "How to Construct Nationally Representative Firm-Level Data from the Orbis Global Database: New Facts on SMEs and Aggregate Implications for Industry Concentration," *American Economic Journal: Macroeconomics*, 16, 353–74.

Kalkuhl, M. and L. Wenz (2020): "The Impact of Climate Conditions on Economic Production. Evidence from a Global Panel of Regions," *Journal of Environmental Economics and Management*, 103, 102360.

Klein Tank, A., J. Wijngaard, G. Können, R. Böhm, G. Demarée, A. Gocheva, M. Mileta, S. Pashiardis, L. Hejkrlik, C. Kern-Hansen, et al. (2002): "Daily dataset of 20th-century surface air temperature and precipitation series for the European Climate Assessment," *International Journal of Climatology: A Journal of the Royal Meteorological Society*, 22, 1441.

Krusell, P. and A. A. Smith (2022): "Climate Change around the World," NBER Working Paper no.30338.

Lai, W., Y. Qiu, Q. Tang, C. Xi, and P. Zhang (2023): "The effects of temperature on labor productivity," *Annual Review of Resource Economics*, 15, 213–232.

Leduc, S. and D. J. Wilson (2023): "Climate Change and the Geography of the US Economy," Federal Reserve Bank of San Francisco, Working Paper Series 2023-17.

Liu, T. and Z. Xu (2024): "The (Mis) Allocation Channel of Climate Change," .

Loecker, J. D. and F. Warzynski (2012): "Markups and Firm-level Export Status," *American Economic Review*, 102, 2437–2471.

Melitz, M. J. (2003): "The impact of trade on intra-industry reallocations and aggregate industry productivity," *Econometrica*, 71, 1695–1725.

Mian, A. and A. Sufi (2014): "What Explains the 2007–2009 Drop in Employment?" *Econometrica*, 82, 2197–2223.

Moll, B. (2021): "The Missing Intercept in Cross-Section Regressions," Available at https://benjaminmoll.com/wp-content/uploads/2021/02/missing_intercept.pdf.

Nath, I. (2024): "Climate Change, the Food Problem, and the Challenge of Adaptation through Sectoral Reallocation," *Accepted for publication Journal of Political Economy*.

Nath, I. B., V. A. Ramey, and P. J. Klenow (2024): "How Much Will Global Warming Cool Global Growth?" NBER Working Paper no.32761.

Newell, R. G., B. C. Prest, and S. E. Sexton (2021): "The GDP-Temperature Relationship:

Implications for Climate Change Damages," *Journal of Environmental Economics and Management*, 108, 102445.

Nordhaus, W. D. (1977): "Economic Growth and Climate: The Carbon Dioxide Problem," *The American Economic Review*, 67, 341–346.

Nordhaus, W. D. and A. Moffat (2017): "A survey of global impacts of climate change: replication, survey methods, and a statistical analysis," NBER Working Paper no.23646.

Osotimehin, S. (2019): "Aggregate Productivity and the Allocation of Resources over the Business Cycle," *Review of Economic Dynamics*, 32, 180–205.

Pankratz, N. M. and C. M. Schiller (2024): "Climate Change and Adaptation in Global Supply-Chain Networks," *The Review of Financial Studies*, 37, 1729–1777.

Ponticelli, J., X. Qiping, and S. Zeume (2023): "Temperature, Adaptation, and Local Industry Concentration," NBER Working Paper no.31533.

Restuccia, D. and R. Rogerson (2008): "Policy Distortions and Aggregate Productivity with Heterogeneous Establishments," *Review of Economic Dynamics*, 11, 707–720.

Seppanen, O., W. J. Fisk, and Q. Lei (2006): "Room Temperature and Productivity in Office Work," Tech. rep., Lawrence Berkeley National Lab.(LBNL), Berkeley, CA (United States).

Solow, R. M. (1957): "Technical Change and the Aggregate Production Function," *The Review of Economics and Statistics*, 312–320.

Somanathan, E., R. Somanathan, A. Sudarshan, and M. Tewari (2021): "The Impact of Temperature on Productivity and Labor Supply: Evidence from Indian Manufacturing," *Journal of Political Economy*, 129, 1797–1827.

Sraer, D. and D. Thesmar (2023): "How to Use Natural Experiments to Estimate Misallocation," *American Economic Review*, 113, 906–938.

Zhang, P., O. Deschenes, K. Meng, and J. Zhang (2018): "Temperature Effects on Productivity and Factor Reallocation: Evidence from a Half Million Chinese Manufacturing Plants," *Journal of Environmental Economics and Management*, 88, 1–17.

Climate Change, Firms, and Aggregate Productivity

Andrea Caggese, Andrea Chiavari, Sampreet S. Goraya, and

Carolina Villegas-Sanchez

Online Appendix

Contents

6.1.2 Counterfactual changes in grid-cell-level temperatures. 31

A Structural Framework **1**

A.1 Aggregate Gross Output TFP 1

A.2 Solow Residual 6

B Data **8**

B.1 Firm-Level Data 8

B.2 Climate Data 9

B.2.1 Description of E-OBS data 9

B.2.2 Distribution of Meteorological Stations 10

B.2.3 Climate Data Summary Statistics 11

B.3 Temperature bins 11

C Empirical Results **12**

C.1 Additional Controls and Alternative Independent Variables 12

C.2 Additional Sample Cuts 17

C.3 Additional Demand-Adjusted Productivity Results 20

C.4 Results across adapted and non adapted regions 20

D Aggregate Results **21**

D.1 Counterfactual Temperature Distributions 21

D.1.1 Counterfactual Temperature Distributions with Mean Change 21

D.1.2 Counterfactual Temperature Distributions with Change in Standard-deviation or/and Mean 24

D.2 Additional Robustness Main Results 27

A Structural Framework

In this section, we show the derivations of the equations in Section 2.2.

A.1 Aggregate Gross Output TFP

To derive the equations (19) and (20), we start from the definition of aggregate gross output TFP, given by

$$TFP_t = \left(\frac{\prod_{X \in \mathcal{X}} X_t^{\alpha^X}}{Y_t} \right)^{-1}, \tag{31}$$

$$= \prod_{X \in \mathcal{X}} \left(\frac{X_t}{Y_t} \right)^{-\alpha^X}; \tag{32}$$

where aggregate real inputs are defined as

$$X_t = \sum_{i=1}^{N_t} X_{it}. \tag{33}$$

To characterize aggregate real inputs X_t, we now need to derive the demand for each input X_{it}. We start recalling that the minimized cost function is given by

$$\mathcal{C}(Y_{it}) = \frac{Y_{it}}{e^{z_{it}(T_{g(i)t})}} \prod_{X \in \mathcal{X}} \left(\frac{e^{\tau_{it}^X (T_{g(i)t})} P^X}{\alpha^X} \right)^{\alpha^X}, \tag{34}$$

$$= \prod_{X \in \mathcal{X}} \left(\frac{P_t^X}{\alpha^X} \right)^{\alpha^X} \frac{Y_{it}}{e^{z_{it}(T_{g(i)t})}} \prod_{X \in \mathcal{X}} \left(e^{\tau_{it}^X (T_{g(i)t})} \right)^{\alpha^X}, \tag{35}$$

$$= C_t \frac{Y_{it}}{e^{z_{it}(T_{g(i)t})}} \prod_{X \in \mathcal{X}} \left(e^{\tau_{it}^X (T_{g(i)t})} \right)^{\alpha^X}; \tag{36}$$

where

$$C_t = \prod_{X \in \mathcal{X}} \left(\frac{P_t^X}{\alpha^X} \right)^{\alpha^X}. \tag{37}$$

Given that the first-order conditions for each input are given by

$$e^{\tau_{it}^X(T_{g(i)t})} P_t^X X_{it} = \alpha^X \mathcal{C}(Y_{it}), \tag{38}$$

$$= \alpha^X C_t \frac{Y_{it}}{e^{z_{it}(T_{g(i)t})}} \prod_{X \in \mathcal{X}} \left(e^{\tau_{it}^X(T_{g(i)t})} \right)^{\alpha^X}; \tag{39}$$

we obtain the following input demand function:

$$X_{it} = \alpha^X \frac{C_t}{P_t^X} \frac{Y_{it}}{e^{\tau_{it}^X(T_{g(i)t})} e^{z_{it}(T_{g(i)t})}} \prod_{X \in \mathcal{X}} \left(e^{\tau_{it}^X(T_{g(i)t})} \right)^{\alpha^X}, \tag{40}$$

This implies the following aggregate level for each input X_t:

$$X_t = \alpha^X \frac{C_t}{P_t^X} \sum_{i=1}^{N_t} \frac{Y_{it}}{e^{\tau_{it}^X(T_{g(i)t})} e^{z_{it}(T_{g(i)t})}} \prod_{X \in \mathcal{X}} \left(e^{\tau_{it}^X(T_{g(i)t})} \right)^{\alpha^X}. \tag{41}$$

Substituting equation (41) back into equation (32) we obtain the following:

$$TFP_t = \prod_{X \in \mathcal{X}} \left(\alpha^X \frac{C_t}{P_t^X} \sum_{i=1}^{N_t} \frac{1}{e^{\tau_{it}^X(T_{g(i)t})} e^{z_{it}(T_{g(i)t})}} \frac{Y_{it}}{Y_t} \prod_{X \in \mathcal{X}} \left(e^{\tau_{it}^X(T_{g(i)t})} \right)^{\alpha^X} \right)^{-\alpha^X}, \tag{42}$$

$$= \prod_{X \in \mathcal{X}} \left(\alpha^X \frac{C_t}{P_t^X} \right)^{\alpha^X} \left(\sum_{i=1}^{N_t} \frac{1}{e^{\tau_{it}^X(T_{g(i)t})} e^{z_{it}(T_{g(i)t})}} \frac{Y_{it}}{Y_t} \prod_{X \in \mathcal{X}} \left(e^{\tau_{it}^X(T_{g(i)t})} \right)^{\alpha^X} \right)^{-\alpha^X}, \tag{43}$$

$$= \prod_{X \in \mathcal{X}} \left(\sum_{i=1}^{N_t} \frac{1}{e^{\tau_{it}^X(T_{g(i)t})} e^{z_{it}(T_{g(i)t})}} \frac{Y_{it}}{Y_t} \prod_{X \in \mathcal{X}} \left(e^{\tau_{it}^X(T_{g(i)t})} \right)^{\alpha^X} \right)^{-\alpha^X}; \tag{44}$$

where the last equality holds because of the definition of C_t in equation (37). Notice that now aggregate gross output TFP in equation (44) depends only on wedges and on each firm relative size Y_{it}/Y_t. Hence, to obtain an expression for aggregate gross output TFP that depends only on wedges, we need to express the relative size of each firm as a function of wedges only. We start by defining a firm's relative size using the demand function:

$$\frac{Y_{it}}{Y_t} = \left(e^{d_{it}(T_{g(i)t})} \right)^{\sigma - 1} \left(\frac{P_{it}}{P_t} \right)^{-\sigma}. \tag{45}$$

Now, recall that the firms' prices are given by

$$P_{it} = \mathcal{MC}'(Y_{it}), \tag{46}$$

$$= \mathcal{MC}_t \frac{1}{e^{z_{it}(T_{g(i)t})}} \prod_{X \in \mathcal{X}} \left(e^{\tau_{it}^X (T_{g(i)t})} \right)^{\alpha^X}; \tag{47}$$

Moreover, we can substitute firm-level prices from equation (47) into the aggregate price index and obtain

$$P_t = \left(\sum_{i=1}^{N_t} \left(\frac{P_{it}}{e^{d_{it}(T_{g(i)t})}} \right)^{1-\sigma} \right)^{\frac{1}{1-\sigma}}, \tag{48}$$

$$= \left(\sum_{i=1}^{N_t} \left(\mathcal{MC}_t \frac{1}{e^{d_{it}(T_{g(i)t})} e^{z_{it}(T_{g(i)t})}} \prod_{X \in \mathcal{X}} \left(e^{\tau_{it}^X (T_{g(i)t})} \right)^{\alpha^X} \right)^{1-\sigma} \right)^{\frac{1}{1-\sigma}}, \tag{49}$$

$$= \mathcal{MC}_t \left(\sum_{i=1}^{N_t} \left(\frac{1}{e^{\tilde{z}_{it}(T_{g(i)t})}} \prod_{X \in \mathcal{X}} \left(e^{\tau_{it}^X (T_{g(i)t})} \right)^{\alpha^X} \right)^{1-\sigma} \right)^{\frac{1}{1-\sigma}}; \tag{50}$$

Finally, substituting equations (47) and (50) into equation (45), we obtain an expression for firms' relative size as a function of wedges only, given by

$$\frac{Y_{it}}{Y_t} = \left(e^{d_{it}(T_{g(i)t})} \right)^{\sigma-1} \left(\frac{\frac{1}{e^{z_{it}(T_{g(i)t})}} \prod_{X \in \mathcal{X}} \left(e^{\tau_{it}^X (T_{g(i)t})} \right)^{\alpha^X}}{\left(\sum_{i=1}^{N_t} \left(\frac{1}{e^{\tilde{z}_{it}(T_{g(i)t})}} \prod_{X \in \mathcal{X}} \left(e^{\tau_{it}^X (T_{g(i)t})} \right)^{\alpha^X} \right)^{1-\sigma} \right)^{\frac{1}{1-\sigma}}} \right)^{-\sigma} \tag{51}$$

Now, we can substitute equation (51) into equation (44) to obtain the following:

$$TFP_t = \prod_{X\in\mathcal{X}} \left(\sum_{i=1}^{N_t} \frac{\left(e^{d_{it}(T_{g(i)t})}\right)^{\sigma-1}}{e^{\tau_{it}^X(T_{g(i)t})} e^{z_{it}(T_{g(i)t})}} \left(\frac{\frac{1}{e^{z_{it}(T_{g(i)t})}} \prod_{X\in\mathcal{X}} \left(e^{\tau_{it}^X(T_{g(i)t})}\right)^{\alpha^X}}{\left(\sum_{i=1}^{N_t} \left(\frac{1}{e^{\tilde{z}_{it}(T_{g(i)t})}} \prod_{X\in\mathcal{X}} \left(e^{\tau_{it}^X(T_{g(i)t})}\right)^{\alpha^X}\right)^{1-\sigma}\right)^{\frac{1}{1-\sigma}}} \right)^{-\sigma} \prod_{X\in\mathcal{X}} \left(e^{\tau_{it}^X(T_{g(i)t})}\right)^{\alpha^X} \right)^{-\alpha^X}, \tag{52}$$

$$= \left(\sum_{i=1}^{N_t} \left(e^{\tilde{z}_{it}(T_{g(i)t})}\right)^{\sigma-1} \prod_{X\in\mathcal{X}} \left(e^{\tau_{it}^X(T_{g(i)t})}\right)^{-(\sigma-1)\alpha^X} \right)^{\frac{\sigma}{\sigma-1}}$$

$$\times \prod_{X\in\mathcal{X}} \left(\sum_{i=1}^{N_t} \frac{\left(e^{\tilde{z}_{it}(T_{g(i)t})}\right)^{\sigma-1}}{e^{\tau_{it}^X(T_{g(i)t})}} \prod_{X\in\mathcal{X}} \left(e^{\tau_{it}^X(T_{g(i)t})}\right)^{-(\sigma-1)\alpha^X} \right)^{-\alpha^X}. \tag{53}$$

Hence, taking logs in equation (53) we obtain the following:

$$\log TFP_t = \frac{\sigma}{\sigma-1} \log \left(\sum_{i=1}^{N_t} \left(e^{\tilde{z}_{it}(T_{g(i)t})}\right)^{\sigma-1} \prod_{X\in\mathcal{X}} \left(e^{\tau_{it}^X(T_{g(i)t})}\right)^{-(\sigma-1)\alpha^X} \right)$$

$$- \sum_{X\in\mathcal{X}} \alpha^X \log \left(\sum_{i=1}^{N_t} \frac{\left(e^{\tilde{z}_{it}(T_{g(i)t})}\right)^{\sigma-1}}{e^{\tau_{it}^X(T_{g(i)t})}} \prod_{X\in\mathcal{X}} \left(e^{\tau_{it}^X(T_{g(i)t})}\right)^{-(\sigma-1)\alpha^X} \right). \tag{54}$$

Equation 54 shows that aggregate gross output TFP in this framework can be expressed as just a function of (i) firm-level wedges, $e^{\tilde{z}_{it}(T_{g(i)t})}$ and $e^{\tau_{it}^X}(T_{g(i)t})$; (ii) the elasticity of substitution across goods σ; and (iii) the production function elasticities α^X.

Notice that if the revenue-based marginal products equalize across firms, i.e., if $e^{\tau_{it}^X(T_{g(i)t})} = 1$, then equation (54) reduces to the efficient aggregate gross output TFP, given by

$$\log TFP_t^* = \frac{1}{\sigma-1} \log \left(\sum_{i=1}^{N_t} \left(e^{\tilde{z}_{it}(T_{g(i)t})}\right)^{\sigma-1} \right). \tag{55}$$

This concludes the derivations to get equations (16) and (17), which define respectively the inefficient and the efficient aggregate gross output TFP. Using these two equations, we can now derive equations (19) and (20). We start by differentiating equation (54) to obtain a relation linking changes in aggregate gross output TFP to changes in grid-cell-level temperatures,

given by

$$d\log TFP_t = \sigma \sum_{i=1}^{N_t} \underbrace{\left(\frac{\left(e^{\tilde{z}_{it}(T_{g(i)t})}\right)^{\sigma-1} \prod_{X\in\mathcal{X}} \left(e^{\tau_{it}^X(T_{g(i)t})}\right)^{-(\sigma-1)\alpha^X}}{\sum_{i=1}^{N_t} \left(e^{\tilde{z}_{it}(T_{g(i)t})}\right)^{\sigma-1} \prod_{X\in\mathcal{X}} \left(e^{\tau_{it}^X(T_{g(i)t})}\right)^{-(\sigma-1)\alpha^X}} \right)}_{\equiv \lambda_{it}\left(e^{\tilde{z}_{it}(T_{g(i)t})}, e^{\tau_{it}^X(T_{g(i)t})}\right)}$$

$$\times \left(\frac{\partial \tilde{z}_{it}(T_{g(i)t})}{\partial T_{g(i)t}} - \sum_{X\in\mathcal{X}} \alpha^X \frac{\partial \tau_{it}^X(T_{g(i)t})}{\partial T_{g(i)t}} \right) dT_{g(i)t}$$

$$- \sum_{X\in\mathcal{X}} \alpha^X \sum_{i=1}^{N_t} \left(\frac{\frac{\left(e^{\tilde{z}_{it}(T_{g(i)t})}\right)^{\sigma-1}}{e^{\tau_{it}^X(T_{g(i)t})}} \prod_{X\in\mathcal{X}} \left(e^{\tau_{it}^X(T_{g(i)t})}\right)^{-(\sigma-1)\alpha^X}}{\sum_{i=1}^{N_t} \frac{\left(e^{\tilde{z}_{it}(T_{g(i)t})}\right)^{\sigma-1}}{e^{\tau_{it}^X(T_{g(i)t})}} \prod_{X\in\mathcal{X}} \left(e^{\tau_{it}^X(T_{g(i)t})}\right)^{-(\sigma-1)\alpha^X}} \right)$$

$$\times \left((\sigma-1) \frac{\partial \tilde{z}_{it}(T_{g(i)t})}{\partial T_{g(i)t}} - \frac{\partial \tau_{it}^X(T_{g(i)t})}{\partial T_{g(i)t}} - \sum_{X\in\mathcal{X}} (\sigma-1)\alpha^X \frac{\partial \tau_{it}^X(T_{g(i)t})}{\partial T_{g(i)t}} \right) dT_{g(i)t}, \tag{56}$$

$$= \sigma \sum_{i=1}^{N_t} \lambda_{it}\left(e^{\tilde{z}_{it}(T_{g(i)t})}, e^{\tau_{it}^X(T_{g(i)t})}\right)$$

$$\times \left(\frac{\partial \tilde{z}_{it}(T_{g(i)t})}{\partial T_{g(i)t}} - \sum_{X\in\mathcal{X}} \alpha^X \frac{\partial \tau_{it}^X(T_{g(i)t})}{\partial T_{g(i)t}} \right) dT_{g(i)t}$$

$$- \sum_{X\in\mathcal{X}} \alpha^X \sum_{i=1}^{N_t} \underbrace{\left(\frac{\sum_{i=1}^{N_t} \left(e^{\tilde{z}_{it}(T_{g(i)t})}\right)^{\sigma-1} \prod_{X\in\mathcal{X}} \left(e^{\tau_{it}^X(T_{g(i)t})}\right)^{-(\sigma-1)\alpha^X}}{\sum_{i=1}^{N_t} \frac{\left(e^{\tilde{z}_{it}(T_{g(i)t})}\right)^{\sigma-1}}{e^{\tau_{it}^X(T_{g(i)t})}} \prod_{X\in\mathcal{X}} \left(e^{\tau_{it}^X(T_{g(i)t})}\right)^{-(\sigma-1)\alpha^X}} \right)}_{\equiv \Omega_t^X\left(e^{\tilde{z}_{it}(T_{g(i)t})}, e^{\tau_{it}^X(T_{g(i)t})}\right)} \lambda_{it}\left(e^{\tilde{z}_{it}(T_{g(i)t})}, e^{\tau_{it}^X(T_{g(i)t})}\right)$$

$$\times \frac{1}{e^{\tau_{it}^X(T_{g(i)t})}} \left((\sigma-1) \frac{\partial \tilde{z}_{it}(T_{g(i)t})}{\partial T_{g(i)t}} - \frac{\partial \tau_{it}^X(T_{g(i)t})}{\partial T_{g(i)t}} - \sum_{X\in\mathcal{X}} (\sigma-1)\alpha^X \frac{\partial \tau_{it}^X(T_{g(i)t})}{\partial T_{g(i)t}} \right) dT_{g(i)t}, \tag{57}$$

$$= \sum_{i=1}^{N_t} \lambda_{it}\left(e^{\tilde{z}_{it}(T_{g(i)t})}, e^{\tau_{it}^X(T_{g(i)t})}\right) \left[\sigma \left(\frac{\partial \tilde{z}_{it}(T_{g(i)t})}{\partial T_{g(i)t}} - \sum_{X\in\mathcal{X}} \alpha^X \frac{\partial \tau_{it}^X(T_{g(i)t})}{\partial T_{g(i)t}} \right) dT_{g(i)t} \right.$$

$$- \sum_{X\in\mathcal{X}} \frac{\alpha^X}{e^{\tau_{it}^X(T_{g(i)t})}} \Omega_t^X\left(e^{\tilde{z}_{it}(T_{g(i)t})}, e^{\tau_{it}^X(T_{g(i)t})}\right)$$

$$\left. \times \left((\sigma-1) \frac{\partial \tilde{z}_{it}(T_{g(i)t})}{\partial T_{g(i)t}} - \frac{\partial \tau_{it}^X(T_{g(i)t})}{\partial T_{g(i)t}} - \sum_{X\in\mathcal{X}} (\sigma-1)\alpha^X \frac{\partial \tau_{it}^X(T_{g(i)t})}{\partial T_{g(i)t}} \right) dT_{g(i)t} \right], \tag{58}$$

$$= \sum_{i=1}^{N_t} \lambda_{it}\left(e^{\tilde{z}_{it}(T_{g(i)t})}, e^{\tau_{it}^X(T_{g(i)t})}\right) \sum_{X\in\mathcal{X}} \frac{\alpha^X}{e^{\tau_{it}^X(T_{g(i)t})}} \Omega_t^X\left(e^{\tilde{z}_{it}(T_{g(i)t})}, e^{\tau_{it}^X(T_{g(i)t})}\right)$$

$$\times \left[\left(\sigma \frac{e^{\tau_{it}^X(T_{g(i)t})}}{\Omega_t^X\left(e^{\tilde{z}_{it}(T_{g(i)t})}, e^{\tau_{it}^X(T_{g(i)t})}\right)} - (\sigma-1) \right) \left(\frac{\partial \tilde{z}_{it}(T_{g(i)t})}{\partial T_{g(i)t}} - \sum_{X\in\mathcal{X}} \alpha^X \frac{\partial \tau_{it}^X(T_{g(i)t})}{\partial T_{g(i)t}} \right) + \frac{\partial \tau_{it}^X(T_{g(i)t})}{\partial T_{g(i)t}} \right]$$

$$\times dT_{g(i)t}; \tag{59}$$

which is exactly the expression in equation (19) in Section (2). We can now follow the strategy as above and differentiate equation (55) to obtain a relation linking changes in efficient aggregate gross output TFP to changes in grid-cell-level temperatures, given by

$$d\log TFP_t^* = \sum_{i=1}^{N_t} \underbrace{\left(\frac{\left(e^{\tilde{z}_{it}(T_{g(i)t})}\right)^{\sigma-1}}{\sum_{i=1}^{N_t}\left(e^{\tilde{z}_{it}(T_{g(i)t})}\right)^{\sigma-1}} \right)}_{\equiv \lambda_{it}^*\left(e^{\tilde{z}_{it}(T_{g(i)t})}\right)} \frac{\partial \tilde{z}_{it}(T_{g(i)t})}{\partial T_{g(i)t}} dT_{g(i)t}, \tag{60}$$

$$= \sum_{i=1}^{N_t} \lambda_{it}^*\left(e^{\tilde{z}_{it}(T_{g(i)t})}\right) \frac{\partial \tilde{z}_{it}(T_{g(i)t})}{\partial T_{g(i)t}} dT_{g(i)t}; \tag{61}$$

which is exactly the expression in equation (20) in Section (2).

A.2 Solow Residual

The model presented in Section 2 has three productive inputs: capital, labor, and materials. This implies that its notion of output is a gross measure, hence, its implied TFP is defined on gross output. However, when normally thinking about productivity as defined by Solow (1957), we think of a concept related to net output, i.e., to GDP. Here, we show how to adjust our measurement to be able to study the effect of climate change on aggregate net output TFP, i.e., on the Solow residual. Our strategy is reminiscent of the insights from Jones (2011).

We start by the definition of GDP, given by

$$GDP_t = Y_t - \frac{P_t^M}{P_t} M_t, \tag{62}$$

$$= TFP_t K^{\alpha^K} L^{\alpha^L} M^{\alpha^M} - \frac{P_t^M}{P_t} M_t; \tag{63}$$

i.e., GDP is defined as gross output net of the aggregate real value of materials. Given equation (63), we can defined the Solow residual as

$$Solow_t = \frac{TFP_t K^{\alpha^K} L^{\alpha^L} M^{\alpha^M} - \frac{P_t^M}{P_t} M_t}{K^{\widehat{\alpha}^K} L^{\widehat{\alpha}^L}}, \tag{64}$$

where $\widehat{\alpha}^K$ and $\widehat{\alpha}^L$ are the aggregate capital and labor elasticities of value added. Taking logs gives

$$\log Solow_t = \log\left(TFP_t K^{\alpha^K} L^{\alpha^L} M^{\alpha^M} - \frac{P_t^M}{P_t} M_t \right) - \log\left(K^{\widehat{\alpha}^K} L^{\widehat{\alpha}^L} \right). \tag{65}$$

Since we are interested in a counterfactual that assesses the implications of a medium- or long-run phenomenon such as climate change, we abstract from the fluctuations in aggregate capital and labor due to it and assume that these two aggregate quantities are fixed in the medium- or long-run, i.e., $K_t = \overline{K}$ and $L_t = \overline{L}$. Notice that this assumption is coherent with the model being in general equilibrium, it just implies that aggregate capital and labor supplies are supplied inelastically. Under these two assumptions, we can differentiate equation (65) and obtain the following:

$$d\log Solow_t = \frac{1}{GDP_t} TFP_t K^{\alpha K} L^{\alpha L} M^{\alpha M} \frac{dTFP_t}{TFP_t} + \frac{\alpha^M}{GDP_t} TFP_t K^{\alpha K} L^{\alpha L} M^{\alpha M} \frac{dM_t}{M_t} - \frac{\frac{P_t^M}{P_t} M_t}{GDP_t} \frac{dM_t}{M_t}, \tag{66}$$

$$= \frac{Y_t}{GDP_t} d\log TFP_t + \alpha^M \frac{Y_t}{GDP_t} d\log M_t - \frac{\frac{P_t^M}{P_t} M_t}{Y_t} \frac{Y_t}{GDP_t} d\log M_t, \tag{67}$$

$$= \frac{Y_t}{GDP_t} \left(d\log TFP_t + \left(\alpha^M - \frac{\frac{P_t^M}{P_t} M_t}{Y_t} \right) d\log M_t \right). \tag{68}$$

The equation (68) says that a percentage change in the Solow residual is proportional to the linear combination of the percentage changes in aggregate gross output TFP and aggregate materials. We further approximate equation (68) by assuming that $\alpha^M - P^M M_t / P_t Y_t$ is close to zero. This assumption is convenient since it allows us to solve the model in closed form.[34] We emphasize two things about this additional assumption: (i) In the likely scenario where the general equilibrium temperature-semielasticity of the aggregate materials is negative, this assumption should be considered conservative because it goes against the effect of temperature on the Solow residual; and (ii) when we test this hypothesis empirically by measuring the difference between α^M and $P^M M_t / P_t Y_t$, we find that it is less than 0.1 in our data.[35] Hence, with this additional assumption at hand, we can derive the following adjustment to our gross

[34] Notice that, while aggregate gross output TFP does not depend on aggregate prices, aggregate materials do depend on them. Therefore, to know their response to changes in temperature we would have to infer the general equilibrium effect of temperature, i.e., their effect on the user cost of capital and wages, which is beyond the scope of our analysis and difficult because of the constraints imposed by the short time frame of our data.

[35] This implies that, even if the temperature-semielasticity of aggregate materials is x, which we consider an unlikely upper bound, given that this is our estimate of partial equilibrium temperature-semielasticity found in Table 2 and that normally general equilibrium effects dampen partial equilibrium estimates, we would lose at *most* 0.1^*x percentage points relative to our main results.

output TFP measure:

$$d \log Solow_t = \frac{Y_t}{GDP_t} d \log TFP_t, \tag{69}$$

which is exactly equation (22) in Section (2).

B Data

B.1 Firm-Level Data

To ensure data quality, we employ firm-level balance sheet information from Orbis, following the data construction and cleaning methodologies outlined by Kalemli-Özcan et al. (2024) and Gopinath et al. (2017). The following steps are implemented: (1) Removal of Missing Information: We drop firm-year observations that have missing data on total assets, operating revenue, sales, and employment. (2) Exclusion of Negative Values: Firms reporting negative values for assets, tangible fixed assets, employment, or sales are excluded from the analysis. (3) Limiting Extreme Values: To enhance the robustness of our findings, we compute three ratios: sales to total assets, employment to total assets, and employment to sales. We then remove observations that fall below the 0.1 percentile or above the 99.9 percentile of the distribution of these ratios. By doing so, we mitigate the potential influence of extreme values on our analysis.

For this specific project, we apply additional filters and exclusions. (1) Removal of Missing Zipcode Information: Firms with missing zipcode information are dropped from the dataset. This ensures that we can accurately associate firms with specific geographic regions. (2) Exclusion of Finance, Insurance, and Utility Sectors: To maintain focus on the sectors relevant to our analysis, we exclude firms operating in the finance and insurance sectors, as well as the utility sector. (3) Exclusion of Firms with Negative Age or Exceeding 100: Firms with negative age or those exceeding 100 years are excluded from the analysis. (4) Time Period Selection: We keep observations from 1999 to 2013.

The final sample used for our analysis consists of approximately 4.3 million observations, representing 1 million unique firms. To account for changes in prices and maintain comparability over time, we deflate operating revenue, material expenditure, and wage bill using gross output price indices at the two-digit industry level, with the base year of 2005 (sourced from the Eurostat database). Additionally, the capital stock is deflated using the economy-wide price of investment goods obtained from the World Development Indicators database. Table B.1 provides an overview of the main variables in our analysis, based on the final Orbis

dataset.

Table B.1: Summary Statistics (1999-2013)

	Sales	Materials	Wage Bill	Employees	Capital	MRPM	MRPL	MRPK
Mean	13.33	11.61	11.66	1.88	11.14	1.72	2.03	2.30
Median	13.34	12.02	11.82	1.79	11.05	1.01	1.77	2.39
Min	5.92	3.55	4.35	0	5.51	-0.04	-0.05	-4.26
Max	17.78	17.32	16.08	5.76	16.68	8.09	7.52	7.27
No. Obs.	4,823,392	4,823,392	3,875,031	2,545,857	4,444,668	4,823,392	3,875,031	4,444,668

Note. Summary statistics of cleaned Orbis dataset between 1999 and 2013. All variables are in logs. All monetary values are deflated using Eurostat two-digit industry price deflators, and capital is deflated using the country-specific price of investment from the World Development Indicators.

B.2 Climate Data

B.2.1 Description of E-OBS data

E-OBS is a land-only gridded daily observational dataset that provides information on precipitation, temperature, sea level pressure, global radiation, wind speed, and relative humidity in Europe.[36] The dataset is derived from meteorological observations collected by the National Meteorological and Hydrological Services (NMHSs) and other data-holding institutes across Europe.

E-OBS is presented on regular latitude-longitude grids with spatial resolutions of 0.1°. It covers a significant portion of the European continent, spanning from northern Scandinavia to southern Spain and extending from Iceland to 40°E in the Russian Federation. Over time, the coverage of E-OBS has progressively expanded since its inception in the 1950s, encompassing a larger area of the European continent due to an increasing number of contributing meteorological stations. The dataset undergoes comprehensive updates twice a year, with provisional monthly updates accessible through the E-OBS website.[37]

Originally developed in 2008 as a validation tool for Europe-wide climate model simulations within the European Union ENSEMBLES project, E-OBS has evolved into a resource for monitoring climate conditions across Europe (Klein Tank et al., 2002). The position of E-OBS in Europe is unique due to its relatively high spatial resolution, daily temporal resolution, multiple variables, and the extensive length of the dataset. The station-level data on which E-OBS is based can be accessed through the webpages of the European Climate Assessment

[36] Official E-OBS website: https://cds.climate.copernicus.eu.
[37] E-OBS monthly updates: http://surfobs.climate.copernicus.eu/dataaccess/access_eobs_months.php.

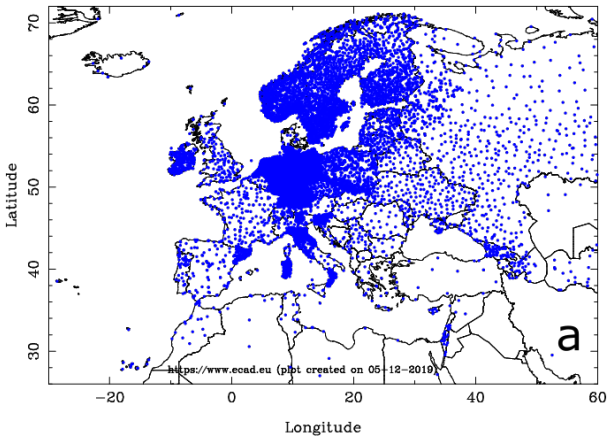
& Dataset (ECA&D), subject to data permissions.[38]

The dataset is daily, meaning the observations cover a 24-hour period per time step. The specific 24-hour period may vary across regions and data providers. The reason for this is that some data providers measure between midnight to midnight while others might measure from morning to morning. Since E-OBS is an observational dataset, no attempts have been made to adjust the time series for this 24-hour offset. However, it ensures that the largest part of the measured 24-hour period corresponds to the day attached to the time step in E-OBS and ECA&D

B.2.2 Distribution of Meteorological Stations

The station data used in the E-OBS dataset are sourced from 84 participating institutions and encompass over 23,000 meteorological stations. For a considerable number of countries, the number of stations used in the E-OBS dataset represents their complete national network, resulting in a much higher density compared to the station network routinely shared among NMHSs, which forms the basis of other gridded datasets.

Figure B.1: Distribution of Meteorological Station Used by E-OBS



Note. Figure B.1 shows the map with the station coverage in ECA&D which is the basis for the E-OBS precipitation dataset v20.0e.

Figure B.1 presents the distribution of meteorological stations used by E-OBS. This map showcases the station coverage in ECA&D, which serves as the basis for the E-OBS precipitation dataset v20.0e., regardless of their start or stop dates. The figure illustrates the high density of stations in many parts of Europe.

[38]ECA&D website: www.ecad.eu.

B.2.3 Climate Data Summary Statistics

Table B.2 displays the distribution of temperatures and rainfall across Italy and within the average grid-cell of Italy. It reveals significant variation in temperature throughout Italy, ranging from a minimum of -25 degrees Celsius to a maximum of 45 degrees Celsius, with an average temperature of 17 degrees Celsius.

Table B.2: Summary Statistics of Climate Data (1950-2020)

	Overall		Within Grid-Cell	
	Temperatures (°C)	Rainfalls (mm)	Temperatures (°C)	Rainfalls (mm)
Mean	16.88	2.28	16.88	2.28
Median	16.73	0.00	16.50	1.09
Min	-25.43	0.00	-2.60	0.00
Max	45.82	308.20	35.02	31.71

Note. Table 1 shows summary statistics of temperature in degrees Celsius (°C) and rainfalls in millimeters (mm) for the period 1999-2013. The first two columns report statistics for the overall sample. The last two columns report statistics on the variation within the average grid-cell, i.e., they show the average temperature distribution among the different grid-cells.

Examining the variation within grid-cells, which is the crucial one to identify our effects, we find slightly lower but still significant temperature variation. Specifically, the average minimum temperature within grid-cells is -3 degrees Celsius, and the average maximum is 35 degrees Celsius, with an average temperature within grid-cells of 17 degrees Celsius.

B.3 Temperature bins

Table B.3 reports summary statistics on the distribution of the number of days across grid-cells within each temperature bin for the period 1999-2013. Several points can be highlighted from these statistics.

Table B.3: Summary Statistics of Days Within Temperature Bins (1999-2013)

	Temperature Bins				
	$(-\infty, 0°C]$	$(0°C, 30°C]$	$(30°C, 35°C]$	$(35°C, 40°C]$	$(40°C, \infty)$
Mean	1.90	316.10	41.87	5.19	0.04
Median	0	317	43	3	0
Min	0	201	0	0	0
Max	164	365	95	56	10

Note. Table B.3 shows the summary statistics on the number of days across grid-cells within each temperature bin for the period 1999-2013.

First, despite the considerable variation in the data, all temperature bins have a positive number of days on average, with the exception of the bin capturing temperatures above 40

degrees Celsius. This shows that there is some representation for each bin across the grid-cells. Second, there is significant variation within each temperature bin across different grid cells. Even in the reference temperature bin $(0°C, 30°C]$, the number of days ranges from a minimum of 201 to a maximum of 365. This observation underscores the substantial variability present across grid-cells, which is important for our regression analysis. Third, it is worth noting that certain grid-cells exhibit a particularly high number of days with temperatures that are typically considered extreme. For instance, the maximum number of days below 0 degrees Celsius can reach as high as 164. This is not surprising considering Italy's diverse geography, which includes areas in the Alps (in the northern part of Italy) that frequently experience subzero temperatures. Additionally, some grid-cells experience a significant number of days with temperatures above 40 degrees Celsius, with some areas recording up to 10 such days.

C Empirical Results

C.1 Additional Controls and Alternative Independent Variables

In this section of the appendix, we present additional regression models to further validate the extent of the robustness of our results obtained from equation (25).

We start by splitting the $(0°C, 30°C]$ range into two bins: $(0°C, 15°C]$ and $(15°C, 30°C]$. We estimate the effects of temperature relative to the $(15°C, 30°C]$ range and report the results in Table C.4. Our findings indicate that one additional day in the $(0°C, 15°C]$ range increases sales by 0.015%. For the bins common to both distributions, we observe similar semielasticities.

Further, we augment the regression framework in equation (25) with a quadratic control for age. Age it has been shown empirically to be an important predictor of firm-level differences related to demand, productivity, and differences in financial frictions (see Fort et al., 2013; Cloyne et al., 2023; and Colciago et al., 2019). Columns 1, 5, 9, and 13 of Table C.5 and columns 1, 5, and 9 of Table C.6 present the estimates of this specification.

Moreover, we also use alternative functions of daily maximum temperatures over the year, such as the piece-wise linear degree days measure used in Somanathan et al. (2021). The calculation of degree days is best explained with an example. A day with a temperature of 35 degrees Celsius contributes 30 degrees Celsius to the first bin (0°C,30°C], 5 degrees Celsius to the third bin (30°C, 35°C], and 0 degree Celsius to the fourth bin (35°C, 40°C]. Thus, when a single day moves from 35 degrees Celsius to 40 degrees Celsius there is an increase of 5

Table C.4: Average Effect of Temperature on Sales and Inputs

Dependent Variable	**Sales** (1)	**Materials** (2)	**Labor** (3)	**Capital** (4)	**MRPL** (5)	**MRPM** (6)	**MRPK** (7)
Temperature Bins							
$(-\infty, 0°C]$	-0.076***	-0.049**	-0.058**	-0.026	-0.003	-0.012	-0.034
	(0.018)	(0.020)	(0.028)	(0.024)	(0.014)	(0.020)	(0.023)
$(0°C, 15°C]$	0.015*	0.017**	0.009	0.008	-0.009	0.004	-0.003
	(0.009)	(0.007)	(0.012)	(0.008)	(0.006)	(0.007)	(0.010)
$(30°C, 35°C]$	-0.014*	0.006	-0.020	0.004	-0.013**	0.006	-0.015
	(0.009)	(0.008)	(0.013)	(0.011)	(0.006)	(0.008)	(0.010)
$(35°C, 40°C]$	-0.043**	0.001	-0.059**	0.006	-0.023*	0.012	-0.046**
	(0.017)	(0.016)	(0.025)	(0.019)	(0.0125)	(0.014)	(0.021)
$(40°C, +\infty]$	-0.806***	-0.369*	-0.557**	0.034	-0.020	-0.209	-0.579**
	(0.1945)	(0.188)	(0.241)	(0.217)	(0.145)	(0.156)	(0.231)
Fixed Effects							
Firm	✓	✓	✓	✓	✓	✓	✓
Sector × Year	✓	✓	✓	✓	✓	✓	✓
GR and SDC × Region	✓	✓	✓	✓	✓	✓	✓
Controls							
Rainfalls	✓	✓	✓	✓	✓	✓	✓
Region Trends	✓	✓	✓	✓	✓	✓	✓
Observations	4,587,926	4,635,108	3,692,934	4,260,946	3,692,934	4,587,926	4,260,946

Note. All dependent variables are in logs. Temperature bins are defined with greater granularity than in the baseline specification. Rows 1-5 present the effect on the log of the dependent variable of adding an extra day in the given temperature range respectively. Standard errors are clustered at the grid-cell level and reported in parentheses. *, **, and *** denote 10, 5, and 1% statistical significance respectively.

degrees Celsius in the fourth-degree-day bin and no change in other bins.

More formally, denote the endpoints of our five temperature bins by $[T^{1\ell}, T^{2\ell})$, ℓ = 1,2,. . . , 5. A daily temperature T contributes positive degree days to all those bins for which $T > T^{1\ell}$ and zero to all others. If $T \geq T^{2\ell}$, the day contributes $T^{2\ell} - T^{1\ell}$ to bin ℓ. If $T^{1\ell} < T \leq T^{2\ell}$, it contributes $T - T^{1\ell}$ to bin ℓ. We now sum the degree days in each bin over the year to obtain D_{it}^{ℓ} for each unit i and estimate the following model:

$$Outome_{it} = \sum_{\ell} \beta_{\ell} D_{it}^{\ell} + \delta Rain_{g(i)t} + \boldsymbol{\lambda}' \mathbf{X}_{r(i)t} + \gamma_{s(i)t} + \alpha_i + \varepsilon_{it}. \tag{70}$$

Columns 2, 6, 10, and 14 of Table C.5 and columns 2, 6, and 10 of Table C.6 present the estimates of this specification.

Furthermore, we present results from an additional model of daily temperatures where the dependent variable depends on polynomial functions of daily maximum temperature, summed over the year. Denoting by T_{dit} the maximum temperature for firm i on day d of year t, the polynomial specification takes the following form:

$$Outome_{it} = \sum_{d}^{365} \beta_1 T_{dit} + \sum_{d}^{365} \beta_2 T_{dit}^2 + \delta Rain_{g(i)t} + \boldsymbol{\lambda}' \mathbf{X}_{r(i)t} + \gamma_{s(i)t} + \alpha_i + \varepsilon_{it}. \tag{71}$$

Columns 3, 9, 15, and 21 of Table C.5 provide and columns 3, 9, and 15 of Table C.6 present the estimates of this specification. Overall, we find patterns qualitatively consistent with our baseline estimates. However, this specification, due to its restrictive parametric assumptions, misses at times some additional effects, particularly for extreme temperatures, highlighting the value added by our semiparametric approach.

Additionally, we also estimate equation (25) allowing for a semiparametric specification of rainfalls instead of the linear baseline one. This allows us to capture the nonlinear effects of rainfall, including the impacts of floods caused by extreme precipitation. We use ten different bins, capturing P10, P20, ..., P100. Columns 4, 10, 16, and 20 of Table C.5 and Columns 4, 10, and 16 of Table C.6 present the estimates of this specification.

Finally, we also estimate equation (25) using the same benchmark definition for temperature bins, but constructing standard errors following Conley (2010) with a radius of 80km and 150km, corresponding to the size of largest NUTS3 and NUTS2 region. Columns 5, 11, 17, and 23 and columns 6, 12, 18, and 2 of Table C.5 and columns 5, 11, and 17 and 6, 12, and 18 of Table C.6 present the estimates of this specification. Estimates remain statistically significant in most cases, even with the very conservative distance of 150 km, considering that Italy covers an area of 301,340km^2, suggesting that our results are robust to considerations of spatial serial correlation.

Tables C.5 and C.6 consistently confirm our main findings through the outlined robustness exercises. Specifically, we observe that extreme temperatures harm sales, materials, and labor, while they do not affect capital substantially. Consequently, the revenue-based marginal products of materials and labor exhibit much sensitivity to extreme temperatures, whereas that of capital does.

Table C.5: Average Effect of Temperature on Sales and Inputs—Robustness

Dependent Variable	Sales						Materials						Labor						Capital					
	(1)	(2)	(3)	(4)	(5)	(6)	(7)	(8)	(9)	(10)	(11)	(12)	(13)	(14)	(15)	(16)	(17)	(18)	(19)	(20)	(21)	(22)	(23)	(24)
Temperature Bins																								
$(-\infty, 0°C]$	-0.088***	0.011**	-0.215***	-0.084***	-0.094***	-0.094***	-0.063**	0.010	-0.228***	-0.061**	-0.068***	-0.068**	-0.065***	0.006	-0.063**	-0.065***	-0.070**	-0.070**	-0.034	-0.001	0.007	-0.035	-0.036	-0.36
	(0.019)	(0.005)	(0.033)	(0.018)	(0.030)	(0.034)	(0.028)	(0.007)	(0.046)	(0.028)	(0.025)	(0.033)	(0.019)	(0.004)	(0.027)	(0.019)	(0.033)	(0.029)	(0.021)	(0.005)	(0.033)	(0.022)	(0.040)	(0.036)
$(30°C, 35°C]$	-0.019**	-0.011***	0.005	-0.013	-0.017	-0.017	-0.024*	-0.012***	-0.007	-0.018	-0.022	-0.022	-0.000	0.001	0.010	0.005	0.002	0.002	0.002	-0.000	0.003	0.004	0.003	0.003
	(0.009)	(0.003)	(0.012)	(0.008)	(0.014)	(0.012)	(0.014)	(0.004)	(0.017)	(0.013)	(0.018)	(0.025)	(0.008)	(0.003)	(0.012)	(0.008)	(0.008)	(0.010)	(0.010)	(0.004)	(0.014)	(0.010)	(0.012)	(0.015)
$(35°C, 40°C]$	-0.043**	-0.019*	-0.018	-0.042**	-0.046*	-0.046	-0.058**	-0.027*	-0.038	-0.055**	-0.060*	-0.060	0.002	-0.006	0.007	0.002	-0.003	-0.003	0.005	-0.008	0.005	0.007	0.004	0.004
	(0.017)	(0.010)	(0.019)	(0.017)	(0.025)	(0.032)	(0.025)	(0.014)	(0.027)	(0.025)	(0.031)	(0.048)	(0.016)	(0.009)	(0.018)	(0.017)	(0.022)	(0.028)	(0.019)	(0.011)	(0.021)	(0.020)	(0.022)	(0.028)
$(40°C, +\infty)$	-0.722***	-0.969***	-0.075**	-0.720***	-0.807**	-0.807**	-0.473**	-0.519*	-0.106**	-0.467*	-0.557	-0.557**	-0.257	-0.438**	-0.004	-0.374*	-0.369**	-0.369*	0.063	0.128	0.009	-0.020	0.033	0.034
	(0.190)	(0.250)	(0.033)	(0.196)	(0.368)	(0.339)	(0.236)	(0.297)	(0.047)	(0.246)	(0.370)	(0.246)	(0.197)	(0.206)	(0.030)	(0.197)	(0.159)	(0.194)	(0.221)	(0.198)	(0.035)	(0.227)	(0.174)	(0.211)
Fixed Effects																								
Firm	✓	✓	✓	✓	✓	✓	✓	✓	✓	✓	✓	✓	✓	✓	✓	✓	✓	✓	✓	✓	✓	✓	✓	✓
Sector × Year	✓	✓	✓	✓	✓	✓	✓	✓	✓	✓	✓	✓	✓	✓	✓	✓	✓	✓	✓	✓	✓	✓	✓	✓
GR and SDC × Region	✓	✓	✓	✓	✓	✓	✓	✓	✓	✓	✓	✓	✓	✓	✓	✓	✓	✓	✓	✓	✓	✓	✓	✓
Controls																								
Rainfalls	✓	✓	✓	✓	✓	✓	✓	✓	✓	✓	✓	✓	✓	✓	✓	✓	✓	✓	✓	✓	✓	✓	✓	✓
Region Trends	✓	✓	✓	✓	✓	✓	✓	✓	✓	✓	✓	✓	✓	✓	✓	✓	✓	✓	✓	✓	✓	✓	✓	✓
Age^2	✓						✓						✓						✓					
Observations	4,687,503	4,687,503	4,687,503	4,687,503	4,687,503	4,687,503	4,687,503	4,687,503	4,687,503	4,687,503	4,687,503	4,687,503	3,767,558	3,767,558	3,767,558	3,767,558	3,767,558	3,767,558	4,328,689	4,328,689	4,328,689	4,328,689	4,328,689	4,328,689

Note. All dependent variables are in logs. Columns 1, 6, 11, and 16 provide estimates from the baseline specification in equation (25), with temperature bins constructed as explained in Section 3.2, augmented with a quadratic age control. Columns 2, 7, 12, and 17 present estimates from the degree-day model in equation (70). Columns 3, 9, 15, and 21 provide estimates from the quadratic specification in equation (71). Columns 4, 10, 16, and 22 provide estimates from the baseline specification in equation (25), with temperature bins constructed as explained in Section 3.2, where rainfall controls are defined semiparametrically by ten bins instead of the linear specification in the benchmark case. Columns 5, 11, 17, and 23 provide estimates from the baseline specification in equation (25), with temperature bins constructed as explained in Section 3.2 but standard errors constructed following Conley (2010) with a radious of 80km. Columns 6, 12, 18, and 24 provide estimates from the baseline specification in equation (25), with temperature bins constructed as explained in Section 3.2 but standard errors constructed following Conley (2010) with a radious of 150km. Rows 1-4 present the effect on the log of the dependent variable of adding an extra day in the given temperature range respectively. Standard errors are clustered at the grid-cell level and reported in parentheses. *, **, and *** denote 10, 5, and 1% statistical significance respectively.

Table C.6: Average Effect of Temperature on Revenue-Based Marginal Products of Inputs—Robustness

Dependent Variable	MRPM						MRPL						MRPK					
	(1)	(2)	(3)	(4)	(5)	(6)	(7)	(8)	(9)	(10)	(11)	(12)	(13)	(14)	(15)	(16)	(17)	(18)
Temperature Bins																		
$(-\infty, 0°C]$	-0.018	-0.000	0.018	-0.016	-0.018	-0.018	0.007	0.000	-0.037*	0.007	0.008	0.008	-0.026	0.005	-0.159***	-0.023	-0.030	-0.030
	(0.019)	(0.005)	(0.024)	(0.019)	(0.020)	(0.019)	(0.013)	(0.003)	(0.021)	(0.013)	(0.015)	(0.007)	(0.022)	(0.004)	(0.036)	(0.022)	(0.038)	(0.030)
$(30°C, 35°C]$	0.006	0.001	0.012	0.006	0.006	0.006	-0.011*	-0.006***	-0.002	-0.012**	-0.012	-0.012	-0.015	-0.008**	0.008	-0.012	-0.014	-0.014
	(0.008)	(0.003)	(0.009)	(0.007)	(0.006)	(0.004)	(0.006)	(0.002)	(0.008)	(0.006)	(0.008)	(0.010)	(0.011)	(0.004)	(0.013)	(0.010)	(0.015)	(0.015)
$(35°C, 40°C]$	0.011	0.005	0.019	0.010	0.011	0.011	-0.022*	-0.002	-0.007	-0.025*	-0.021	-0.021	-0.044**	-0.009	-0.008	-0.046**	-0.045*	-0.045*
	(0.014)	(0.008)	(0.014)	(0.015)	(0.013)	(0.011)	(0.013)	(0.007)	(0.012)	(0.013)	(0.015)	(0.016)	(0.022)	(0.013)	(0.021)	(0.022)	(0.026)	(0.028)
$(40°C, +\infty)$	-0.209	-0.412**	0.032	-0.212	-0.209	-0.209	-0.049	-0.034	-0.018	0.060	-0.019	-0.019	-0.523**	-0.803***	-0.048	-0.443**	-0.578**	-0.578***
	(0.156)	(0.179)	(0.024)	(0.157)	(0.229)	(0.212)	(0.148)	(0.169)	(0.021)	(0.138)	(0.204)	(0.156)	(0.225)	(0.246)	(0.036)	(0.227)	(0.290)	(0.203)
Fixed Effects																		
Firm	✓	✓	✓	✓	✓	✓	✓	✓	✓	✓	✓	✓	✓	✓	✓	✓	✓	✓
Sector × Year	✓	✓	✓	✓	✓	✓	✓	✓	✓	✓	✓	✓	✓	✓	✓	✓	✓	✓
GR and SDC × Region	✓	✓	✓	✓	✓	✓	✓	✓	✓	✓	✓	✓	✓	✓	✓	✓	✓	✓
Controls																		
Rainfalls	✓	✓	✓	✓	✓	✓	✓	✓	✓	✓	✓	✓	✓	✓	✓	✓	✓	✓
Region Trends	✓	✓	✓	✓	✓	✓	✓	✓	✓	✓	✓	✓	✓	✓	✓	✓	✓	✓
Age^2	✓					✓					✓							
Observations	4,687,503	4,687,503	4,687,503	4,687,503	4,687,503	4,687,503	3,767,558	3,767,558	3,767,558	3,767,558	3,767,558	3,767,558	4,328,689	4,328,689	4,328,689	4,328,689	4,328,689	4,328,689

Note. All dependent variables are in logs. Columns 1, 7, and 13 provide estimates from the baseline specification in equation (25), with temperature bins constructed as explained in Section 3.2, augmented with a quadratic age control. Columns 2, 8, and 14 present estimates from the degree-day model in equation (70). Columns 3, 9, and 15 provide estimates from the quadratic specification in equation (71). Columns 4, 10, and 16 provide estimates from the baseline specification in equation (25), with temperature bins constructed as explained in Section 3.2, where rainfall controls are defined semiparametrically by ten bins instead of the linear specification in the benchmark case. Columns 5, 11, and 17 provide estimates from the baseline specification in equation (25), with temperature bins constructed as explained in Section 3.2 but standard errors constructed following Conley (2010) with a radious of 80km. Columns 6, 12, and 18 provide estimates from the baseline specification in equation (25), with temperature bins constructed as explained in Section 3.2 but standard errors constructed following Conley (2010) with a radious of 150km. Rows 1-4 present the effect on the log of the dependent variable of adding an extra day in the given temperature range respectively. Standard errors are clustered at the grid-cell level and reported in parentheses. *, **, and *** denote 10, 5, and 1% statistical significance respectively.

C.2 Additional Sample Cuts

In this section, we present additional sample custs. To mitigate concerns associated with the presence of multiplant firms, as discussed in Section 3.3, we conduct regression analysis where we exclude specific subsets of firms from our sample. First, we exclude all foreign firms, as presented in Columns 1, 6, 11, and 16 of Table C.7 and Columns 1, 6, and 11 of Table C.8. Next, we exclude all listed firms, as displayed in Columns 2, 7, 12, and 17 of Table C.7 and Columns 2, 7, and 12 of Table C.8. Furthermore, we exclude all firms that report consolidated accounts, as illustrated in Columns 3, 8, 13, and 18 of Table C.7 and Columns 3, 8, and 13 of Table C.8. Finally, we drop firms within the top 5 percent of the sales distribution, as depicted in Columns 4, 9, 14, and 19 of Table C.7 and Columns 4, 9, 14 of Table C.8.

Tables C.7 and C.8 consistently indicate that extreme temperatures adversely affect sales, materials, and labor, but not capital. Consequently, the revenue-based marginal products of materials and labor display no systematic sensitivity to extreme temperature fluctuations, in contrast to capital. Notably, our estimates are if anything larger, confirming the downward bias produced by firms more likely to be multiplant. Nevertheless, the consistency of results across these specifications underscores that the presence of multiplant firms does not significantly impact our fundamental conclusions.

Finally, Columns 5, 10, 15, and 20 of Table C.7 and Columns 5, 10, and 15 of Table C.8 include only firm-year observations where none of the revenues, wage bill, material costs, or capital are missing. Although the results are qualitatively similar, the lower number of observations introduces some quantitative differences, particularly with the revenue semi-elasticity for days above 40°C appearing slightly lower.

Table C.7: Average Effect of Temperature on Sales and Inputs—Robustness II

Dependent Variable	**Sales**					**Materials**					**Labor**					**Capital**				
	(1)	(2)	(3)	(4)	(5)	(6)	(7)	(8)	(9)	(10)	(11)	(12)	(13)	(14)	(15)	(16)	(17)	(18)	(19)	(20)
Temperature Bins																				
$(-\infty, 0°C]$	-0.095***	-0.095***	-0.092***	-0.085***	-0.047***	-0.070**	-0.069**	-0.065**	-0.057*	-0.058***	-0.070***	-0.070***	-0.069***	-0.069***	-0.063***	-0.033	-0.036*	-0.037*	-0.035	-0.024
	(0.020)	(0.019)	(0.019)	(0.020)	(0.015)	(0.022)	(0.029)	(0.029)	(0.031)	(0.019)	(0.021)	(0.019)	(0.020)	(0.020)	(0.021)	(0.022)	(0.021)	(0.021)	(0.022)	(0.021)
$(30°C, 35°C]$	-0.017*	-0.017*	-0.017*	-0.018**	-0.009	-0.023	-0.022	-0.020	-0.023	0.005	-0.001	0.002	0.004	0.002	-0.017*	-0.000	0.003	0.004	0.004	0.000
	(0.009)	(0.009)	(0.009)	(0.009)	(0.006)	(0.014)	(0.014)	(0.014)	(0.014)	(0.007)	(0.008)	(0.008)	(0.008)	(0.008)	(0.009)	(0.010)	(0.011)	(0.011)	(0.011)	(0.011)
$(35°C, 40°C]$	-0.050***	-0.046***	-0.047***	-0.045***	-0.019	-0.068**	-0.060**	-0.057**	-0.056**	0.008	-0.010	-0.003	-0.003	-0.004	-0.035*	0.001	0.004	0.006	0.006	0.003
	(0.017)	(0.017)	(0.017)	(0.017)	(0.013)	(0.026)	(0.025)	(0.026)	(0.025)	(0.016)	(0.017)	(0.017)	(0.017)	(0.017)	(0.018)	(0.019)	(0.019)	(0.020)	(0.020)	(0.020)
$(40°C, +\infty)$	-0.827***	-0.806***	-0.829***	-0.889***	-0.357**	-0.571**	-0.560**	-0.554**	-0.645**	-0.343*	-0.433**	-0.367**	-0.363*	-0.456**	-0.121	0.040	0.033	0.024	0.001	0.119
	(0.191)	(0.194)	(0.194)	(0.200)	(0.144)	(0.243)	(0.242)	(0.243)	(0.254)	(0.181)	(0.194)	(0.187)	(0.190)	(0.195)	(0.211)	(0.204)	(0.216)	(0.220)	(0.211)	(0.235)
Fixed Effects																				
Firm	✓	✓	✓	✓	✓	✓	✓	✓	✓	✓	✓	✓	✓	✓	✓	✓	✓	✓	✓	✓
Sector × Year	✓	✓	✓	✓	✓	✓	✓	✓	✓	✓	✓	✓	✓	✓	✓	✓	✓	✓	✓	✓
GR and SDC × Region	✓	✓	✓	✓	✓	✓	✓	✓	✓	✓	✓	✓	✓	✓	✓	✓	✓	✓	✓	✓
Controls																				
Rainfalls	✓	✓	✓	✓	✓	✓	✓	✓	✓	✓	✓	✓	✓	✓	✓	✓	✓	✓	✓	✓
Region Trends	✓	✓	✓	✓	✓	✓	✓	✓	✓	✓	✓	✓	✓	✓	✓	✓	✓	✓	✓	✓
Observations	4,463,602	4,685,250	4,603,410	4,394,813	3,653,159	4,463,602	4,685,250	4,603,410	4,394,813	3,653,159	4,463,602	4,685,250	4,603,410	4,394,813	3,653,159	4,463,602	4,685,250	4,603,410	4,394,813	3,653,159

Note. All dependent variables are in logs. Columns. Columns 1, 6, 11, and 16 provide estimates from the baseline specification in equation (25) excluding foreign firms. Columns 2, 7, 12, and 17 provide estimates from the baseline specification in equation (25) excluding listed firms. Columns 3, 8, 13, and 18 provide estimates from the baseline specification in equation (25) excluding firms reporting consolidated accounts. Columns 4, 9, 14, and 19 provide estimates from the baseline specification in equation (25) excluding firms with sales above top 5%. Columns 5, 10, 15, and 20 provide estimates from the baseline specification in equation (25) but the sample has been restricted to ensure consistency in number of observations across all variables. Rows 1-4 present the effect on the log of the dependent variable of adding an extra day in the given temperature range respectively (temperature bin coefficients). Standard errors are clustered at the grid-cell level and reported in parentheses. *, **, and *** denote 10, 5, and 1% statistical significance respectively.

Table C.8: Average Effect of Temperature on Revenue-Based Marginal Products of Inputs—Robustness II

Dependent Variable	**MRPM**					**MRPL**					**MRPK**				
	(1)	(2)	(3)	(4)	(5)	(6)	(7)	(8)	(9)	(10)	(11)	(12)	(13)	(14)	(15)
Temperature Bins															
$(-\infty, 0°C]$	-0.016	-0.018	-0.019	-0.021	0.015	0.005	0.008	0.009	0.014	0.010	-0.034	-0.030	-0.027	-0.025	-0.021
	(0.020)	(0.019)	(0.020)	(0.021)	(0.014)	(0.014)	(0.013)	(0.013)	(0.014)	(0.013)	(0.023)	(0.022)	(0.022)	(0.024)	(0.021)
$(30°C, 35°C]$	0.007	0.006	0.004	0.006	0.007	-0.010*	-0.012**	-0.012**	-0.011*	-0.013**	-0.012	-0.014	-0.014	-0.015	-0.009
	(0.007)	(0.008)	(0.008)	(0.008)	(0.006)	(0.006)	(0.006)	(0.006)	(0.006)	(0.005)	(0.010)	(0.010)	(0.010)	(0.011)	(0.010)
$(35°C, 40°C]$	0.014	0.011	0.007	0.009	0.014	-0.021	-0.021	-0.022*	-0.017	-0.025**	-0.046**	-0.045**	-0.048**	-0.048**	-0.026
	(0.015)	(0.014)	(0.015)	(0.015)	(0.011)	(0.013)	(0.013)	(0.013)	(0.014)	(0.013)	(0.020)	(0.021)	(0.022)	(0.022)	(0.021)
$(40°C, +\infty)$	-0.220	-0.206	-0.234	-0.217	-0.196	-0.016	-0.020	-0.017	0.001	-0.004	-0.638***	-0.579**	-0.583**	-0.604***	-0.482**
	(0.160)	(0.156)	(0.162)	(0.164)	(0.147)	(0.148)	(0.145)	(0.149)	(0.152)	(0.142)	(0.217)	(0.231)	(0.239)	(0.229)	(0.212)
Fixed Effects															
Firm	✓	✓	✓	✓	✓	✓	✓	✓	✓	✓	✓	✓	✓	✓	✓
Sector × Year	✓	✓	✓	✓	✓	✓	✓	✓	✓	✓	✓	✓	✓	✓	✓
GR and SDC × Region	✓	✓	✓	✓	✓	✓	✓	✓	✓	✓	✓	✓	✓	✓	✓
Controls															
Rainfalls	✓	✓	✓	✓	✓	✓	✓	✓	✓	✓	✓	✓	✓	✓	✓
Region Trends	✓	✓	✓	✓	✓	✓	✓	✓	✓	✓	✓	✓	✓	✓	✓
Observations	4,463,602	4,685,250	4,603,410	4,394,813	3,576,070	3,576,070	3,765,341	3,687,667	3,480,405	3,576,070	4,120,335	4,326,444	4,246,524	4,040,241	3,576,070

Note. All dependent variables are in logs. Columns provide estimates from the baseline specification in equation (25). Columns 1, 6, and 11 estimate from the baseline specification in equation (25) excluding foreign firms. Columns 2, 7, and 12 provide estimates from the baseline specification in equation (25) excluding listed firms. Columns 3, 8, and 13 provide estimates from the baseline specification in equation (25) excluding firms reporting consolidated accounts. Columns 4, 9, and 14 provide estimates from the baseline specification in equation (25) excluding firms with sales above top 5%. Columns 5, 10, and 15 provide estimates from the baseline specification in equation (25) but the sample has been restricted to ensure consistency in number of observations across all variables. Rows 1-4 present the effect on the log of the dependent variable of adding an extra day in the given temperature range respectively (temperature bin coefficients). Standard errors are clustered at the grid-cell level and reported in parentheses. *, **, and *** denote 10, 5, and 1% statistical significance respectively.

C.3 Additional Demand-Adjusted Productivity Results

Table C.9 presents sector-level losses in demand-adjusted productivity due to a 2-degree Celsius increase in temperature.

Table C.9: Sector-Level Demand-Adjusted Productivity Losses

Sector	NACE 1	Sector-level loss	α^K
Services	G-S	-0.35	0.05
Manufacturing	C	-0.37	0.07
Construction	F	-0.38	0.08
Mining and Quarrying	B	-0.46	0.21
Agriculture, Forestry and Fishing	A	-0.51	0.27

Note. Table C.9 presents sector-level losses in demand-adjusted productivity due to a 2-degree Celsius increase in temperature. Column 1 lists the sector names, Column 2 provides the corresponding NACE codes, Column 3 shows the loss levels, and Column 4 indicates the capital intensity.

To obtain these numbers, we applied equation (11) using our estimates from Table 2, along with the sector-level production function elasticities as explained in Section 3. For conciseness, we report a single number summarizing the sector-level losses. This was done by applying the temperature bin-specific semiparametric losses for each sector to the homogeneous 2-degree Celsius temperature increase from our benchmark scenario explained in Section 6.1.1. Our losses are broadly in line with those reported in the literature, such as the high damages to agriculture and lower damages for manufacturing noted by Addoum et al. (2020) and Ponticelli et al. (2023).

C.4 Results across adapted and non adapted regions

Table C.10 illustrates the full set of results when distinguishing between adapted and non adapted regions, as explained in Section 5.3.2 of the paper. Columns 2 and 5 of Table C.10 use an indicator variable set to one if the number of extreme temperature days in a grid-cell exceeds the national mean, while columns 3 and 6 use the national median as the threshold. In this specification, the estimated coefficients $\beta_{1,\ell}$ represent the temperature-semielasticity of sales common to firms in regions with both high and low exposure to extreme temperatures. In contrast, the coefficients $\beta_{2,\ell}$ capture the differential effect of temperature on firms in more adapted grid-cells.

Table C.10: Effect of Temperature on Sales and MRPK Conditional on Adaptation

Dependent Variable	**Sales** (1)	**Sales** (2)	**Sales** (3)	**MRPK** (4)	**MRPK** (5)	**MRPK** (6)
Temperature Bins						
$(-\infty, 0°C]$	-0.094***	-0.080***	-0.079***	-0.030	-0.004	-0.001
	(0.019)	(0.021)	(0.021)	(0.022)	(0.027)	(0.028)
$(30°C, 35°C]$	-0.017*	-0.029***	-0.023**	-0.014	-0.019	-0.018
	(0.009)	(0.010)	(0.009)	(0.010)	(0.012)	(0.013)
$(35°C, 40°C]$	-0.046***	-0.035	-0.024	-0.045**	-0.049	-0.061
	(0.017)	(0.033)	(0.037)	(0.021)	(0.036)	(0.042)
$(40°C, +\infty)$	-0.807***	-1.864***	-2.039***	-0.578**	-1.225**	-1.393***
	(0.194)	(0.505)	(0.524)	(0.231)	(0.536)	(0.551)
Temperature Bins$\times I^H_{g(i)}$						
$(-\infty, 0°C]$		-0.019	-0.019		-0.039	-0.041
		(0.028)	(0.027)		(0.031)	(0.031)
$(30°C, 35°C]$		0.018	0.009		0.017	0.019
		(0.011)	(0.011)		(0.014)	(0.013)
$(35°C, 40°C]$		-0.003	-0.012		0.025	0.042
		(0.032)	(0.036)		(0.038)	(0.043)
$(40°C, +\infty)$		1.146**	1.344**		0.653	0.826
		(0.540)	(0.559)		(0.581)	(0.595)
Fixed Effects						
Firm	✓	✓	✓	✓	✓	✓
Sector × Year	✓	✓	✓	✓	✓	✓
GR and SDC × Region	✓	✓	✓	✓	✓	✓
Controls						
Rainfalls	✓	✓	✓	✓	✓	✓
Region Trends	✓	✓	✓	✓	✓	✓
Observations	4,687,524	4,687,503	4,687,503	4,328,710	4,328,689	4,328,689

Note. All dependent variables are in logs. Temperature bins are constructed as explained in Section 3.2. In columns 2 and 5 the variable $I^H_{g(i)}$ is an indicator function that takes the value of one if firm i belongs to a grid-cell g with the number of extreme days above the national mean. In columns 3 and 6 the variable $I^H_{g(i)}$ is an indicator function that takes the value of one if firm i belongs to a grid-cell g with the number of extreme days above the national median. Rows 1-4 present the effect on the log of sales of adding an extra day in the given temperature range respectively. Rows 5-12 present the extra effect coming from being exposed to extreme temperatures. Standard errors are clustered at the grid-cell level and reported in parentheses. *, **, and *** denote 10, 5, and 1% statistical significance respectively.

D Aggregate Results

D.1 Counterfactual Temperature Distributions

D.1.1 Counterfactual Temperature Distributions with Mean Change

This appendix describes the counterfactual distribution of days within temperature bins under different warming scenarios compared to the observed data. The different counterfactuals are computed as follows.

For the "MS" counterfactuals, we add the specified temperature increase to each grid-cell's daily temperatures throughout the year. This produces a new distribution of days within each temperature range for each grid-cell. We then partition these distributions into temperature

bins, as outlined in Section 3.2, represented by the vector $\boldsymbol{T_c} = \{T_c^\ell\}_\ell$. Figure 3a illustrates the average counterfactual distributions of days within each bin across grid-cells, while Table D.11 in Appendix D.1.1 provides the complete distribution for all grid-cells and scenarios. Using these partitions, we compute the counterfactual changes in the number of days per temperature bin relative to those in Section 3.2, which form the basis of our analysis. Table D.12 in Appendix D.1.1 presents the distribution of changes in number of days across temperature bins $\boldsymbol{T_c}$.

For the "MP" counterfactuals, we compute counterfactual daily temperature $T^{daily} = \mu_T + (1 + \beta * \Delta T) \times (T - \mu_T)$, where T is the current daily temperature, μ_T is the current mean temperature and ΔT is the counterfactual change in mean temperature. Figure 3b illustrates the average counterfactual distributions of days within each bin across grid-cells. Table **??** and D.13 in Appendix D.1.1 present the distribution of changes in number of days across temperature bins $\boldsymbol{T_c}$.

For the "Full" counterfactuals, we compute counterfactual daily temperature $T^{daily} = \mu_T + (1 + \beta * \Delta T) \times (T - \mu_T) + \Delta T$. We choose $\beta = 0.08$ consistently with the projections of Fischer and Schär (2010).

Table D.11 provides summary statistics of the distribution of days within temperature bins, while Table D.12 presents the changes in the distribution of days under each warming scenario.

Table D.11 summarizes the distribution of days within temperature bins for the observed data and various warming scenarios. The temperature bins are categorized from below 0 degrees Celsius to 40 degrees Celsius or higher, as explained in Section 3.2. The table includes statistical measures such as mean, median, minimum, and maximum values for each temperature bin.

The first four rows present the distribution of days within each temperature bin in the data for the period 1999-2013. The second four rows present the distribution of days within each temperature bin for the 1-degree Celsius temperature increase counterfactual scenario. The third four rows present the distribution of days within each temperature bin for the 2-degree Celsius temperature increase counterfactual scenario. The fourth four rows present the distribution of days within each temperature bin for the 4-degree Celsius temperature increase counterfactual scenario. The fifth four rows present the distribution of days within each temperature bin for the RCP4.5 counterfactual scenario. The sixth four rows present the distribution of days within each temperature bin for the RCP8.5 counterfactual scenario. Overall, we see that the more extreme the counterfactual warming scenario, the larger the

Table D.11: Summary Statistics of Counterfactual Distribution of Days Within Temperature Bins

		Temperature Bins				
		$(-\infty, 0°C]$	$(0°C, 30°C]$	$(30°C, 35°C]$	$(35°C, 40°C]$	$(40°C, +\infty)$
Warming Scenario	*Variable*					
1999-2013	Mean	1.90	316.10	41.87	5.08	0.04
	Median	0	317	44	3	0
	Min	0	201	0	0	0
	Max	164	365	95	56	10
1°C	Mean	1.14	304.04	50.38	9.31	0.13
	Median	0	304	51	6	0
	Min	0	212	0	0	0
	Max	153	365	105	64	17
2°C	Mean	0.66	291.22	57.53	15.18	0.41
	Median	0	289	59	11	0
	Min	0	221	0	0	0
	Max	140	365	105	70	32
4°C	Mean	0.23	265.02	65.142	32.06	2.55
	Median	0	264	65	31	1
	Min	0	198	0	0	0
	Max	111	365	117	87	52
RCP4.5	Mean	0.83	298.21	57.89	16.37	0.7
	Median	0	289	59	11	0
	Min	0	208	0	0	0
	Max	142	365	113	74	37
RCP8.5	Mean	0.30	265.37	64.46	31.92	2.95
	Median	0	266	65	30	0
	Min	0	190	0	0	0
	Max	104	365	122	92	58

Note. Table D.11 summarizes the distribution of days within temperature bins in the data and under different warming scenarios. It includes statistics such as mean, median, minimum, and maximum values for each temperature bin. The temperature bins range from below 0 degrees Celsius to 40 degrees Celsius or higher as defined in Section 3.2.

shift in the number of days toward higher temperatures.

Table D.12 presents the changes in the distribution of days within temperature bins under different warming scenarios. The values indicate the deviation in the number of days compared to the observed data. Negative values represent a decrease, while positive values indicate an increase in the number of days.

The first four rows present the change relative to the data in the distribution of days within each temperature bin for the 1-degree Celsius temperature increase counterfactual scenario. The second four rows present the change relative to the data in the distribution of days within each temperature bin for the 2-degree Celsius temperature increase counterfactual scenario. The third four rows present the change relative to the data in the distribution of days within each temperature bin for the 4-degree Celsius temperature increase counterfactual scenario. The fourth four rows present the change relative to the data in the distribution of days within each temperature bin for the RCP4.5 counterfactual scenario. The fourth and the fifth rows

Table D.12: Summary Statistics of Counterfactual Change in Distribution of Days Within Temperature Bins

		Temperature Bins				
		$(-\infty, 0°C]$	$(0°C, 30°C]$	$(30°C, 35°C]$	$(35°C, 40°C]$	$(40°C, +\infty)$
1°C	Mean	-0.76	-12.07	8.51	4.23	0.09
	Median	0	-12	9	3	0
	Min	-27	-33	-21	-2	0
	Max	0	27	33	25	10
2°C	Mean	-1.24	-24.88	15.66	10.10	0.37
	Median	0	-251	17	8	0
	Min	-56	-64	-31	-10	0
	Max	0	56	57	39	22
4°C	Mean	-1.67	-51.09	23.27	26.98	2.51
	Median	0	-52	24	27	1
	Min	-84	-100	-48	-15	0
	Max	0	84	86	71	44
RCP4.5	Mean	-1.07	-26.89	16.02	11.28	0.66
	Median	0	-24	16	8	0
	Min	-71	-79	-41	-10	0
	Max	0	71	70	57	35
RCP8.5	Mean	-1.60	-50.82	22.59	26.83	2.91
	Median	0	-51	23	25	0
	Min	-100	-120	-49	-22	0
	Max	0	101	100	85	56

Note. Table D.12 presents the changes in the distribution of days within temperature bins under various warming scenarios. It provides statistical measures such as mean, median, minimum, and maximum values for each temperature range. Negative values indicate a decrease, while positive values represent an increase in the number of days.

present the change relative to the data in the distribution of days within each temperature bin for the RCP8.5 counterfactual scenario. Overall, we see that the more extreme the counterfactual warming scenario, the larger the increase in the number of days with higher temperatures and the decline in the number of days with lower temperatures.

D.1.2 Counterfactual Temperature Distributions with Change in Standard-deviation or/and Mean

Here, we consider a climate change scenario where the standard deviation in the temperature increases while the mean remains constant. We define this as the Mean-preserving spread (MP), where the daily temperature is,

$$T_{mp} = \mu_T + (1 + \Delta T * \beta) * (T - \mu_T) \tag{72}$$

where the standard deviation increases by $\Delta T * \beta \times 100$ percent with a change in temperature ΔT. We define the full distribution that consider the mean shift in temperature distribution, The new distribution is

$$T_{full} = \mu_T + (1 + \Delta T * \beta) * (T - \mu_T) + \Delta T. \tag{73}$$

We use $\beta = 0.08$ as in Fischer and Schär (2010). ITable D.13 presents the counterfactual temperature distribution under the mean-preserving spread (MP) scenario, while Table D.14 shows the distribution under the full scenario, which combines both mean shifts and increased variability. The tables report changes in the number of days falling within each temperature bin under different warming scenarios, relative to the observed distribution. Positive values indicate an increase in the number of days in that bin, while negative values indicate a decrease.

Table D.13: Summary Statistics of Counterfactual Change in Distribution of Days Within Temperature Bins–Mean preserving spread with $\beta = 0.080$

		Temperature Bins				
		$(-\infty, 0°C]$	$(0°C, 30°C]$	$(30°C, 35°C]$	$(35°C, 40°C]$	$(40°C, +\infty)$
1°C	Mean	1.73	-11.53	5.05	4.59	0.16
	Median	0.00	-11.00	6.00	4.00	0.00
	Min	-0.00	-34.00	-23.00	-8.00	0.00
	Max	20.00	0.00	26.00	24.00	18.00
2°C	Mean	4.32	-22.69	7.58	10.05	0.74
	Median	2.00	-22.00	9.00	9.00	0.00
	Min	0.00	-57.00	-34.00	-18.00	0.00
	Max	33.00	-1.00	41.00	41.00	29.00
4°C	Mean	11.45	-44.32	6.89	21.66	4.32
	Median	8.00	-42.00	7.00	21.00	2.00
	Min	0.00	-96.00	-53.00	-26.00	0.00
	Max	54.00	-4.00	56.00	64.00	48.00
RCP4.5	Mean	3.52	-22.24	7.34	10.33	1.04
	Median	1.00	-22.00	9.00	8.00	0.00
	Min	-0.00	-68.00	-41.00	-18.00	0.00
	Max	41.00	0.00	48.00	46.00	36.00
RCP8.5	Mean	10.13	-42.29	6.92	20.99	4.25
	Median	7.00	-40.00	7.00	20.00	2.00
	Min	0.00	-107.00	-56.00	-29.00	0.00
	Max	60.00	-4.00	63.00	60.00	53.00

Note. Table D.13 presents the changes in the mean-preserving distribution of days within temperature bins under various warming scenarios as defined in Equation 72. Negative values indicate a decrease, while positive values represent an increase in the number of days.

Table D.14: Summary Statistics of Counterfactual Change in Distribution of Days Within Temperature Bins–Full effect with $\beta = 0.080$

		Temperature Bins				
		$(-\infty, 0°C]$	$(0°C, 30°C]$	$(30°C, 35°C]$	$(35°C, 40°C]$	$(40°C, +\infty)$
1°C	Mean	0.36	-22.37	11.40	10.08	0.53
	Median	0.00	-22.00	13.00	9.00	0.00
	Min	-19.00	-50.00	-32.00	-18.00	0.00
	Max	9.00	19.00	48.00	41.00	29.00
2°C	Mean	0.74	-42.40	14.21	24.02	3.43
	Median	0.00	-42.00	15.00	24.00	1.00
	Min	-31.00	-84.00	-51.00	-23.00	0.00
	Max	13.00	31.00	70.00	64.00	47.00
4°C	Mean	1.55	-74.64	8.71	41.43	22.96
	Median	0.00	-76.00	9.00	43.00	20.00
	Min	-51.00	-121.00	-56.00	-29.00	0.00
	Max	20.00	49.00	88.00	82.00	85.00
RCP4.5	Mean	0.64	-42.86	13.11	23.99	5.12
	Median	0.00	-41.00	14.00	22.00	1.00
	Min	-45.00	-99.00	-56.00	-31.00	0.00
	Max	12.00	45.00	87.00	74.00	66.00
RCP8.5	Mean	1.37	-73.23	8.23	40.96	22.67
	Median	0.00	-74.00	8.00	43.00	18.00
	Min	-62.00	-133.00	-58.00	-25.00	0.00
	Max	18.00	54.00	80.00	86.00	88.00

Note. Table D.14 presents the changes in the full distribution of days within temperature bins under various warming scenarios as defined in Equation 73. Negative values indicate a decrease, while positive values represent an increase in the number of days.

D.2 Additional Robustness Main Results

Table D.15 provides the aggregate productivity decline under 1°C, 2°C and 4°C. Under 1°C, losses are half of the 2°C scenario, while under 4°C, the losses are almost three times that of 2°C, highlighting strong convexity in productivity losses. Adaptation helps cushion against the losses due to climate change, but only to a certain extent.

Table D.15: Effect of Climate Change on Aggregate Productivity

	ΔTotal	ΔTechnology	ΔAllocative Efficiency
1°C			
1°C MS	0.77%	0.31%	0.46%
1°C MP	0.94%	0.50%	0.44%
1°C Long-run	1.51%	1.07%	0.44%
2°C			
2°C MS	1.68%	0.81%	0.87%
2°C MP	3.32%	1.59%	1.73%
2°C Long-run	5.61%	3.88%	1.73%
4°C			
4°C MS	6.81%	3.33%	3.48%
4°C MP	8.74%	4.92%	3.82%
4°C Long-run	22.11%	18.29%	3.82%
1°C with Adaptation			
Adaptation MS	0.65%	0.30%	0.35%
Adaptation MP	0.73%	0.36%	0.37%
Adaptation + Long-run	1.15%	0.78%	0.37%
2°C with Adaptation			
Adaptation MS	1.27%	0.58%	0.69%
Adaptation MP	2.63%	1.21%	1.42%
Adaptation + Long-run	4.36%	2.94%	1.42%
4°C with Adaptation			
Adaptation MS	5.30%	2.46%	2.84%
Adaptation MP	6.85%	3.82%	3.03%
Adaptation + Long-run	18.59%	15.56%	3.03%

Note. This table reports the percentage losses in aggregate productivity due to climate change. Column 1 reports total productivity losses (ΔTotal), while columns 2 and 3 decompose these into losses from within-firm technology reductions (ΔTechnology) and misallocation (Δ Allocative Efficiency). Panels differ by temperature scenario and model assumptions: **2°C MS:** Assumes a mean-shift (MS) by 2°C in temperature. "MP" consider mean-preserving spread to capture increased variability. "Long-run" assumes allocative efficiency effects due to mean shifts in temperature are zero and Δtechnology captures both effects by mean shifts and increased variability in temperature. **2°C with Adaptation:** includes adaptation effects captured by the regression model in Equation 27. Comparisons across rows isolate the effect of average temperature increases, variability increases, and the combination of the average + variability increases.

Table D.15 presents the impact of controlling for adaptation on the scenarios used as robustness exercises in Section 6.1.3. Under the MS distributions, introducing adaptation in the 1°C scenario reduces productivity losses to 0.60, and in the 4°C scenario, it decreases losses

to 21.95 percent.

Overall, adaptation lowers the aggregate productivity losses of the different scenarios by an average of 20 percent under the low-warming scenario. Adaptation has little bite or even slightly worsens the losses under extreme warning scenarios. This is driven by the fact that the majority (around 95 percent) of the firms have already adapted under the low warming scenario.